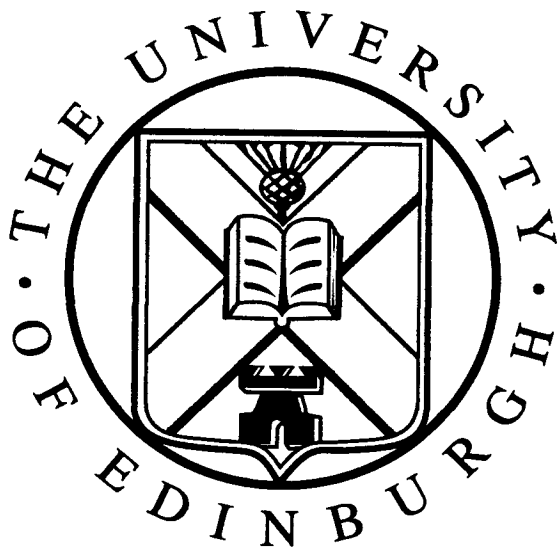


**Post-Translational Regulation of Mad3p
in *Saccharomyces cerevisiae***



Emma King

Thesis presented for the degree of Doctor of Philosophy
at the Univeristy of Edinburgh, 2005



Declaration of Authenticity

I declare that this thesis was composed by myself and that the research presented within is my own work, except where explicitly stated and acknowledgement is given.

Acknowledgements

First and foremost my thanks go to Kevin Hardwick. Over the last 5 years he has provided me with exceptional inspiration, direction, faith and support as supervisor and friend.

I am also grateful to the Hardwick lab members, past and present, and innumerable other researchers and friends at ICMB for making my work environment motivating and fun.

Thank you to Najma Rachidi and Mike Stark for their invaluable input into our studies of Mad3p phosphorylation.

Thank you to Stuart MacNeill for telling me what I should do with my life and the BBSRC for funding my studies to make it possible.

Recognition is also due to my schoolteachers, specifically Mrs Ingle, Mrs Hickman and Mrs Walker. Their teaching, guidance and perseverance got me through school and to university – who knows what would have happened without their influence?!

Throughout the years an invaluable source of strength has come from my friends. You know who you are and I have told you how amazing you are on many occasions, but thank you once again.

My final acknowledgement goes to my family, without whose unfaltering love I would not have achieved anything.

Life

Look to this day
for it is life,
the very life of life.
In its brief course lie all
the realities of existence;
the joy of growth,
the splendor of action,
the glory of power.
For yesterday is but a memory
and tomorrow is only a vision,
but today well lived
makes every yesterday
a memory of happiness
and every tomorrow
a vision of hope.
Look well, therefore,
to this day!

--Ancient Sanskrit Poem

Abstract

Post-Translational Regulation of Mad3p in *Saccharomyces cerevisiae*

The spindle checkpoint in eukaryotic cells maintains the integrity of the genome by ensuring equal chromosome segregation during mitosis. Mad3p is a component of the spindle checkpoint in *Saccharomyces cerevisiae*.

Mad3p is known to be in a constitutive complex with another checkpoint component Bub3p and upon checkpoint activation it interacts with Mad2p and Cdc20p to form the mitotic checkpoint complex. Recent analysis also suggests that the Mad proteins, in addition to the direct inhibition of Cdc20p through formation of the mitotic checkpoint complex, have an additional role in the down-regulation of Cdc20p levels in the cell.

The results presented in this thesis show Mad3p to be a protein that is phosphorylated during every mitosis and consequently upon spindle checkpoint activation. Such phosphorylation does not require any other checkpoint components. Experiments also show that Mad3p is phosphorylated on serine 337 by Ipl1p kinase *in vitro* and the phosphorylation of Mad3p *in vivo*, due to an absence of tension at the kinetochore, requires Ipl1p.

Mad3p contains two KEN box motifs that are conserved between species. Evidence in this thesis demonstrates that mutation of either of these KEN boxes renders cells sensitive to microtubule depolymerising drugs. Further analysis of these KEN box mutants shows that Cdc20p binding is reduced in both but they can both still bind Bub3p. Mutation of the N-terminal KEN box increases the half-life of Cdc20p and consequently the total levels of Cdc20p in the cell. Cdc20p turnover is also reduced in the absence of Bub1p and Bub3p, but to a lesser extent. Mutation of the second KEN box in Mad3p leads to a dominant phenotype that perturbs mitosis even in the presence of wild-type Mad3p.

Common Abbreviations

Amp	Ampicillin
APC/C	Anaphase promoting complex/cyclosome
ATP	Adenosine-5'-triphosphate
BUB	Budding uninhibited by benomyl
C-terminus	Carboxy-terminus (of a protein)
CDE	Centromere DNA element
CDK	Cyclin-dependent kinase
CTP	Cytosine-5'-triphosphate
DNA	Deoxyribonucleic acid
DTT	Dithiothreitol
ECL	Enhanced chemiluminescence
EDTA	Ethylenediamine tetra acetic acid
EGTA	1,2-Di (2-aminoethoxy) ethane-N,N,N',N'-tetra acetic acid
GST	Glutathione S-Transferase
GTP	Guanine-5'-triphosphate
<i>H. sapiens</i>	<i>Homo sapiens</i>
HRP	Horse radish peroxidase
IP	Immunoprecipitation
Kan	Kanamycin
LB	Luria-Bertani Medium
MAD	<u>M</u> itotic <u>A</u> rrest <u>D</u> eficient
MTOC	Microtubule organising centre
N-terminus	Amino-terminus (of a protein)
PAGE	Polyacrylamide gel electrophoresis
PBS	Phosphate buffered saline
PBSS	PBS with Sorbitol
PBST	PBS with Tween-20
PCR	Polymerase chain reaction
PEG	Polyethylene glycol
PMSF	Phenyl methyl sulphonyl fluoride
RNA	Ribonucleic acid
<i>S. cerevisiae.</i>	<i>Saccharomyces cerevisiae</i>
<i>S. pombe</i>	<i>Schizosaccharomyces pombe</i>
SCF	Skp1-cullin-F-box ubiquitin ligase protein complex
SDM	Site-directed mutagenesis
SDS	Sodium dodecyl sulphate
SGD	<i>Saccharomyces</i> genome database
TAE	Tris acetate EDTA solution

TAP	Tandem affinity purification
Tet	Tetracycline
TTP	Thiamine-5'-triphosphate
<i>Xenopus</i>	<i>Xenopus laevis</i>
YMM	Yeast minimal media
YPDA	Yeast peptone with dextrose and adenine
YPD	Yeast peptone with dextrose

Table of Contents

Declaration of Authenticity	i
Acknowledgements	ii
‘Life’	iii
Abstract	
Post-Translational Regulation of Mad3p in <i>Saccharomyces cerevisiae</i>	iv
Common Abbreviations	v
Table of Contents	vii
Chapter 1	
Introduction	
1.1 Introduction to the cell cycle	1
1.2 Cyclins and CDKs	3
1.3 Sister chromatid cohesion	4
1.4 Kinetochore structure, interactions and dependencies	6
1.5 Microtubule-kinetochore attachment and regulation of kinetochore complexes	8
1.6 Aurora and Ipl1p	10
1.7 Polo and Cdc5p	15
1.8 APC/C and irreversible cell cycle progress through mitosis	17
1.9 The spindle checkpoint	20
1.10 Other spindle associated checkpoints	28
Chapter 2	
Materials and Methods	
2.1 Supplier Information	30
2.2 General Information	30
2.2.1 Sterilisation	30
2.2.2 Commonly used buffers and solutions	31
2.3 Microbiological Methods	31
2.3.1 Bacterial and yeast strains and growing conditions	31
2.3.2 Transformations	38
2.3.3 <i>S. cerevisiae</i> cell cycle arrests	40
2.3.4 Mating of <i>S. cerevisiae</i> haploid strains	41
2.3.5 Tetrad dissection	42

2.3.6	Benomyl sensitivity assay	43
2.4	Nucleic Acids Methods	43
2.4.1	Plasmids used in this study	43
2.4.2	Phenol-chloroform extraction of DNA	46
2.4.3	Precipitation of nucleic acids	46
2.4.4	Plasmid mini-prep by spin column	47
2.4.5	Agarose gel electrophoresis	47
2.4.6	Extraction of DNA from agarose gels	47
2.4.7	Restriction digest of DNA	47
2.4.8	Amplification of DNA using the Polymerase Chain Reaction (PCR)	48
2.4.9	PCR mediated site-directed mutagenesis	52
2.4.10	Purification of PCR products	54
2.4.11	Ligation of DNA molecules	54
2.5	Protein Methods	55
2.5.1	Crude total cell lysate preparation	55
2.5.2	Total cell lysate preparation for use in (co-)immunoprecipitation	56
2.5.3	Lambda phosphatase treatment	56
2.5.4	SDS-PAGE	57
2.5.5	Coomassie staining	58
2.5.6	Western blotting	58
2.6	Sister Separation assay	60
2.6.1	Fixation of cells for visualisation of GFP marked chromosomes	60
2.7	Mad3-intein purification	60
2.7.1	Soluble extract preparation	60
2.7.2	Column preparation and incubation with soluble extract	61
2.7.3	Cleavage induction and elution	61
2.8	Tandem Affinity Purification (TAP) protocol	61
2.8.1	Soluble extract preparation	62
2.8.2	Bead preparation and purification of Mad3-TAP	62
2.9	TNT coupled transcription/translation system	63
2.10	<i>In vitro</i> binding assay	63

Chapter 3

Analysis of Putative Mad3p Phosphorylation by Cdc5p and Ipl1p

3.1	Preliminary analysis of Mad3p modification	64
3.1.1	Mad3p is modified through an unperturbed cell cycle	64
3.1.2	Arresting cells at various stages of the cell cycle confirms Mad3p modification is cell cycle dependent and peaks during mitosis	65
3.1.3	Over-expression of Mps1p induces modification of Mad3p	66

3.1.4	The modification of Mad3p is phosphorylation	66
3.1.5	The phosphorylation of Mad3p is unaffected in checkpoint mutants	67
3.2	The identification of putative phosphorylation sites within Mad3p	69
3.3	Analysis of Mad3p mutated at sites putatively phosphorylated by Cdc5p	71
3.3.1	A Mad3p mutant at putative sites of phosphorylation by Cdc5p is sensitive to microtubule depolymerising drugs	71
3.3.2	Mad3p phosphorylation is unaffected by mutation of putative sites of Cdc5p phosphorylation	72
3.4	Mad3p phosphorylation, in response to a lack of tension at kinetochores, requires Ipl1p kinase function <i>in vivo</i>	73
3.4.1	Mad3p phosphorylation is reduced in response to reduced cohesion between sister chromatids in an <i>ipl1-321</i> mutant	73
3.4.2	Mad3p phosphorylation in response to <i>CDC6</i> repression is reduced in an <i>ipl1-321</i> mutant	75
3.4.3	Mad3p phosphorylation is subtly reduced in a <i>ipl1-321</i> Mutant when spindle microtubules are depolymerised	76
3.4.4	Mad3p is required for the metaphase delay seen in a cohesin mutant	77
3.5	Mad3p is phosphorylated <i>in vitro</i> by Ipl1p kinase	78
3.5.1	Mad3-intein purification	78
3.5.2	Mad3, but not the N-terminus of Bub1 or Mad1 is phosphorylated <i>in vitro</i> by Ipl1p	80
3.6	<i>In vivo</i> analysis of <i>mad3</i> mutants at putative sites of phosphorylation by Ipl1p	81
3.6.1	The mutation to aspartate of all Ipl1p and Cdc5p putative phosphorylation sites within Mad3p renders cells sensitive to microtubule depolymerisation	81
3.6.2	Mad3p phosphorylation is not obviously affected by mutation of putative sites of Ipl1p and/or Cdc5p phosphorylation	82
3.6.3	Mad3p stability is increased in the quintuple S222/T229/S380/S303/S337D mutant	82
3.7	Discussion	83

Chapter 4

The Role of KEN boxes in Mad3p

4.1	Mad3p Contains Two Conserved KEN Boxes	90
4.1.1	Mutagenesis to make pKH535 KEN mutants	90
4.2	<i>mad3</i> KEN mutants are sensitive to microtubule depolymerisation	91
4.2.1	<i>mad3</i> KEN mutants do not grow on medium containing benomyl	91

4.2.2	Microcolony analysis of KEN30AAA reveals a classic checkpoint mutant phenotype	91
4.2.3	All KEN box mutants die rapidly following exposure to the microtubule depolymerising drug, nocodazole	93
4.2.4	All KEN box mutants experience premature separation of their sister chromatids	93
4.3	KEN296AAA displays a phenotype that is dominant	94
4.3.1	KEN296AAA mutants remain sensitive to benomyl in the presence of wildtype Mad3p	94
4.3.2	KEN296AAA in the presence of wildtype Mad3p cannot divide beyond 3 divisions on medium containing benomyl	95
4.3.3	KEN296AAA dies rapidly following exposure to the microtubule depolymerising drug nocodazole with endogenous Mad3p present	96
4.3.4	KEN296AAA experiences premature sister separation in the presence of nocodazole and endogenous Mad3p	97
4.4	Role of the APC/C and its activators, Cdc20p and Cdh1p, in Mad3p stability	97
4.4.1	Mad3p is stabilised in APC/C mutants	97
4.4.2	Mad3p stability is unaffected by Cdh1p and Cdc20p mutants	98
4.5	Biochemical analysis of KEN mutants	100
4.5.1	<i>mad3</i> KEN mutants can still bind Bub3p	100
4.5.2	<i>mad3</i> KEN mutants have reduced Cdc20p binding	101
4.6	The spindle checkpoint and <i>mad3</i> KEN mutants have a role in Cdc20p turnover	102
4.6.1	The role of spindle checkpoint components in Cdc20p turnover	102
4.6.2	KEN30AAA and KEN30/296AAA increase Cdc20p stability as seen in a <i>mad3Δ</i> mutant	103
4.7	Discussion	103
Chapter 5		
Final Discussion		108
Appendix		
A.1	Anti-Mad3p Antibody Production and Purification	112
A.2	Mad3p-TAP Purification	112
A.2.1	Strain generation	113
A.2.2	Extraction and purification of TAP-tagged Mad3p	114
A.3	Expression and purification of Bub1-GST	115
A.4	Bub1p N-terminal analysis	116
A.4.1	Alignment of Bub1p across species reveals several	

conserved residues in the N-terminus	117
A.4.2 Generation and integration of Bub1p Region I mutants	117
A.4.3 Bub1p Region I mutants have a benomyl sensitive phenotype	118
A.4.4 Several <i>bub1</i> region I mutants are unstable, reflecting their benomyl sensitive phenotype	118
A.4.5 Portions of Bub1p and Cdc20p can be expressed <i>in vitro</i> using the reticulocyte lysate method of coupled transcription and translation	119
A.4.6 Region I of Bub1p is sufficient for binding Cdc20p <i>in vitro</i>	119
Bibliography	121

Chapter One

Introduction

1.1 Introduction to the Cell Cycle

An understanding of the cell cycle is vital to decipher the mechanisms behind medical conditions, such as cancer, that result from a lack of correct cell cycle control.

The eukaryotic cell cycle can be split into four discrete phases: G1, S, G2 and M. Interphase encompasses G1, S and G2 phases, during which the cell is growing and, in S-phase, replicates its DNA. During interphase chromosomes are found in a relaxed form. In prophase of mitosis, a pre-mitotic spindle is formed and replicated, cohesed, chromosomes begin to condense. The process of condensation continues until metaphase. During prometaphase, the nuclear membrane breaks down, chromosomes become individually identifiable and the kinetochore is assembled on centromeres. The kinetochore is a proteinaceous structure that allows chromosomes to become attached via the mitotic spindle to each pole of the cell; bi-orientation. Metaphase sees chromosomes aligned in the middle of the cell, in higher eukaryotes on the metaphase plate, ready for the separation of sister chromatids equally into two daughter cells. During anaphase, the mitotic spindle elongates and sister chromatids are pulled to opposite poles of the cell. Subsequently telophase ensues, chromosomes decondense and the cell undergoes cytokinesis (Murray and Hunt, 1993).

In all eukaryotes, chromosome condensation requires the action of an aptly named complex, condensin I, and topoisomerase II. The condensin I complex consists of two Smc proteins Smc2 and Smc4 and three non-Smc components (budding yeast homologues given in parenthesis) CAP-D2 (Ycs4p), CAP-G (Ycs5p/Ysg1p) and CAP-H (Brn1p) (reviewed in (Hagstrom and Meyer, 2003) (Gassmann et al., 2004b). In HeLa cells Condensin I and topoisomerase II localise in a non-

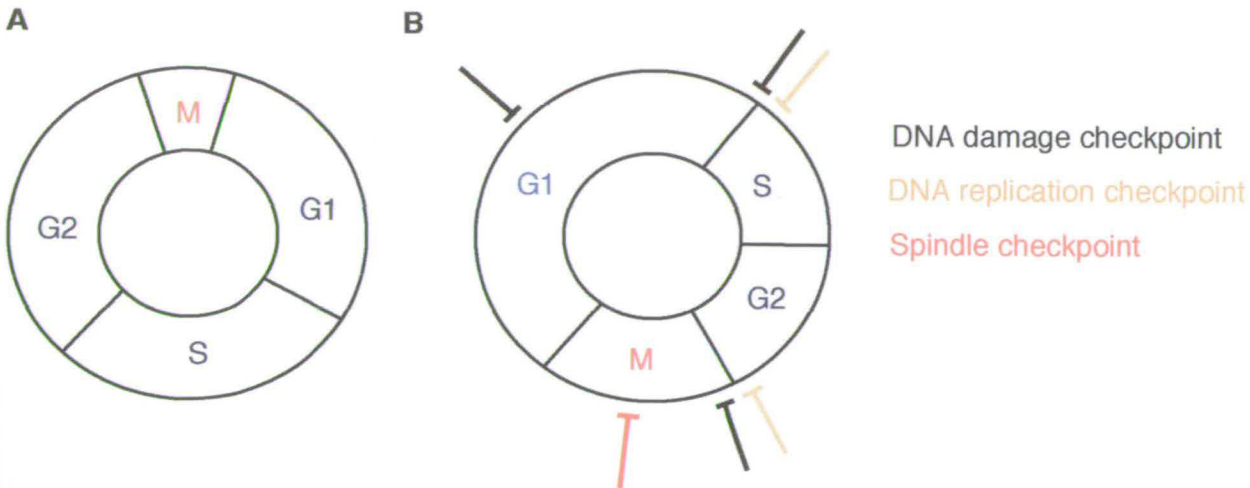


Figure 1.1 The Eukaryotic Cell Cycle

A The *H. sapiens* somatic cell cycle. **B** The *S. cerevisiae* cell cycle and where different checkpoints control it.

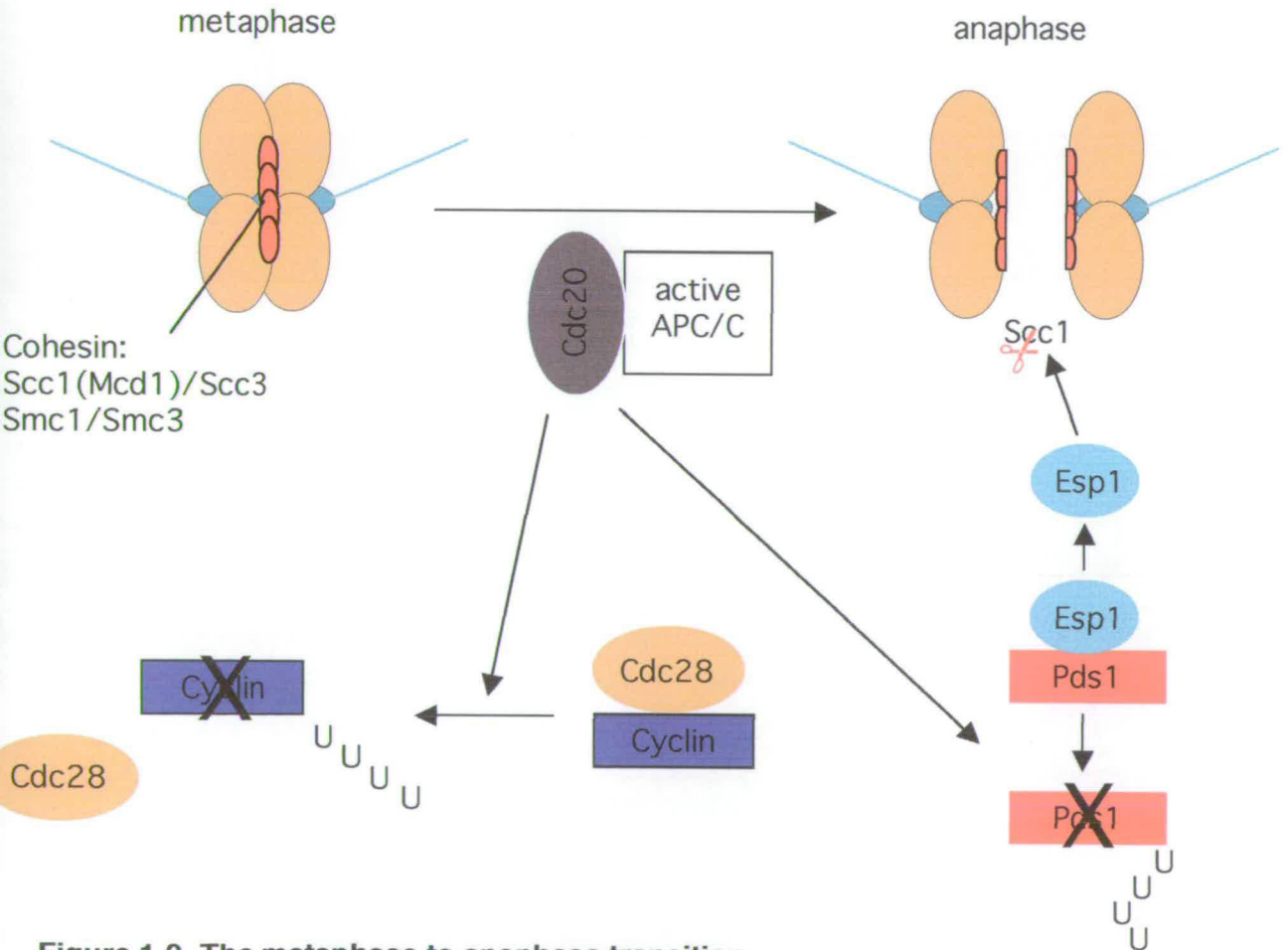


Figure 1.2 The metaphase to anaphase transition

The metaphase to anaphase transition. Cdc20p and the APC/C interact to enable the ubiquitination of cyclins and Pds1p (securin). Subsequently Cdc28p activity is reduced and sister chromatids separate following the release of Esp1p to cleave Scc1p.

overlapping bead-like fashion to the chromosome axis (Maeshima and Laemmli, 2003). Localisation of condensin I to centromeres has been demonstrated in *S. pombe* (Aono et al., 2002) and *brn1* mutants demonstrate defects in kinetochore-microtubule attachment in budding yeast (Lavoie et al., 2000; Ouspenski et al., 2000). Together these results infer an additional secondary role of condensin at kinetochores. In vertebrate cells there is a second condensin complex that also contributes to chromosomal architecture (Ono et al., 2004; Ono et al., 2003). Condensin II contains the same two Smc proteins, but the non-SMC, CAP-D3, CAP-G2 and CAP-H2 (Ono et al., 2003).

Biochemical and physical advances through the cell cycle are coordinated by the post-translational regulation of key substrates. Achieved by kinases, phosphatases and the ubiquitination pathway, the combination of reversible modification and irreversible degradation ensures directed and regulated progression.

Cyclin dependent kinase Cdk1 (Cdc28p in *S. cerevisiae*, Cdc2 in *S. pombe*) is the major kinase responsible for driving the cell division cycle in eukaryotes. There are however other important kinases that operate at different stages of the cell cycle and during mitosis. These include Polo and AuroraB. Transition from metaphase to anaphase of mitosis requires the activity of the anaphase-promoting complex/cyclosome (APC/C). The APC/C is a ubiquitin ligase that targets proteins for destruction via the 26S proteasome when associated with one of two known activating factors: Cdc20p and Cdh1p/Hct1p (reviewed in (Murray, 2004; Nasmyth, 2002)). The functions of these proteins and complexes are discussed in later sections.

Transition between phases of the cell cycle are regulated and coordinated by specific checkpoints. The DNA damage checkpoint can act at G1/S, S and G2/M, depending on which stage the cell cycle is in when the defect is detected (Elledge, 1996). Its function at G1/S may be to facilitate repair by increasing transcription of genes involved in replication and repair (Hartwell and Weinert, 1989), delaying replication as a consequence (Rhind and Russell, 2000). At G2/M the DNA damage

checkpoint arrests cells in a Pds1p phosphorylation dependent manner (Cohen-Fix and Koshland, 1997; Wang et al., 2001a), but independent of APC/C^{Cdc20} activity and spindle checkpoint function (Wang et al., 2001a). The replication checkpoint also acts at G2/M and in S-phase, utilising a common signal transduction pathway to the DNA damage checkpoint, including Mec1p, Rad53p and the effector molecule, Chk1p (Elledge, 1996). The spindle checkpoint functions in mitosis at the metaphase/anaphase transition.

1.2 Cyclins and CDKs

In *S. cerevisiae* Cdc28p is the cyclin-dependent kinase (CDK) principally involved with the cell cycle. Its activation is regulated by phosphorylation and complex formation with a regulatory subunit; the cyclin (reviewed in (Murray, 2004)). There are three G1 cyclins: Cln1-3p, two S-phase cyclins: Clb5p and Clb6p, and four mitotic cyclins: Clb1-4p in *S. cerevisiae*.

In the budding yeast cell cycle START defines the point at which cells have reached a critical size and there are sufficient nutrients available for continued cell cycle progression. Once cells have passed through START they can no longer mate and are committed to a mitotic cell cycle (reviewed in Murray and Hunt, 1993). When cells reach a critical size, Cln3p/Cdc28p activates the transcription factors SBF and MBF to increase levels of Cln1/2p. Cln1p and Cln2p are therefore present in the cell at high levels at START and form a complex with Cdc28p and spindle pole body duplication is initiated (Zachariae, 1999). Cln1/2p bring about the proteolysis of Sic1p, a Clb/Cdc28p inhibitor, and so levels of Clb/Cdc28p complexes rise. The S-phase cyclins are responsible for the initiation of DNA replication and, through switching off proteolysis mediated by the APC/C, give rise to high levels of the mitotic cyclins that can form a complex with and activate a phosphorylated form of Cdc28p, a requirement for entry into mitosis. This activity induces chromosome condensation and the formation of a mitotic spindle, pushing cells into metaphase. The level of the complexes remains high until anaphase when Clb3/5p are targeted for destruction by the APC/C bound to Cdc20p. Following the release of Cdc14p

from Cfi1p/Net1p at the end of the mitotic exit pathway, Sic1p becomes active and Cdh1p de-phosphorylated so it can bind the APC/C, targeting Clb2/3p for destruction by the 26S proteasome, rendering Cdc28p inactive. The reduced activity of Cdc28p prompts cytokinesis and allows another round of chromosome replication to begin (reviewed in (Murray, 2004)).

1.3 Sister Chromatid Cohesion

Sister chromatid cohesion is established during S-phase and maintained until the metaphase-anaphase transition. Cohesion is the means by which replicated chromosomes are held together until separation during anaphase of mitosis. Significantly, defects in cohesion can result in premature anaphase and subsequent chromosome mis-segregation.

A conserved cohesin complex, consisting of Scc1p, Scc3p, Smc1p and Smc3p is thought to be responsible for maintaining cohesion between sister chromatids (Guacci et al., 1997; Losada et al., 1998; Michaelis et al., 1997; Sonoda et al., 2001; Vass et al., 2003) (reviewed in (Nasmyth, 2002)). The cohesin complex is distributed along the arms of metazoan chromosomes (Losada et al., 1998) in addition to centromeric regions, where it is predominantly found in budding yeast (Tanaka et al., 1999). At centromeric regions in budding yeast the localisation of cohesin requires Cse4p (CENP-A), (Tanaka et al., 1999) while in *S. pombe* the methylation of histone H3 required for the recruitment of HP1 (Swi6p) leads to the association of cohesin with heterochromatin (Bernard et al., 2001; Nonaka et al., 2002). Kinetochore proteins, including Ndc10p and Mif2p (Tanaka et al., 1999) are also required for correct localisation of cohesin in *S. cerevisiae* and further studies have revealed an interaction between another kinetochore protein Ndc80p/Hec1p and Smc1p (Zheng et al., 1999).

In budding yeast cohesin the two Smc proteins form a heterodimer with intramolecular coiled coils. A globular domain situated in the central coil-coil allows formation of the hinge region and gives the structural appearance of a 'V'

(Anderson et al., 2002). The Smc proteins are joined at their globular 'head' domains by Scc1p that has Scc3p bound to its central domain (Haering et al., 2002). Currently the interaction between cohesin and chromatin is under great debate; ideas and proposals are reviewed in Haering and Nasmyth (2003). It has been suggested that a single complex forms a ring around the two sisters (Gruber et al., 2003), which is supported in part by electron micrograph data from Anderson *et al.* (2002). In a similar model, two cohesin complexes interact to form a larger ring around two sister chromatids either through the connection of head domains or two separate rings that are catenated or joined by an unknown factor around each sister.

The cohesin subunits also have a role in kinetochore/microtubule attachment and may play a part in presenting kinetochores to microtubules by ensuring a back-to-back presentation of sister chromatids to aid biorientation. In *S. pombe* and *Drosophila*, disruption of the cohesin complex results in mis-localisation of the chromosomal passenger complex (AuroraB, INCENP, Survivin and Borealin/dasraB) required for the re-orientation of maloriented sister chromatids (Gassmann et al., 2004a; Sampath et al., 2004; Sonoda et al., 2001; Tanaka et al., 1999; Vass et al., 2003).

scc1/mcd1 mutants, in addition to defects in sister chromatid cohesion, demonstrate defects in microtubule-kinetochore interactions and exhibit monopolar attachment of sister chromatids to spindle poles (Sonoda et al., 2001; Tanaka et al., 2000). This phenotype mimics that seen in mutants of Ipl1p and members of the DASH kinetochore complex (see later section).

The separation of sister chromatids during anaphase, in all eukaryotes, is accomplished by cleavage of the cohesin subunit Scc1p (Uhlmann et al., 1999). Ubiquitin mediated proteolysis of securin (Pds1p) releases separase (Esp1p) to cleave Scc1p, allowing sister chromatids to separate and be pulled to either pole of the cell by microtubules attached to their kinetochores (reviewed in (Nasmyth, 2002)). In budding yeast, optimum cleavage requires phosphorylation of residues adjacent to cleavage sites by Cdc5p (Alexandru et al., 2001), the budding yeast

homologue of Polo, whose function (and that of Aurora B) is required for the removal of cohesin from the arms of chromosomes in higher eukaryotes during prophase (Losada et al., 1998; Losada et al., 2002; Waizenegger et al., 2000).

1.4 Kinetochore Structure, Interactions and Dependencies

The kinetochore is a complex of proteins assembled at the centromere of each chromosome that mediates microtubule attachment and is required for tension generation and correct chromosome segregation. The simple budding yeast kinetochore has provided a useful model for the structure of kinetochores across species especially as one kinetochore binds only one microtubule.

In *S. cerevisiae*, the centromere is a 125bp sequence of DNA, encompassing the CDE I, II and III elements. In *S. pombe* and metazoans, the centromeric region is much larger, up to several (2-4) megabases in length, and frequently contains repetitive sequences that embed the kinetochore in surrounding regions of heterochromatin (reviewed in (Pidoux and Allshire, 2004). CDEII is the central element of the budding yeast centromere - an 80bp DNA sequence flanked by CDEI and CDEIII. CDEI binds two proteins Cbf1p (CENP-B) (Sorger et al., 1994) and Mif2p (CENP-C) (De Wulf et al., 2003).

The centromeric region of chromosomes has modified nucleosomes that include the presence of a histone H3-like protein Cse4p (CENP-A) (Basrai and Hieter, 1995). The complex provides a protein interface to mediate looping of centromeric DNA.

The composition of the budding yeast kinetochore has largely been facilitated by the development of Tandem Affinity Purification (TAP) methods and subsequent identification of proteins by mass-spectrometry. Refinement of this technique has provided further insight into the clarification of specific sub-complexes and interactions between proteins (Cheeseman et al., 2002; Cheeseman et al., 2001; De Wulf et al., 2003). The application of TAP derivatives to the purification of C.

elegans kinetochore complexes has also proved successful and has revealed a conserved molecular core (Cheeseman et al., 2004).

At least six kinetochore subcomplexes are now thought to exist with complex internal interactions and dependencies throughout (Figure 1.3). De Wulf *et al.* (2003) propose that the core CBF3 complex is linked by three sub-complexes; COMA - Ctf19p, Okp1p, Mcm21p and Ame1p (De Wulf et al., 2003; Ortiz et al., 1999), MIND - Mtw1p, Nsl1p, Nnf1p and Dsn1p (De Wulf et al., 2003) and the Ndc80p complex – Ndc80p, Spc34p, Spc25p and Nuf2p to the outer kinetochore complexes. The outer kinetochore complexes include such proteins as the Mcm proteins, Ctf3p and the DASH complex - Dam1p, Duo1p, Dad1p, Spc19p, Spc34p, Ask1p, Dad2p, Dad3p and Dad4p, which is thought to mediate microtubule binding (Cheeseman et al., 2002; Cheeseman et al., 2001).

The kinetochore complex CBF3, consisting of Ndc10p and associated proteins Skp1p, Cft13p and Cep3p (Connelly and Hieter, 1996; Goh and Kilmartin, 1993; Ng et al., 1986; Sorger et al., 1995; Strunnikov et al., 1995), is assembled on the CDEIII element of centromeric DNA and is required for the formation of all complexes *in vivo*, with the exception of the modified histone complex containing Cse4p (Measday et al., 2002; Ortiz et al., 1999).

Assembly of the COMA complex on kinetochores requires the presence of the Cse4p nucleosome and is perturbed by mutations in the CBF3 complex component, Ndc10p (Measday et al., 2002; Ortiz et al., 1999). While its function and composition does not affect the formation of MIND, Ndc80p or DASH complexes, COMA is required for loading of Mcm16p, Mcm22p, Ctf3p and Chl4p (De Wulf et al., 2003; Measday and Hieter, 2004; Pot et al., 2003). Ctf19p has been shown to co-purify with no less than 19 kinetochore proteins. Though it has also been shown that Mcm16p, Mcm22p and Ctf3p form a separate sub-complex from Chl4p that interacts with another outer kinetochore component, Iml3p (De Wulf et al., 2003; Pot et al., 2003).

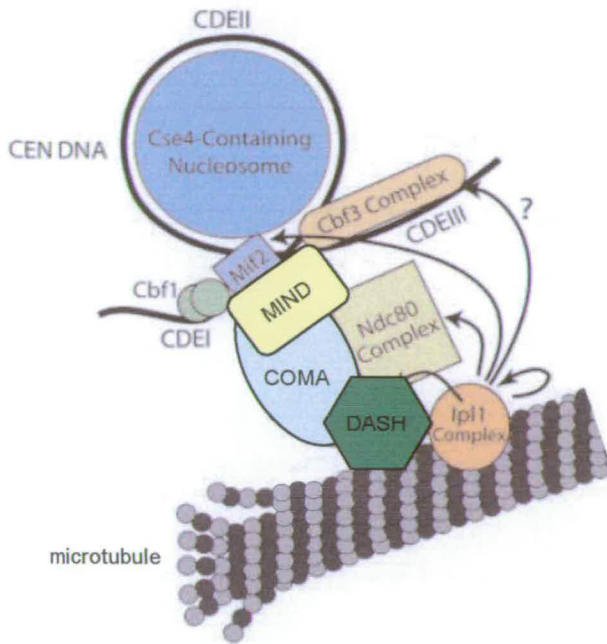


Figure 1.3 Sub-complexes at the budding yeast kinetochore

Model (adapted from Westerman *et al.*, 2003) showing the position and interactions of budding yeast kinetochore complexes with themselves, the centromere and a microtubule.

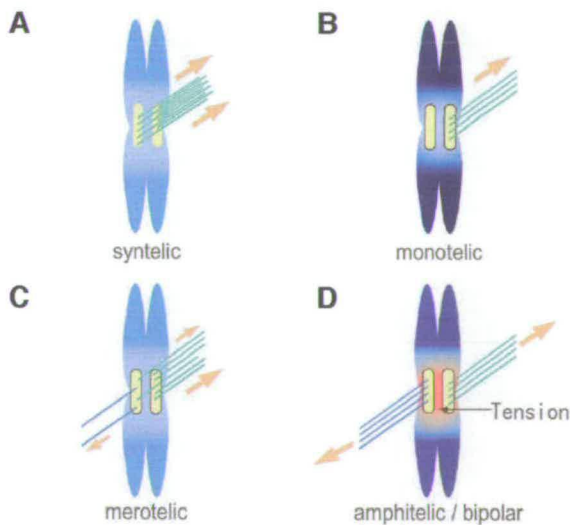


Figure 1.4 Microtubule-kinetochore attachments

Model showing different genres of kinetochore-microtubule attachments. **A-C** illustrate maloriented chromosomes. **A** Illustrates syntely where both sister chromatids are attached to the same pole. **B** Demonstrates monotelly where only one sister is attached to one pole. **C** Illustrates merotelly that can occur in higher eukaryotes (that have multiple microtubule-kinetochore attachments) where sisters are unequally attached to one pole. **D** Shows correct bipolar attachment of one sister chromatid to each pole - amphitelic attachment (taken from Tan *et al.*, 2004)

The MIND complex again requires the CBF3 complex for its kinetochore association as demonstrated by a requirement for Ndc10p for correct localisation and its interaction with centromeres. As yet, no outer kinetochore or other sub-complexes depend upon MIND for function or localisation (Goshima and Yanagida, 2000; Measday and Hieter, 2004).

The Ndc80p complex has been shown to localise to kinetochores and has a role in chromosome segregation (Janke et al., 2001; Wigge and Kilmartin, 2001). Biochemical and 2-hybrid studies have shown an interaction between Ndc80p complex members and COMA but Ndc80p complex integrity is not required for COMA components' kinetochore localisation (Janke et al., 2001). The kinetochore localisation of the Ndc80p complex is abrogated in *ndc10* mutants and the Ndc80p complex itself is required for the localisation of DASH components Spc34p and Dad2p and another outer kinetochore component Stu2p (He et al., 2001; Janke et al., 2001; Janke et al., 2002).

1.5 Microtubule-Kinetochore Attachment and Regulation of Kinetochore Complexes

It is from replicated spindle pole bodies (the budding yeast equivalent of centrosomes) that microtubules emanate to form the mitotic spindle. The spindle pole body is a complex structure composed of a half-bridge and inner and outer plates that sits in the nuclear envelope (reviewed in (Jaspersen and Winey, 2004). Microtubules are dynamic polymers that grow inside and outside the nucleus. The minus ends of nuclear microtubules are associated with spindle pole bodies while plus ends form kinetochore-microtubule interactions or interdigitate in the middle of the spindle (reviewed in (Wittmann et al., 2001). The separation of spindle pole bodies and the forces generated by the attachment of microtubules to both spindle pole bodies and kinetochores is required for the poleward movement of sister chromatids during anaphase and thus the successful segregation of DNA into daughter cells. The cell cycle of *S. cerevisiae* differs from other eukaryotic cell

cycles as the spindle cycle is initiated by spindle pole body duplication in late G1 or early S-phase. A pre-mitotic spindle is formed during S-phase that matures into a mitotic spindle during G2. During anaphase of mitosis, the spindle is responsible for chromosome segregation between mother cell and bud (reviewed in (Winey and O'Toole, 2001)).

Chromosome attachment to the mitotic spindle happens in stages. Initially, kinetochores are captured by microtubules from one pole (monotelic attachment), then subsequently by microtubules emanating from the opposite pole (amphitelic attachment) that generates tension at kinetochores. Rarely, and in some specific mutants, malorientation can occur. If both sister kinetochores are attached to one pole, attachment is 'syntelic'. In higher eukaryotes, kinetochores can capture more than one microtubule. 'Merotelic' attachment is used to describe both sister chromatids predominantly attached to one pole and one sister attached to a few microtubules from the opposite pole, but not sufficiently to generate tension (Figure 1.4).

Proteins associated with both kinetochores and microtubules include the outer kinetochore DASH complex, microtubule motors and chromosomal passenger protein complexes. Together they form an integral structure that is dynamic and highly regulated to maintain stable kinetochore-microtubule interactions.

Budding yeast Dam1p was shown to interact directly with microtubules and has since been characterised as a component of the outer kinetochore DASH complex. DASH assembles at the kinetochore in a CBF3 and Ndc80p complex dependent manner and interacts physically with members of the Ndc80p and Ctf3p complexes (Cheeseman et al., 2002; Cheeseman et al., 2001; Courtwright and He, 2002; Enquist-Newman et al., 2001; Hofmann et al., 1998; Janke et al., 2002; Jones et al., 2001; Kang et al., 2001; Li et al., 2002). Interestingly, Ndc80p complex mutants lack kinetochore-microtubule attachment but their kinetochores remain intact (Janke et al., 2001), though no direct physical link between the complex and microtubules has been observed. The *dam1-1* mutant identified in a screen as synthetically lethal

with an *mps1* kinase mutant exhibits a 'broken' spindle phenotype (Jones et al., 1999). This and other *dam1* mutants were examined further and also found to suffer from chromosome mis-segregation defects at their restrictive temperature (Cheeseman et al., 2001).

Non-motor proteins found at the outer kinetochore include Stu2p (XMAP215) that has been demonstrated to stabilise microtubules at their plus end and is proposed to interact with MIND (De Wulf et al., 2003; Kosco et al., 2001; van Breugel et al., 2003). Bik1p (CLIP-170) and Bim1p (EB1) may also have a role in kinetochore structure and function, though no specific interaction between the proteins and kinetochore components has been established. Bim1p contributes to kinetochore-microtubule attachment and stability in budding yeast (Schwartz et al., 1997) and has also recently been shown to play a role in efficient sister chromatid cohesion (Mayer et al., 2004). Implicated motor proteins include Cin8p, Kar3p and Kip3p (De Wulf et al., 2003).

As the link between kinetochores and microtubules varies throughout the cell cycle and correct attachment generating tension is integral to chromosome segregation, a mechanism is required for regulating and monitoring the kinetochore-microtubule interaction. Biggins *et al.* (1999) were the first to propose that at least part of this process is regulated by the kinase Ipl1p, the budding yeast Aurora kinase.

1.6 Aurora and Ipl1p

Metazoans possess three Aurora kinases (A, B and C) in comparison to the single Ipl1p in budding yeast. All of them have important roles in cell cycle progression and regulation.

While Aurora A is principally involved in spindle assembly and centrosome maturation and separation, with predominant localisation reflecting these two functions, Aurora C is localised to centrosomes only during telophase and is expressed only in testis (reviewed in REF - Carmena and Earnshaw, 2003).

Aurora B is a convincing orthologue of Ipl1p in higher eukaryotes. Both proteins exist in conserved and well characterised chromosomal passenger complexes that include Aurora B (Ipl1p), INCENP (Sli15p), Survivin (Bir1p) (reviewed in (Adams et al., 2001), in yeast (Cheeseman et al., 2002; Kang et al., 2001; Kim et al., 1999)) and the recently identified Borealin/dasraB (Gassmann et al., 2004a; Sampath et al., 2004). No yeast homologue of Borealin has been identified to date. The passenger complex localisation is concentrated on chromosomal arms in prophase and is transferred to the inner centromere during metaphase and finally to the spindle mid-zone and midbody from anaphase until cytokinesis (reviewed in (Carmena and Earnshaw, 2003) (Adams et al., 2001).

The mitotic functions of Ipl1p ensure correct microtubule-kinetochore attachment (Biggins et al., 1999; Cheeseman et al., 2002), re-orientation of mal-oriented chromatids (Courtwright and He, 2002; Tanaka et al., 2002) and mitotic spindle disassembly (Buvelot et al., 2003). *ipl1* mutants experience massive chromosome mis-segregation as they do not arrest in response to the defects and can subsequently inherit chromosomes in an asymmetric manner (Biggins et al., 1999; Francisco et al., 1994; Kim et al., 1999). Subsequent research by several groups set out to characterise this defect by looking for potential substrates.

Ipl1p in budding yeast is capable of auto-phosphorylation and has also been shown to phosphorylate Sli15p (Kang et al., 2001). In higher eukaryotes, substrates of Aurora B include INCENP (Bishop and Schumacher, 2002), Survivin (Wheatley et al., 2004) CENP-A (Cse4p) (Zeitlin et al., 2001) and Histone H3 (Giet and Glover, 2001; Goto et al., 2002; Hsu et al., 2000). The phosphorylation of other components of the chromosomal passenger complexes has shown to be important for both stimulating the kinase activity of Ipl1p/AuroraB and for its (and the complex') localisation.

As described earlier, Ipl1p has been shown to localise to centromeres during mitosis (reviewed in Carmena and Earnshaw, 2003). Purification of kinetochore complexes

and subsequent identification of sites phosphorylated by Ipl1p *in vivo* in combination with *in vitro* kinase assays has demonstrated that three components of DASH (Dam1p, Spc34p and Ask1p) and Ndc80p are substrates in budding yeast (Cheeseman et al., 2002). In addition, Biggins *et al.* (1999) demonstrated that Ndc10p was also a substrate *in vitro*, though this has not been confirmed *in vivo*.

Mutational analysis of the identified sites within *dam1* showed that alanine site mutants, that can no longer be phosphorylated by Ipl1p, are sensitive to benomyl, a microtubule depolymerising agent, and demonstrate chromosome mis-segregation defects similar to *ipl1* mutants. Aspartate mutants (sites mutated to mimic phosphorylation by Ipl1p) could suppress the temperature sensitive phenotype of an *ipl1* mutant and analysis by microscopy revealed the presence of lagging chromosomes, suggesting defects in kinetochore-microtubule attachment (Cheeseman et al., 2002). These phenotypes are distinct from previous reports on the *dam1-1* mutant (Cheeseman et al., 2001; Jones et al., 1999) as they did not affect spindle structure.

The lack of kinetochore-microtubule attachment seen in *dam1* mutants that mimic constitutive phosphorylation by Ipl1p is consistent with data that Ipl1p promotes microtubule release from mal-oriented chromosomes (Tanaka et al., 2002). These elaborate and elegant experiments demonstrated a requirement for Ipl1p function in establishing sister kinetochore connections to opposite poles of the cell. In the absence of Ipl1p function, sister kinetochores remained attached to a single pole and segregated accordingly during anaphase. Leading on from these conclusions, a role for Aurora B in metazoans, in the correction of improper chromosome attachments has been proposed. The removal of small molecule inhibitors of Aurora B from cells with maloriented chromosomes, allowed correction of chromosome malorientation through microtubule disassembly (Lampson et al., 2004). Interestingly, phosphorylation by Aurora B has recently been shown to control the centromere localisation and activity of the microtubule depolymerase MCAK (Andrews et al., 2004; Lan et al., 2004) (reviewed in (Gorbsky, 2004) (Moore and Wordeman, 2004).

Monitoring of kinetochore-microtubule attachment is performed by the spindle checkpoint. An increasing body of evidence has demonstrated a role for Ipl1p/Aurora B in the spindle checkpoint response.

Work in budding yeast has suggested a role for Ipl1p only in the spindle checkpoint activated by a lack of tension at the kinetochore (Biggins and Murray, 2001; Stern and Murray, 2001). In addition to cohesion defects and attached but unreplicated chromosomes, Ipl1p function was also required for the checkpoint response in an *mtw1-1* (kinetochore protein) mutant that exhibits predominantly mono-oriented chromosomes (Pinsky et al., 2003). However, Ipl1p function is not required in budding yeast for a checkpoint response induced by microtubule depolymerisation (Biggins and Murray, 2001).

Further evidence from experiments performed on higher eukaryote cells and *S. pombe* however also suggest a role for Aurora B (*S. pombe* Ark1) in the spindle attachment checkpoint (Ditchfield et al., 2003; Hauf et al., 2003; Murata-Hori and Wang, 2002; Petersen and Hagan, 2003). Correct localisation of checkpoint components to kinetochores and formation of the mitotic checkpoint complex (MCC) is thought to be essential for a proper checkpoint response (see section 1.9). The evidence from these publications, with the exception of Hauf *et al.*, 2003, demonstrated perturbed Mad2 localisation in the absence of Aurora B/Ark1 function. In addition, where analysed, BubR1 localisation was affected (Ditchfield et al., 2003; Hauf et al., 2003) and MCC formation was abolished (Petersen and Hagan, 2003). Conflicting results of the effect of Aurora B inhibition on CENP-E localisation have been published (Ditchfield et al., 2003; Hauf et al., 2003).

Working in opposition to kinases are phosphatases. Responsible for the removal of phosphate groups from phosphorylated residues, their action is, again, often regulatory but they tend to have a much more diverse set of substrates and are therefore likely to perform multiple roles in the cell. Phosphatases have a catalytic

sub-unit that is regulated by the association of regulatory subunits that can either inhibit or activate their activity and control substrate specificity.

The *GLC7* gene in budding yeast encodes the catalytic subunit of type 1 protein phosphatase (PP1) (Feng et al., 1991). Conditional alleles of this gene when grown at their restrictive temperature induce an arrest characteristic of mutants that cannot pass through the metaphase to anaphase transition as they have activated the spindle checkpoint. Some *glc7* mutants isolated have large buds, replicated DNA, short spindles, and maintain high Cdc28 and H1 kinase activity upon arrest (Andrews and Stark, 2000; Bloecher and Tatchell, 1999; Hisamoto et al., 1994). The arrest is both spindle checkpoint and Ndc10p (kinetochore protein) dependent (Bloecher and Tatchell, 1999; Hisamoto et al., 1994). In addition, microtubule-kinetochore association *in vitro* is reduced in *glc7-10* mutants, inferred to be a result of hyperphosphorylation of Ndc10p by Ipl1p *in vitro* (Biggins et al., 1999). The result fits with the suggestion that PP1 works in opposition to Ipl1p kinase, also demonstrated by the dosage dependent ability of a truncated version to suppress *ipl1* mutants and the partial rescue of *ipl1-1* by *glc7-1* (Francisco et al., 1994). PP1 has also been shown to affect histone H3 phosphorylation (Hsu et al., 2000; Murnion et al., 2001), another substrate of Ipl1p and Aurora B.

In addition to *glc7* mutants indicating a role for PP1 in mitotic progression, mutations in regulatory sub-units (Cdc55p and Rts1p) of PP2A have also demonstrated defects in mitosis (Wang and Burke, 1997).

A *cdc55* mutant was identified in a screen looking for genes involved in the spindle checkpoint, as it was synthetically lethal with a *ctf13* kinetochore mutant (Wang and Burke, 1997). Further analysis showed that abolition of Cdc55p function rendered cells partially checkpoint deficient, they became benomyl sensitive and separated sister chromatids in the presence of nocodazole, but Cdc28 activity was down-regulated (it remains high in a wild-type checkpoint response) though the protein was not degraded (Minshull et al., 1996; Wang and Burke, 1997).

Rts1p was identified in a yeast 2 hybrid assay using Mad3p as bait. Subsequent deletion analysis showed that these cells were sensitive to benomyl, though no further characterisation has been performed (Kevin Hardwick, *pers comm*). Rts1p has also been shown to localise to kinetochore (Gentry and Hallberg, 2002), the predicted source of a spindle checkpoint response.

Functions of the pre-described phosphatases appear to be important in the early stages of mitosis. Cdc14p, however, plays a vital role in mitotic exit (reviewed in (D'Amours and Amon, 2004) when Cdc5p controls its activity by regulating its localisation.

1.7 Polo and Cdc5p

Polo like kinases (PLKs) exhibit multiple roles throughout the cell cycle. Their diverse applications can both inhibit and stimulate the activity of substrates to provide control over cell cycle progression and regulation (reviewed in (Barr et al., 2004). The several PLKs present in metazoans are replaced with one orthologue, Cdc5p in budding yeast.

All PLKs contain a conserved kinase domain at their N-terminus and a regulatory domain containing two polo-boxes at their C-terminus (reviewed in (Barr et al., 2004). The POLO boxes are responsible for mitotic progression, subcellular localisation and substrate recognition. They are known to optimally bind proteins containing the sequence [P/F] [ϕ /P] [ϕ /A] [T/Q/H/M] S [pT/pS] P/X, though several substrates do not fit this optimal sequence and S [pT/pS] P/X has been shown to be sufficient (Elia et al., 2003a; Elia et al., 2003b). Interestingly this recognition motif is very reminiscent of the CDK1 consensus sequence required for substrate phosphorylation.

PLK activity peaks during mitosis and in budding yeast is regulated in-part by degradation during anaphase in an APC/C^{Cdh1}/destruction-box dependent manner

(Charles et al., 1998; Jaspersen et al., 1998; Schwab et al., 2001; Shirayama et al., 1998).

PLKs are involved in mitotic entry through the stimulation of CDK activity to promote biochemical progression into mitosis and subsequently centrosome maturation, spindle assembly and the dissolution of cohesed sister chromatids at the metaphase-anaphase transition by phosphorylation of Scc1p cleavage sites that promotes cleavage by the protease, Esp1 (separase) (Alexandru et al., 2001).

Initially thought to regulate APC/C activity by direct phosphorylation; Rudner and Murray (2000) showed that while Cdc5p could phosphorylate APC/C subunits Cdc16p and Cdc27p *in vitro*, this activity was not conferred *in vivo*. It is now believed that Cdc5p acts through the degradation of APC/C inhibitor Emi1 (see later section) though this protein does not exist in yeast. Cdc5p activity is required for the APC/C activity responsible for the destruction of Clb2p but not Pds1p. The reduction in CDK activity mediated by the destruction of Cdc13 is required for the initiation of septation in *S. pombe*. In *plo1* mutants septation is impaired and when Plo1 is overexpressed septum position can be aberrant (Ohkura et al., 1995).

During late mitosis the action of Cdc5p/PLK controls the localisation of FEAR (Cdc fourteen early anaphase release) component Cdc14p through the phosphorylation of Net1p (Shou et al., 2002; Yoshida et al., 2002). When Net1p is de-phosphorylated it sequesters Cdc14p in the nucleolus, and upon phosphorylation it releases Cdc14p into the nucleus where it can perform its role in mitotic exit (reviewed in (D'Amours and Amon, 2004)). Another way Polo/Cdc5p promotes mitotic exit is through the phosphorylation of Bfa1p in opposition to the actions of the spindle assembly and orientation checkpoints that inhibit the phosphorylation of Bfa1p to delay cell cycle progression in response to a checkpoint stimulus (Geymonat et al., 2003; Hu et al., 2001).

Budding yeast Cdc5p also has two roles in meiosis: first to promote the monopolar attachment of sister chromatids and secondly as a regulator of sister chromatid

cohesion through the phosphorylation of the meiotic cohesin Rec8p to allow its dissociation from chromosome arms, but not centromeres at the first meiotic division and subsequently probably to potentiate cleavage of Rec8p at the second meiotic division as is its role in Scc1p cleavage during mitosis (reviewed in (Cohen-Fix, 2003)).

1.8 APC/C and irreversible cell cycle progress through mitosis

The APC/C is one of two major ubiquitin-ligase complexes that control cell cycle progression. The other is SCF-Skp1/Cullin/F-box protein. The APC/C and SCF are responsible for targeting proteins for destruction via the 26S proteasome. They are E3 ubiquitin ligases, that transfer a ubiquitin chain, in collaboration with an E2 ubiquitin-conjugating enzyme, to a specific substrate. Initially an E1 ubiquitin-activating enzyme and ATP activate ubiquitin allowing the trans-esterification of the molecule to a conserved cysteine of an E2 enzyme. Subsequently the E2 enzyme and E3 ligase can assemble a multi-ubiquitin chain on the substrate. The substrate can now be recognised and degraded by the 26S proteasome, composed of a core 20S subunit and two flanking 19S regulatory subunits, (reviewed in (Jackson et al., 2000)).

While the APC/C functions from early mitosis to late G1 of the next cell cycle it commits the cell to irreversible transitions of the cell cycle by specific degradation of proteins such as the mitotic cyclins and Pds1p. SCF activity is considerably more versatile as it acts at all stages of the cell cycle. Substrates include transcription factors and regulation of proteins involved in cell cycle control eg. Sic1p, that regulates CDK activity in early mitosis and cyclins Cln1p and Cln2p in G1 to allow replication initiation (reviewed in (Jackson and Eldridge, 2002)). SCF recognises a specific sequence in target proteins, DSGXXS. In the case of EMI1 (an APC/C inhibitor not present in yeast, described later) phosphorylation by CDK1 and PLK1 is required before it can be recognised and subsequently degraded (Margottin-Goguet et al., 2003).

In vertebrates, 11 APC/C subunits have been identified, this number increases to 13 in yeast (Yoon et al., 2002). Apc11p the RING finger protein in APC/C that is proposed to interact with Apc2p a cullin-like protein, to mediate interaction between APC/C and the E2 enzyme (Tang et al., 2001b). Four TPR proteins exist in the yeast APC/C, Apc5p, Cdc16p (Apc6), Cdc23p (Apc8) and Cdc27p (Apc3), and their structure suggests a role in protein-protein interactions. Indeed, in budding yeast and humans, TPR proteins are required for interactions between the APC/C and the APC/C activator Cdh1/Hct1p (Schwab et al., 2001; Vodermaier et al., 2003). It is reasonable to predict, due to the presence of conserved IR motifs that mediate the predescribed interaction, that the alternative APC/C activator Cdc20p and the Doc1/Apc10p subunit may also interact with the TPR proteins.

In budding yeast Pds1p, protein kinases (Cdc5p and Hsl1p), regulatory subunits of protein kinases (including Clb2p), Cdc20p, motor, spindle and kinetochore proteins have been identified as substrates of the APC/C. Spatial regulation of substrates for degradation is possible through the localisation of the APC/C to centrosomes, kinetochores and possibly the nuclear periphery where the proteasome can be found (reviewed in (Peters, 2002; Pines, 1999).

At present, substrate recognition is thought to be achieved through selection and interaction with one of two activating proteins Cdc20p or Cdh1p that can be found in association with the APC/C. Cdc20p is thought to recognise proteins through a D-box motif while Cdh1p recognises proteins through D-box motifs and/or KEN boxes (Pfleger and Kirschner, 2000). The first D-box motif was identified in the N-terminus of mitotic cyclins (Glutzer et al., 1991), while the first KEN box was identified in Cdc20p (Pfleger and Kirschner, 2000).

There is also evidence that APC/C substrates can interact with either Cdc20p or Cdh1p independently of the APC/C. Pds1p, an important APC/C substrate, can interact directly with Cdc20 *in vitro* and using the yeast two-hybrid system (Hilioti et al., 2001; Schwab et al., 2001) and Cdh1p can be co-immunoprecipitated with

Cib2p (Schwab et al., 2001). Cdh1p is dispensable in yeast (Schwab et al., 2001) as Sic1p can down-regulate Cdc28p activity in the absence of cyclin destruction.

Conversely, it has recently been reported that, in *Xenopus* egg extracts, repeated D-boxes of cyclin B bind the APC/C directly, in a cell cycle dependent manner, in the absence of either Cdc20p or Cdh1p (Yamanò et al., 2004).

The activity of the APC/C is controlled by the abundance and/or modification of Cdc20, Cdh1 and itself. The APC/C is activated by mitotic phosphorylation of core subunits by Cdk1 and possibly Cdc5, though there remains some controversy (reviewed in (Peters, 2002; Zachariae and Nasmyth, 1999)). In budding yeast mutation of Cdc28p phosphorylation sites on Cdc16p, Cdc23p, Cdc27p reduced Cdc20-APC/C binding *in vivo* (Rudner and Murray, 2000). In fact, Cdc28p activity ensures the inactivity of Cdh1p through G2 and early mitosis, by controlling its phosphorylation, a modification that is removed in a Cdc14p-dependent manner, before Cdh1p can interact with the APC/C from anaphase through to late G1 of the following cell cycle. While Cdh1p levels remain constant through the cell cycle, Cdc20p levels increase from G2/M, as its transcription is up-regulated, until anaphase when it is targeted for destruction by APC/C^{Cdh1}.

In higher eukaryotes a further method of regulation exists in the form of EMI1 (reviewed in (Peters, 2003)). This protein can regulate both APC/C^{Cdc20} and APC/C^{Cdh1} activity in early mitosis (Reimann et al., 2001a; Reimann et al., 2001b) and is required in *Xenopus* embryos for cyclin B accumulation and mitotic entry while its destruction is required for mitotic exit (Reimann et al., 2001a). This function is conserved in human cell lines (Hansen et al., 2004).

The final mode of APC/C regulation is by the spindle checkpoint, a complex mechanism that targets and subsequently inhibits the APC/C activator, Cdc20p (reviewed in (Musacchio and Hardwick, 2002)).

1.9 The Spindle Checkpoint

The spindle checkpoint is a monitoring system designed to ensure that during metaphase of mitosis all chromosomes are correctly attached, via kinetochore/microtubule interactions, to a bipolar spindle before anaphase proceeds and sister chromatids are separated.

Activation of the checkpoint may be a result of spindle or kinetochore defects (Hardwick et al., 1999), monopolar spindles (Hardwick et al., 1999; Weiss and Winey, 1996) or simply mis-aligned chromosomes (Rieder et al., 1995). Two intrinsic methods of activation have been proposed: 1. unattached kinetochores (Rieder et al., 1995) or 2. a lack of tension at kinetochores (Li and Nicklas, 1997).

Mantid spermatocytes contain unpaired sex chromosomes that activate the checkpoint due to a lack of tension at their kinetochores, identified through increased intensity of the 3F3 phospho-epitope at kinetochores. Li and Nicklas (1997) showed that by 'pulling' on chromosomes, using micromanipulation, the tension generated was sufficient to switch off the checkpoint, subsequently reducing the 3F3 phospho-epitope signal at kinetochores.

The importance of kinetochore-microtubule attachment in relieving the spindle checkpoint was highlighted using Ptk1 cells. The progression of these cells through mitosis was visualised by video microscopy. Laser irradiation of unattached kinetochores relieved the spindle checkpoint and demonstrated the requirement of a signal generated at the kinetochore for checkpoint delay (Rieder et al., 1995).

The checkpoint can be activated artificially by over-expression of the checkpoint protein Mps1p in budding yeast (Hardwick et al., 1996) or the introduction of microtubule depolymerising drugs, e.g. nocodazole/benomyl, into the media. The effect of adding nocodazole to metazoans cell is consistent with the effects seen in budding yeast.

Li and Murray (1991) and Hoyt et al. (1991) isolated mutant strains that, in the presence of microtubule depolymerising drugs, were found to be mitotic arrest deficient (*mad*) and budding uninhibited by benzimidazole (*bub*) respectively. Mutant cells proceeded through the cell cycle regardless of their spindle defects; consequently cells had increased rates of chromosome loss and were often aneuploid. In yeast these genes are non-essential for growth under optimal conditions as chromosomes are bioriented from S-phase until the end of mitosis and so do not activate the checkpoint. However, in vertebrates the checkpoint is essential and knockouts of checkpoint components are lethal. The metazoan cell cycle generates unattached sister chromatids every mitosis and requires checkpoint regulation to prevent premature anaphase even in the absence of artificial checkpoint induction.

The original genetic screen for *mad* and *bub* mutants identified the components of the spindle checkpoint Mad1p, Mad2p, Mad3p, Bub1p, and Bub3p (Hoyt et al., 1991; Li and Murray, 1991). The pathway also requires Mps1p, a kinase identified as a spindle checkpoint component by Weiss and Winey (1996) in addition to its role in spindle pole body duplication (Winey et al., 1991).

New proteins required for mitotic checkpoint function in higher eukaryotes are being discovered all the time. Work in *Drosophila* and humans identified two new components Rough Deal/Rod and Zw10/hZw10 respectively (Basto et al., 2000; Chan et al., 2000). These proteins do not have homologues in yeast. The proteins have been shown to form a complex *in vivo* (Chan et al., 2000) that includes another protein Zwilch (Williams et al., 2003). Depletion of either Rod or Zw10, or in a *zwilch* mutant, leads to premature sister separation and bypass of the spindle checkpoint. In human cells, neither Rod nor Zw10 were required for the recruitment of several checkpoint proteins to kinetochores (Chan et al., 2000). Rod has been shown to localise to kinetochores in early mitosis but is redistributed to spindles and predominantly to spindle poles by anaphase (Chan et al., 2000). The microtubule motor protein dynein colocalises during mitosis and mutants in dynein

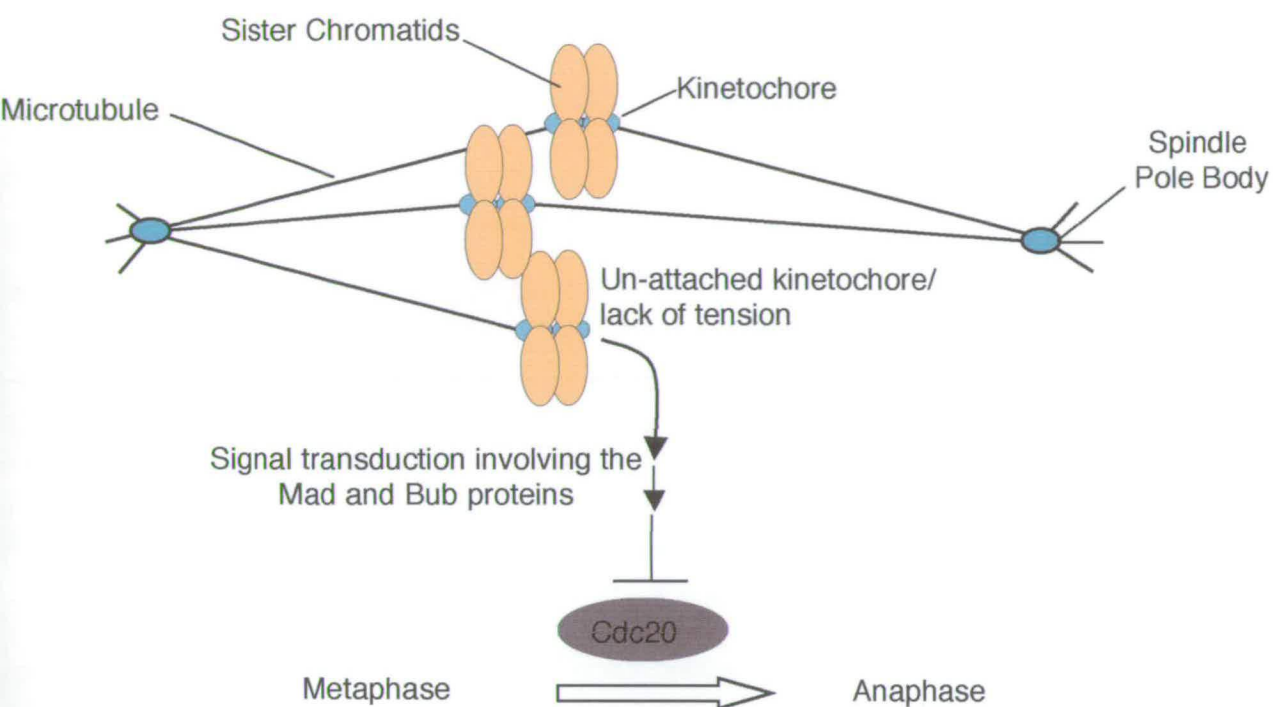
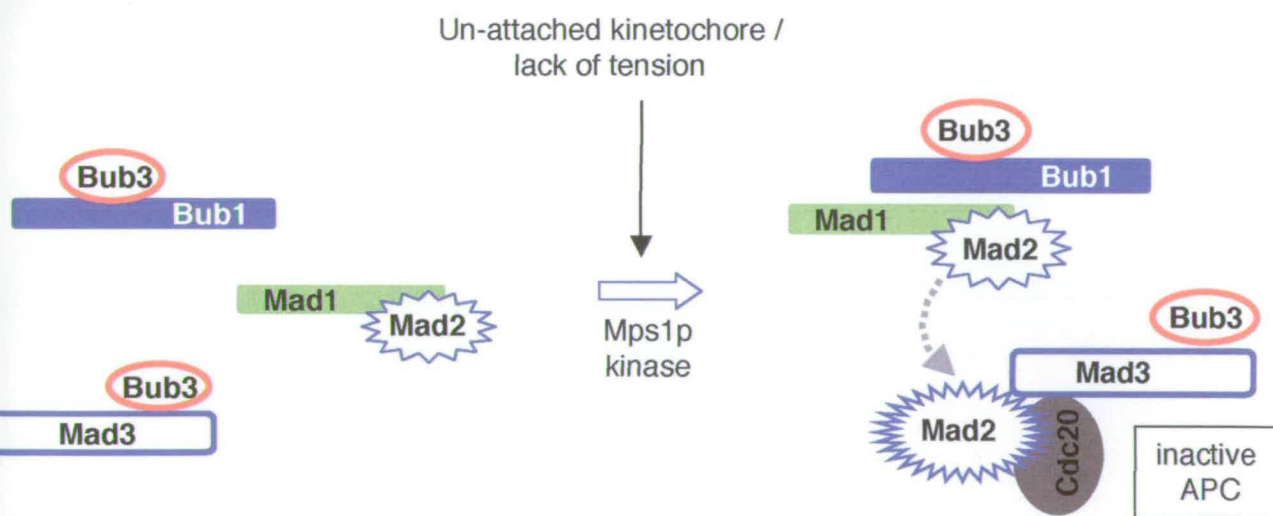
A**B**

Figure 1.5 The Spindle Checkpoint

A Overview of the spindle checkpoint acting at the metaphase-anaphase transition to ensure correct attachment of sister chromatids to the mitotic spindle. **B** Complex formation upon spindle checkpoint activation and the inhibition of Cdc20 that results in an inactive APC/C and prevention of sister chromatid separation.

that prevent its redistribution onto microtubules also prevent the relocalisation of Rod (Wojcik et al., 2001).

To establish an arrest at the metaphase to anaphase transition the spindle checkpoint needs to inhibit APC/C activity, thus preventing sister chromatid separation and cyclin B destruction. This is achieved through inhibiting the target of the spindle checkpoint, Cdc20p, from activating the APC/C (Hwang et al., 1998; Kim et al., 1998).

Metaphase arrest is achieved by four different modes of Cdc20p regulation; direct inhibition through Mad2p-Cdc20p binding, mitotic checkpoint complex (MCC) formation, Cdc20p degradation and finally inhibitory phosphorylation of Cdc20p (reviewed in (Musacchio and Hardwick, 2002).

Structural insights into the mechanism of Mad2p release from Mad1p and subsequent direct Cdc20p binding have identified conformational changes in Mad2p upon Mad1p and Cdc20p binding and identified a common Mad2-binding motif present in Mad1p and Cdc20p (Luo et al., 2000; Luo et al., 2002; Sironi et al., 2002; Sironi et al., 2001).

Inhibition of Cdc20p is also thought to be mediated by binding of the MCC containing Mad2p, Bub3p and Mad3p (Hardwick et al., 2000; Millband and Hardwick, 2002; Sudakin et al., 2001; Sudakin and Yen, 2004). Conflicting *in vitro* data have been presented claiming that Mad2p or BubR1 are capable of inhibiting APC/C activity independently (Fang, 2002; Tang et al., 2001a), though the potency of this inhibition is greatly increased by the presence of the other protein and this may be a requirement for successful inhibition *in vivo*.

Recently it has been proposed that the checkpoint also regulates the levels of Cdc20p present in the cell through APC/C dependent degradation (Pan and Chen, 2004).

Mad1p was identified as a phosphoprotein component of the spindle checkpoint by Hardwick and Murray (1995). The protein is constitutively bound to Mad2p throughout the cell cycle in an unphosphorylated form. In humans, HsMad1 and HsMad2 were found to associate with nuclear pore complexes in interphase (Campbell et al., 2001), this corresponds to the nuclear localisation of Mad1p in *S. cerevisiae* under normal cellular conditions (Gillett et al., 2004; Hardwick and Murray, 1995; Iouk et al., 2002). Preliminary work has also suggested that this localisation pattern is dependent upon a putative bi-partite nuclear localisation signal. In *S. pombe* during a normal mitosis, Mad1p can be found localised to the kinetochores and spindle poles (Karen May, *pers comm.*) though this cannot be detected in budding yeast (Gillett et al., 2004). Upon checkpoint arrest Mad1p, in all eukaryotes studied, is enriched at kinetochores and depends upon several other members of the spindle checkpoint (reviewed in (Musacchio and Hardwick, 2002)). In addition to Mad1, Mad2 can also be found at kinetochores, spindle pole bodies and moving along microtubules during mitosis (Howell et al., 2000). In Ptk2 cells the majority of Mad1 exhibits a stable association at kinetochores but the remainder cycles at $t_{1/2} = 6$ secs during a normal mitosis and half the speed in the presence of nocodazole. At spindle poles, 80% of Mad1 is stably bound and the remainder cycles with $t_{1/2} = 6.6$ seconds while Mad2 cycles at $t_{1/2} = 7.7$ seconds (Shah et al., 2004) (Howell et al., 2004). Upon activation of the checkpoint Mad1p becomes hyperphosphorylated (Hardwick and Murray, 1995; Seeley et al., 1999) and forms a complex with Bub1p and Bub3p, in a Mad2p and Mps1p dependent manner. The interactions between Mad1p and Bub3p/Bub1p require the RLK motif found in its C-terminus and are only observed when the checkpoint is activated (Brady and Hardwick, 2000).

Spindle checkpoint function is totally dependent on the CBF3 complex (Gardner et al., 2001) and two members of the Ndc80p complex, Spc24p and Spc25p (Janke et al., 2001; McClelland et al., 2003). Mutations in these components remove the cells' ability to detect the presence of microtubule depolymerisation, presumably as they form part of the signalling network required for a checkpoint arrest. However, mutations in Ndc80p and Nuf2p do not abrogate a checkpoint response (Janke et al.,

2001) suggesting subtly different roles for these proteins. Disruption of the Ndc80 complex has also been implicated in destabilising interactions between the checkpoint components Mad1 and Mad2 and kinetochores in human cells (DeLuca et al., 2003; Martin-Lluesma et al., 2002; McClelland et al., 2003). Though co-immunoprecipitation experiments in yeast have failed to confirm any stable physical interaction (Michelle Brady, unpublished) an interaction has been shown by yeast two-hybrid using vertebrate proteins (Martin-Lluesma et al., 2002). De Wulf *et al* (2003) recently revealed a biochemical interaction between Mad1p and Nnf1p of MIND.

Sequence analysis of Mad3p has revealed two regions of homology with Bub1p and a conserved N-terminal KEN box. Homology Region I is needed to bind Mad2p and Cdc20p (in a Mad2p dependent manner) upon checkpoint activation, homology region II is necessary and sufficient for Bub3p binding, throughout the cell cycle. Mutations in either of these two regions render cells benomyl sensitive and the spindle checkpoint inactive (Hardwick et al., 2000; Li and Murray, 1991). A new role for Mad3p in Cdc20p turnover has recently been highlighted. Though *mad1* and *mad2* mutants also appeared to stabilise Cdc20p in budding yeast, *mad3* mutants had the most profound effect (Pan and Chen, 2004). The data also demonstrated that only a two-fold increase in the amount of Cdc20p present in the cell was enough to override the checkpoint and render cells sensitive to microtubule depolymerisation, as they were no longer capable of establishing a mitotic arrest (Pan and Chen, 2004).

BubR1, the vertebrate homologue of Mad3p, has a kinase domain at its C-terminus. hBubR1 has been shown to localise to kinetochores (Chan et al., 1999; Jablonski et al., 1998) and specifically bind the kinesin CENP-E (Yao et al., 2000) upon activation of the checkpoint in a homology region II dependent manner (Taylor et al., 1998). In *Xenopus* CENP-E has been shown to activate the kinase activity of BubR1 and upon microtubule capture is required for BubR1 kinase silencing (Mao et al., 2003). hBubR1 is also known to co-immunoprecipitate with three sub-units of the APC/C during mitosis; HsCdc27, HsCdc16 and APC7 (Chan et al., 1999) and

hCdc20/p55 (Wu et al., 2000). Visualisation of Mad3-GFP in *S. pombe* confirmed the result seen in humans and also demonstrated that Bub1p, Bub3p and Mph1p (Mps1p) were required for the correct localisation (Millband and Hardwick, 2002). Cdc20 and BubR1 exhibit biphasic dynamics at unattached kinetochores in Ptk cells. Slower exchanging pools have a $t_{1/2}$ = 23 seconds and 21 seconds respectively and a faster pool with $t_{1/2}$ = 1 second and 3 seconds respectively. The slower exchanging pool of Cdc20 is lost upon attachment and also requires Mad2-Cdc20 interaction (Shah et al., 2004) (Howell et al., 2004). Ditchfield *et al.*, 2003 have demonstrated that BubR1 phosphorylation seen when the spindle checkpoint is active requires AuroraB activity, though to date no direct phosphorylation by AuroraB has been demonstrated.

In metazoans, kinetochore and checkpoint-independent roles for Mad2 and BubR1 in mitotic timing have been demonstrated. Investigation by Meraldi *et al.*, 2004 using siRNA and time-lapse imaging of H2B in HeLa cells confirmed the result and demonstrated that the effects of knocking down Mad2 and BubR1 were a shorter prometaphase, and a very short or no metaphase, though no effect on the length of anaphase was noted. The same group demonstrated that knockdown of Mad1, Bub1 or Bub3 did not affect mitotic timing (Meraldi et al., 2004).

The final two components of the spindle checkpoint, as yet not addressed, are Bub1 and Bub3.

Bub1p is a protein kinase highly conserved between species that is localised to the kinetochore every cell cycle in all eukaryotes analysed and is required for the localisation of Bub3p and Mad3p in *S. pombe* (Millband and Hardwick, 2002; Vanoosthuyse et al., 2004). Homology Region I, conserved between both Bub1p and Mad3p (BubR1) appears to be required for this localisation and removal of this region in *S. pombe* and budding yeast renders cells checkpoint deficient (Vanoosthuyse et al., 2004) (Laura Boyes, *pers comm.*). However, the kinetochore localisation of the protein is not required for other as yet undefined functions of Bub1p as a *bub1* mutant that could no longer localise to kinetochores did not

experience an increased rate of lagging chromosomes as seen in a *bub1Δ* (Vanoosthuyse et al., 2004). Studies on the dynamic localisation of checkpoint proteins in higher eukaryotes showed that Bub1 is stably associated with kinetochores during a normal mitosis and when nocodazole is added (Howell et al., 2004; Shah et al., 2004).

Kinase dead versions of Bub1p in fission yeast maintain a partially competent spindle checkpoint (Vanoosthuyse et al., 2004; Yamaguchi et al., 2003) while a robust checkpoint remains following removal of the kinase domain from the budding yeast protein (Warren et al., 2002). However, experiments in *Xenopus* showed a requirement for Bub1 kinase activity in establishing a checkpoint arrest in response to low (but not high) doses of nocodazole (Sharp-Baker and Chen, 2001). Controversy reigns over possible substrates of Bub1 kinase activity. It has recently been published that HsBub1 can phosphorylate the spindle checkpoint effector Cdc20 (Tang et al., 2004). Though this work shows that the MCC can still be formed and kinetochore localisation of Cdc20 is unaffected, Cdc20 mutated at sites phosphorylated in a Bub1 dependent manner has a dominant negative effect and the spindle checkpoint appears to be partially abrogated (Tang et al., 2004). Work performed in *Xenopus* extracts identified residues within Cdc20 phosphorylated by MAP-kinase. Mutation of these sites, so they could no longer be phosphorylated, resulted in inhibited MCC formation and abrogation of the spindle checkpoint (Chung and Chen, 2003). A Bub1p interaction with Cdc20p in budding yeast has been seen using the yeast two-hybrid assay (Hardwick et al., 2000) but the interaction has not been confirmed *in vivo* under normal physiological conditions. Presently, Bub1p is only known to form a complex with another checkpoint protein, Bub3p via a conserved GLEBS domain that is conserved with Mad3p as well, and Mad1p in mitosis and upon checkpoint activation in budding yeast (Brady and Hardwick, 2000), though this has not been observed in immunoprecipitation experiments in higher eukaryotes. Roberts *et al.*, 1994 had shown that Bub3p is a substrate for Bub1p, but no functional significance of this phosphorylation event has been demonstrated *in vivo*.

Bub3 is a WD-repeat protein with structural, and some functional similarities, to another protein Rae1 (Wang et al., 2001b). Bub3p forms conserved constitutive complexes with Bub1p and Mad3p, and through interaction with the latter, forms part of the MCC with Cdc20p (Fraschini et al., 2001b) (reviewed in (Musacchio and Hardwick, 2002)).

Overexpression of Bub1p (and Bub3p) in budding yeast induces the highest rate of chromosome loss seen in all checkpoint mutants (Warren et al., 2002) though it is thought that these results demonstrate additional functions of these proteins. Data from *S. pombe* suggests that part of this additional function is conferred by the Bub1p kinase domain (Vanoosthuyse et al., 2004).

In humans, aneuploidy contributes to a loss of heterozygosity at various loci, including those of tumour suppresser genes, leading to accelerated cancer progression and tumourigenesis (Orr-Weaver and Weinberg, 1998). Further evidence for the role of the mitotic checkpoint in tumourigenesis has come from mice. Michel et al. (2001) deleted one allele of Mad2 from a mouse line that as a result was seen to have an increased rate of chromosome mis-segregation and the development of lung tumours after long latencies. Chromosomal instability (CIN) resulting in aneuploidy has been identified in 30% of colorectal adenomas and 75% of early cancer and adenocarcinomas (Mihich and Hartwell, 1997). An investigation by Cahill et al. (1998) concluded that mutations of mitotic checkpoint genes in colorectal cancers could be potentially linked with cells exhibiting a CIN phenotype. Of 19 cell lines selected, 2 demonstrated mutations in the checkpoint gene for hBub1. Very recently, germline biallelic mutations in BubR1 have been identified and shown to confer pre-disposition to several cancers (Hanks et al., 2004).

1.10 Other Spindle Associated Checkpoints

Spindle Orientation Checkpoint (SOC)

In these experiments Latrunculin was used to inhibit the polymerisation of actin in *S. pombe*. Use of this drug leaves the mitotic spindle, composed of tubulin, intact but interferes with interactions between astral microtubules and cortical actin. The perturbation of this interaction generates problems with spindle orientation in the cell (Gachet et al., 2004).

On encountering spindles that are not correctly oriented the cell induces a mitotic delay. Initially this was characterised as being independent of APC/C inhibition as Cut2p (securin) and Cdc13p (cyclin B) were grossly degraded, though sister chromatids remained cohesed (Gachet et al., 2001). Upon closer examination of spindle associated Cut2p and Cdc13p it was found that localisation was maintained, presumably as a result of localised APC/C inhibition (Tournier et al., 2004). The mitotic delay experienced relies on a subset of checkpoint proteins, including Bub1p, Mph1p and Mad3p, but independently of Mad2p (Gachet et al., 2001; Rajagopalan et al., 2004; Tournier et al., 2004).

Spindle Position Checkpoint

A second spindle checkpoint pathway involving Bub2p and Byr4p is thought to recognise aberrant spindle (pole) position in budding yeast (Bloecher et al., 2000; Fraschini et al., 1999) and delay exit from mitosis and cytokinesis (Hoyt, 2000). The effect of the pathway is similar to that of the Mad2p dependent spindle checkpoint, in that it prevents mitotic exit, but the signal transducers, Bub2p/Byr4p, suppress the mitotic exit network (MEN) rather than sister chromatid separation and therefore act later in mitosis. Active Tem1p-GTP, activates the MEN proteins that in turn activate Sic1p and Cdh1p via Cdc14p (Burke, 2000; Hoyt, 2000), resulting in the proteolysis of mitotic cyclins, as discussed previously, and exit from mitosis.

Current opinion is that Bub2/Byr 4 force the GTPase Tem1p into its inactive GDP form, disabling the MEN and inducing a mitotic arrest (Hoyt, 2000).

Chapter 2

Materials and Methods

2.1 Supplier information

Chemicals were purchased from the following sources, except where stated otherwise: BDH, Boehringer Mannheim, Fisher, Fisons, Gibco BRL, Melford and Sigma.

Restriction enzymes, DNA polymerases, DNA modifying enzymes and other enzymes used in this work were obtained from the following sources, except where otherwise stated: Boehringer Mannheim, New England Biolabs, Promega, Qiagen, Stratagene.

Reagents for all growth media were obtained from the following sources, except where stated otherwise: Biogene, Difco, Oxoid, Sigma.

2.2 General information

2.2.1 Sterilisation

Solutions and media were typically sterilised by autoclaving at 120°C and 15 pounds/inch² for fifteen minutes. Alternatively, solutions and media were sterilised by filtration. Small volumes were filtered through acrodisc syringe filters (0.45 µm, Gelman Sciences). Large volumes of solutions were filtered through 250 ml or 500 ml filter units (0.45 µm, Nalgene). Glassware was dry sterilised by baking in an oven at 250°C for 16 hours.

2.2.2 Commonly used buffers and solutions

Buffer or Solution	Components
10x TBE	54 gl^{-1} Tris (445mM) 27.5 gl^{-1} Boric acid (445mM) 20 ml^{-1} 0.5M EDTA pH 8.0 (100mM)
1x Transfer Buffer	3.03 gl^{-1} Tris (25mM) 14.4 gl^{-1} Glycine (192mM) 200 ml^{-1} Methanol
5x Running Buffer	30 gl^{-1} Tris (250mM) 144 gl^{-1} Glycine (1.92M) 50 ml^{-1} 10% (w/v) SDS
10x PBS	8 gl^{-1} NaCl (137mM) 0.2 gl^{-1} KCl (2.7mM) 1.44 gl^{-1} Na_2PO_4 (10.1M) 0.24 gl^{-1} KH_2PO_4 (1.76mM)

Table 2.1: Commonly Used Buffers and Solutions

2.3 Micro-biological methods

2.3.1 Bacterial and yeast strains, media and growth conditions

2.3.1.1 Bacterial strains

XL1-Blue electrocompetent cells were used for cloning and Site Directed Mutagenesis. TG1 cells were used for the propagation of plasmid DNA. BL21 cells were used in the production of bacterially expressed GST and intein fusion proteins.

Strain	Genotype	Origin
XL1-Blue	<i>F'</i> ::Tn10 <i>proA</i> ⁺ <i>B</i> ⁺ <i>lacI</i> ^q Δ (<i>lacZ</i>)M15/ <i>recA1 end A1</i> <i>gyrA96 (Nal^r) thi hsdR17 (r_k⁻m_k⁺) glnV44 relA1 lac</i>	Stratagene
TG1	<i>glnV thi-1</i> Δ (<i>lac-proAB</i>) Δ (<i>mcrB-hsdSM</i>)5 (<i>rK-mK-</i>) [<i>F'</i> <i>traD36 proAB lacIqZDM15</i>]	Stratagene
ER2566	<i>F</i> λ <i>fhuA2 [lon] ompT lacZ::T7 gene1 gal sulA11</i> Δ (<i>mcrC-mrr</i>) 114:: <i>IS10 R(mcr-73::miniTn10-TetS)2</i> <i>R(zgb-210)::Tn10 (tetS) end A1 [dcm]</i>	NEB
BL21	<i>E. coli B F dcm ompT hsdS(r_B⁻m_B⁻) gal</i>	Stratagene

Table 2.2: Bacterial Strains

Bacterial Media	Media Components
LB ^ψ	1% (w/v) Bacto-tryptone 0.5% (w/v) Bacto-yeast extract 0.5% (w/v) NaCl pH adjusted to pH 7.2 with %M NaOH

Table 2.3: Bacterial Growth Media

For solid media, 2% (w/v) agar was added prior to autoclaving.

2.3.1.2 Bacterial nutrients and supplements

Supplement	Abbreviation	Stock Solution Solvent and Conc. (mg/ml)	Final Conc. (μg/ml)
Ampicillin (1000x)	Amp	Water 100	100
Kanamycin (250x)	Kan	Water 10	40
Isopropylthiogalactoside	IPTG	Water	1M

Table 2.4: Bacterial Growth Media and Reagents

2.3.1.3 Bacterial growth conditions

Bacteria were typically grown at 37°C on solid LB medium or at 37°C with aeration in liquid LB. To maintain selection for plasmid DNA, transformed bacteria were grown in medium containing the appropriate antibiotic.

2.3.1.4 *Saccharomyces cerevisiae* strains used in this study

All strains are isogenic with W303.

Common name	Strain	MAT	Genotype	Origin
BM13 <i>mad3Δ</i>	RJ10	<i>a</i>	<i>mad3Δ2, BUB3-(myc)₁₃::G418 ura3-1, leu2, 3-112, his3-11, trp1-1, ade2-1, can1-100</i>	Hardwick et al., 2001
<i>mad3Δ</i>	KH173	<i>a</i>	<i>mad3Δ2::URA3 ura3-1, leu2, 3-112, his3-11, trp1-1, ade2-1, can1-100 bar⁻</i>	Hardwick et al., 2001
<i>mad3Δ</i>	KH174	<i>a</i>	<i>mad3Δ2::URA3 ura3-1, leu2, 3-112, his3-11, trp1-1, ade2-1, can1-100 bar⁻</i>	Hardwick et al., 2001
Wild-type <i>bar⁻</i>	KH186	<i>a</i>	<i>bar ura3-1, leu2, 3-112, his3-11, trp1-1, ade2-1, can1-100⁻</i>	Kevin Hardwick
Wild-type	KH34	<i>a</i>	<i>ura3-1, leu2, 3-112, his3-11, trp1-1, ade2-1, can1-100</i>	Rodney Rothstein
<i>cdc26Δ</i>	KH243	<i>a</i>	<i>cdc26Δ::URA ura3-1, leu2, 3-112, his3-11, trp1-1, ade2-1, can1-100</i>	Hwang and Murray, 1997
<i>ipl1-321</i>	NRY38a	<i>a</i>	<i>ipl1-321 ura3-1, leu2, 3-112, his3-11, trp1-1, ade2-1, can1-100</i>	Biggins et al., 1999
<i>glc7-10</i>	PAY700a	<i>a</i>	<i>GLC7:TRP glc7-10:LEU ura3-1, leu2, 3-112, his3-11, trp1-1, ade2-1, can1-100</i>	Andrews and Stark, 2000
<i>mcd1-1</i>	SBY870	<i>a</i>	<i>mcd1-1, his3-11:pCUP1-GFP12-lacI12:HIS3, trp1-1:lacO:TRP1, lys2Δ:PDS1-myc18:LEU2, bar⁻, leu2, 3-112, can1-100, ura3-1, ade2-1</i>	Biggins and Murray, 2001
<i>mcd1-1 ipl1-321</i>	SBY871	<i>a</i>	<i>mcd1-1, ipl1-321, his3-11:pCUP1-GFP12-lacI12:HIS3, trp1-1:lacO:TRP1, lys2Δ:PDS1-myc18:LEU2, bar⁻, leu2, 3-112, can1-100, ura3-1, ade2-1</i>	Biggins and Murray, 2001
<i>GALCDC6</i>	SBY771	<i>a</i>	<i>cdc6:pGAL-UBI-R-CDC6:URA3:ura3-1, his3-11:pCUP1-GFP12-lacI12:HIS3, trp1-1:lacO:TRP1, lys2Δ:PDS1-myc18:LEU2 leu2, 3-112, bar⁻ can1-100, ade2-1</i>	Biggins and Murray, 2001
<i>GALCDC6 ipl1-321</i>	SBY772	<i>a</i>	<i>cdc6:pGAL-UBI-R-CDC6:URA3, ura3-1 his3-11:pCUP1-GFP12-lacI12:HIS3, trp1-1:lacO:TRP1, lys2Δ:PDS1-myc18:LEU2, leu2, 3-112, bar⁻, can1-100, ade2-1</i>	Biggins and Murray, 2001
<i>mcd1-1 mad3Δ</i>	EK12	<i>a</i>	<i>mad3Δ, mcd1-1, his3-11:pCUP1-GFP12-lacI12:HIS3, trp1-1:lacO:TRP1, lys2Δ:PDS1-myc18:LEU2, leu2, 3-112, bar⁻, can1-100, ura3-1, ade2-1</i>	This study
<i>cdc26Δ bub1Δ</i>	MB090	<i>a</i>	<i>bub1Δ::HIS3 cdc26Δ::URA3 ura3-1, leu2, 3-112, his3-11, trp1-1, ade2-1, can1-100</i>	Hardwick et al., 2001
<i>cdc26Δ bub3Δ</i>	MB094	<i>a</i>	<i>bub3Δ::TRP1 cdc26Δ::URA3 ura3-1, leu2, 3-112, his3-11, trp1-1, ade2-1, can1-100</i>	Hardwick et al., 2001
<i>GAL1-10MPS1</i>	KH153	<i>a</i>	<i>GAL1-10MPS1::URA3 ura3-1, leu2, 3-112, his3-11, trp1-1, ade2-1, can1-100</i>	Hardwick et al., 1996
<i>cdc26Δ mad2Δ</i>	KH246	<i>a</i>	<i>cdc26Δ, mad2Δ, ura3-1, leu2, 3-112, his3-11, trp1-1, ade2-1, can1-100</i>	Hardwick et al., 2001
<i>mad2Δ</i>	MB106	<i>a</i>	<i>mad2Δ::LEU2 ura3-1, leu2, 3-112, his3-11, trp1-1, ade2-1, can1-100</i>	Brady and Hardwick, 2000
<i>bub1Δ</i>	MB060	<i>a</i>	<i>bub1Δ::HIS3 ura3-1, leu2, 3-112, his3-11, trp1-1, ade2-1, can1-100</i>	Brady and Hardwick, 2000
<i>bub3Δ</i>	MB003	<i>a</i>	<i>bub3Δ::LEU2 ura3-1, leu2, 3-112, his3-11, trp1-1, ade2-1, can1-100</i>	Brady and Hardwick, 2000
<i>mad3-1</i>	KH45	<i>a</i>	<i>mad3-1 ura3-1, leu2, 3-112, his3-11, trp1-1, ade2-1, can1-100</i>	Hardwick and Murray, 1995
<i>Mad3p-TAP</i>	EK001	<i>a</i>	<i>MAD3-TAP::URA3 ura3-1, leu2, 3-112, his3-11, trp1-1, ade2-1, can1-100</i>	This study

<i>Mad3p-TAP BM13</i>	EK002	<i>a</i>	<i>MAD3-TAP::TRP1 BUB3-(myc)₁₃::G418 ura3-1, leu2, 3-112, his3-11, trp1-1, ade2-1, can1-100</i>	This study
GFP chromosomes	SBY215	<i>a</i>	<i>his3-11::pCUP1-GFP12-lacI12:HIS3, trp1-1::lacO:TRP1ura3-1, leu2, 3-112, bar-, ade2-1, can1-100</i>	Biggins et al., 2001
<i>mad3Δ</i> GFP chromosomes	EK13	<i>a</i>	<i>mad3Δ2::URA3 ura3-1, his3-11::pCUP1-GFP12-lacI12:HIS3, trp1-1::lacO:TRP1, bar-, ade2-1, can1-100, leu2, 3-112</i>	This study
<i>cdc23-1</i>	ADR719A	<i>a</i>	<i>cdc23-1 ura3-1, leu2, 3-112, his3-11, trp1-1, ade2-1, can1-100</i>	Rudner et al., 2000
<i>cdc16-1</i>	ADR34	<i>a</i>	<i>cdc16-1 ura3-1, leu2, 3-112, his3-11, trp1-1, ade2-1, can1-100</i>	Rudner et al., 2000
<i>cdh1Δ</i>	331	<i>a</i>	<i>cdh1Δ ura3-1, leu2, 3-112, his3-11, trp1-1, ade2-1, can1-100</i>	Rudner et al., 2000
<i>cdc20-1</i>	KH112	<i>a</i>	<i>cdc20-1::LYS,cdc20-1::URA3 ura3-1,ura3-1 leu2,3-112,leu2,3-112 his3-11,his3-11 trp1-1, trp1-1 ade2-1,ade2-1 can1-100, can1-100</i>	Hwang et al., 1998
GALCDC20	KH319	<i>a/α</i>	<i>cdc20Δ::LEU2 GALCDC20::TRP1 ura3-1, leu2, 3-112, his3-11, trp1-1, ade2-1, can1-100</i>	Hwang et al., 1998
<i>mad3Δ</i> myc18-CDC20	LB4	<i>a</i>	<i>mad3Δ2::URA3 (myc)₁₈-CDC20::LEU2 ura3-1, leu2, 3-112, his3-11, trp1-1, ade2-1, can1-100</i>	Laura Boyes
Myc18-CDC20	LB3	<i>a</i>	<i>(myc)₁₈-CDC20::TRP1 ura3-1, leu2, 3-112, his3-11, trp1-1, ade2-1, can1-100</i>	Laura Boyes
<i>mad1Δ</i> myc18-CDC20	KH302	<i>a</i>	<i>(myc)₁₈-CDC20::TRP1 mad1Δ::URA3 ura3-1, leu2, 3-112, his3-11, trp1-1, ade2-1, can1-100</i>	Kevin Hardwick
<i>mad2Δ</i> myc18-CDC20	KH340	<i>a</i>	<i>(myc)₁₈-CDC20::TRP1 mad2Δ::URA3 ura3-1, leu2, 3-112, his3-11, trp1-1, ade2-1, can1-100</i>	Kevin Hardwick
<i>bub3Δ</i> myc-18CDC20	KH345	<i>a</i>	<i>(myc)₁₈-CDC20::TRP1 bub3Δ::LEU2 ura3-1, leu2, 3-112, his3-11, trp1-1, ade2-1, can1-100</i>	Kevin Hardwick
<i>bub1Δ</i> myc18-CDC20	LB1	<i>a</i>	<i>(myc)₁₈-CDC20::LEU2 bub1Δ::HIS3 ura3-1, leu2, 3-112, his3-11, trp1-1, ade2-1, can1-100</i>	Laura Boyes

Table 2.5 *Saccharomyces cerevisiae* strains used in this study

2.3.1.5 *Saccharomyces cerevisiae* growth media

Growth Media	Media Components
YPD(A)	1% w/v Yeast Extract 2% w/v Bacto-peptone 2% w/v Glucose (0.003% w/v Adenine sulphate)
Sporulation Media	0.3% w/v Potassium Acetate 0.02% Raffinose
Minimal media (YMM)	0.67% w/v Yeast Nitrogen Base w/o amino acids 2% w/v Glucose 1 Pellet Sodium Hydroxide
Selective media ^ψ	YMM Plus amino acids required from: 90mg/l each of Adenine, Tryptophan, Histidine, Lysine, Methionine, Uracil 220mg/l Leucine 87mg/l each of Cysteine, Isoleucine, Serine, Alanine, Glutamic acid, Arginine, Threonine, Glutamine, Tyrosine, Asparagine, Glycine, Phenylalanine, Aspartic acid, Proline, Valine
YEP GAL/RAFF	1% w/v Yeast Extract 2% w/v Bacto-peptone 2% w/v Galactose 2% w/v Raffinose 0.003% w/v Adenine sulphate
YEP RAFF	1% w/v Yeast Extract 2% w/v Bacto-peptone 2% w/v Raffinose 0.003% w/v Adenine sulphate

Table 2.6 *Saccharomyces cerevisiae* media used in this study

For solid media, 2% (w/v) agar was added prior to autoclaving.
Galactose and Raffinose were substituted for glucose where required.

2.3.1.6 *Saccharomyces cerevisiae* supplements

Supplement	Stock solution	Working Concentration
Benomyl	30 mg/ml in DMSO	As stated in text
Nocodazole	10 mg/ml in DMSO	15µg/ml unless stated otherwise
Hydroxyurea	100 mg/ml in dH ₂ O	5mg/ml
Alpha mating Factor	10 mg/ml in DMSO	10µg/ml in <i>BAR+</i> , 1µg/ml in <i>bar-</i> strains

Table 2.7 Supplements to media for *Saccharomyces cerevisiae* growth

2.3.1.7 *Saccharomyces cerevisiae* growth conditions

Wild type *S. cerevisiae* were grown at 30°C either upturned on solid media or in liquid media, shaking to provide aeration (180-200rpm). Strains with a temperature sensitive phenotype were typically grown at a permissive temperature of 23°C and a restrictive temperature of 37°C. To maintain selection for plasmid DNA and/or for auxotrophic markers inserted on the genome, cells were grown on selective media lacking the appropriate amino acid(s).

2.3.1.8 Storage of bacteria and yeast strains

Strains were stored for short periods on solid media at 4°C and longer term at -80°C in liquid YPD supplemented with 15% v/v glycerol.

2.3.2 Transformations

2.3.2.1 Preparation of chemically competent *E. coli* cells

100ml of DH5 α (GIBCO, BRL) *E. coli* cells in LB liquid medium were grown at 37°C to OD_{600nm}=0.5-0.7. Cells were then placed on ice for 10-15 minutes after which they were subjected to centrifugation for 5 minutes at 5000 rpm (4°C, Beckman JLA 10.500 rotor). Cells were resuspended, gently, on ice in 20ml of 0.1M CaCl₂ (pre-chilled) then collected by centrifugation for 5 minutes at 4000rpm. Cells were then resuspended as before in 10ml of 0.1M CaCl₂ buffer (pre-chilled). Glycerol was added to 20% w/v and cells measured into 100 μ l aliquots and stored at -80°C.

2.3.2.2 Transformation of chemically competent cells

Competent cells were thawed on ice. Typically, 50 μ l of cells were added to up to 100ng of DNA for transformation. The *E. coli*/DNA mixture was incubated on ice for 10 minutes then transferred, for heat shock, to a 37°C waterbath for 5 minutes. 200 μ l of LB media was added and the cells were allowed to recover, shaking (200rpm) at 37°C, without selection, for a minimum of 30 minutes. Cells were then plated onto LB agar supplemented with the appropriate antibiotic required for selection and incubated at 37°C.

2.3.2.3 Transformation of XL-1 Blue electro-competent *E. coli*

XL-1 Blue electro-competent *E. coli* (Stratagene) were purchased electro-competent. 40-50 μ l of cells were thawed slowly on ice then added to DNA for transformation. The mixture was then transferred to a pre-chilled electroporation cuvette (0.2cm electrode gap) on ice. Electroporation was performed using a BioRad Gene PulserII at 200 Ω resistance, 25mF capacitance and 1.7kV voltage. A time constant between 4-5 milliseconds was aimed for. Immediately following

electroporation, 200µl of LB medium was added and cells were allowed to recover, shaking, (200rpm) at 37°C without selection for a minimum of 30 minutes. Cells were then plated onto LB agar supplemented with the appropriate antibiotic required for selection and incubated at 37°C.

2.3.2.4 Lithium acetate transformation of *Saccharomyces cerevisiae*

(Ito et al., 1983)

A 50 ml culture of the strain to be transformed, OD₆₀₀ of 0.5-0.8, was harvested by centrifugation at 2500rpm for 2.5 minutes, washed in 1ml LiOAc mix harvested, then washed again, harvested and resuspended in 500µl LiOAc mix.

1-2.5µg DNA plus 15µl of boiled salmon sperm carrier DNA (10mg/ml) were added to a 100µl of the LiOAc yeast cell mix. 700µl of PEG mix was then added and the mixture incubated at room temperature for 30 minutes.. The transformation mix was then heat shocked at 42°C for 15 minutes, unless the strain was temperature sensitive., pelleted by centrifugation at 8000rpm for 30 seconds, the supernatant removed and the pellet resuspended in 200µl of YPDA. The transformation was plated onto the relevant selective media and incubated at a permissive temperature until colonies were formed. Transformants were re-streaked onto selective media prior to further use.

Reagents:

Reagent	Constituents
5M LiOAc	
1M Tris pH7.4	
500mM EDTA	
LiOAc mix	100mM LiOAc 10mM Tris pH7.4 1mM EDTA Filter sterilised
PEG mix	40% PEG 2000 100mM LiOAc 10mM Tris pH7.4 1mM EDTA Filter sterilised

Table 2.8 Reagents used in lithium acetate transformation of yeast

2.3.3 *Saccharomyces cerevisiae* cell cycle arrests**2.3.3.1 G1 arrest by growth in alpha mating pheromone factor**

S. cerevisiae MATA cells were grown to mid-log phase $OD_{600nm} = 0.5 - 0.8$ in liquid YPDA. Cells were then harvested by centrifugation for 3 minutes at 2500rpm and resuspended in 1/10th initial volume of liquid media. Alpha-factor mating pheromone was then added to *bar*⁻ strains at a final concentration of 1 μ g/ml and *BAR*⁺ strains at a

final concentration of 10 μ g/ml. *BAR* encodes a protease that breaks down alpha-factor. The use of *bar*- cells reduced the amount of alpha-factor required for G1 arrest as cells were more sensitive to the peptide. Cells were then grown at a permissive temperature for 3 hours after which cells were collected by centrifugation for 3 minutes at 2500 rpm. For release from an alpha-factor arrest cells were washed twice in fresh media and resuspended in a volume where the OD_{600nm} = 0.5 - 0.8 unless several samples were to be collected and alpha-factor was added back where they were resuspended again in 1/10th the initial volume of liquid media.

2.3.3.2 S-phase arrest by growth in hydroxyurea

S. cerevisiae cells were grown to mid-log phase OD_{600nm} = 0.5 - 0.8 in the appropriate media for strain propagation. Hydroxyurea (HU) was added at a final concentration of 5mg/ml. The cells were then grown at the required temperature (see specific experiments) for 2 hours.

2.3.3.3 Mitotic arrest by growth in nocodazole

S. cerevisiae cells were grown to mid-log phase OD_{600nm} = 0.5 - 0.8 in the appropriate media for strain propagation. Nocodazole was added at a final concentration of 15 μ g/ml for arrest at 23°C or 20 μ g/ml for arrest at 37°C. The cells were then grown at the required temperature (see specific experiments) for 2 hours unless otherwise stated.

2.3.4 Mating of *Saccharomyces cerevisiae* haploid strains

S. cerevisiae strains of opposite mating types (a and α) were streaked onto YPDA and grown overnight at their permissive temperature. The following day, strains were mixed together, to mate, in a drop of sterile dH₂O water on a YPDA plate. The mating

mix was incubated at a permissive temperature 23-30°C for 4 hours. Either diploid yeast cells were identified as two cells that had formed a schmoo and were picked using a micromanipulator (Singer Instruments MSM System Series 300) or the mating mix was streaked onto selective media to allow growth of only diploid strains. In both instances cells were left to grow at their permissive temperature until colonies were visible, approximately 2 days.

The colonies were tested for diploid status by mating with strains 604 (mat a) and 605 (mat α). Following mating, the mixtures were replica plated onto minimal media plates. Diploid strains from the original cross were identified by their lack of ability to grow on minimal media as they were unable to mate with the mating type tester strains. True diploids were subsequently grown in liquid sporulating media at room temperature for 3-7 days.

2.3.5 Tetrad dissection

The cells were then examined by light microscopy for sporulation and tetrad formation. 1ml of the sporulated culture was centrifuged at 8000rpm for 1 minute and resuspended in 190 μ l of sterile dH₂O and 10 μ l β -gluco-uronidase (1700 Units/ml) was added and mixed gently. The cells were incubated at room temperature for 10-15 minutes until the walls of the tetrad appeared to be digested. 20 μ l of tetrad mix was dripped onto YPDA and the tetrads were dissected using a Singer Instruments MSM System Series 300 micromanipulator and grown at a permissive temperature until colonies were visible. The tetrads were replica plated onto selective plates to identify and isolate the required strain genotype. The mating type of spores was tested by their ability to mate with either 604 (mata) or 605 (mat α).

2.3.6 Benomyl sensitivity assay

Strains/transformants were freshly streaked out onto selective plates and incubated upturned at a permissive temperature overnight. Small amounts of the streak outs were resuspended in 200µl of sterile dH₂O in the first row of a 96-well plate. The cells were diluted 1:10 and 1:100 into the second and third rows of the plate with gentle mixing. The serially diluted cells were stamped onto YPD plates supplemented with 0, 10, 12.5 and 15µg/ml Benomyl using a sterile stamper. The plates were incubated upturned at 23°C for 2-3 days. Growth was then analysed and compared to relevant controls (see individual experiments).

2.4 Nucleic acid methods

2.4.1 Plasmids used in this study

Name	Further Information	Source
pKYB1	Intein fusion protein expression vector	NEB
pM3R1intein	pKYB1 plus Region I of <i>MAD3</i> amplified by PCR from pKH535 using primers IN1A and IN1B. Insert and vector cut with <i>Sall</i> and <i>EcoRI</i> .	This study
pM3R2intein	PKYB1 plus Region II of <i>MAD3</i> amplified by PCR from pKH535 using primers IN2A and 3M3intein. Insert and vector cut with <i>Sall</i> and <i>EcoRI</i> .	This study
pM3intein	PKYB1 plus <i>MAD3</i> amplified by PCR from pKH535 using primers IN1A and 3M3intein. Insert and vector cut with	This study

	<i>Sall</i> and <i>EcoRI</i>	
pM3IS337A	PKYB1 plus <i>mad3</i> with serine 337 mutated to alanine	This study
pKH535	Ycplac22 backbone plus <i>MAD3</i> and it's promoter	Kevin Hardwick
pM3S337A	pKH535 with serine 337 mutated to alanine by multi-SDM using primer M3S337A	This study
pM3S303A	pKH535 with serine 303 mutated to alanine by SDM using primers M3S303A and M3S303AR	This study
pM3S303/337A	pKH535 with serines 303 and 337 mutated to alanine. Derived from pM3S303A mutated by multi-SDM using primer M3S337A to create double mutant.	This study
pM3S303D	pKH535 with serine 303 mutated to aspartate	Najma Rachidi
pM3S337D	pKH535 with serine 337 mutated to aspartate	Najma Rachidi
pM3S303/337D	pKH535 with serines 303 and 337 mutated to aspartate	Najma Rachidi
pM3S380A	pKH535 with serine 380 mutated to alanine by multi-SDM using primer M3S380A.	This study
pM3S222/229/380A	pKH535 with serines 222, 229 and 380 mutated to alanine by multi-SDM using primers M3S380A and M3ST222/9AA.	This study
pM3S380D	pKH535 with serine 380 mutated to	This study

	aspartate by multi-SDM using primer M3S380D.	
pM3S222/229/380D	pKH535 with serines 222, 229 and 380 mutated to aspartate by multi-SDM using primers M3S380D and M3ST222/9DD.	This study
pKH535KEN30AAA	pKH535 with lysine 30, glutamate 31 and asparagine 32 mutated to alanine by multi-SDM using primer M3KEN31AAA .	This study
pKH535KEN296AAA	pKH535 with lysine 296, glutamate 297 and asparagine 298 mutated to alanine by multi-SDM using primer M3KEN297AAA.	This study
pKH535KEN30/296AA	pKH535 with lysines 30 and 296, glutamates 31 and 297 and asparagines 32 and 298 mutated to alanine. Created by replacing a <i>HindIII/EcoRI</i> fragment in pKH535KEN30AAA with a <i>HindIII/EcoRI</i> fragment from pKH535KEN296AAA to create the double mutant.	This study
pBS1479	<i>TRP</i> marked TAP plasmid used as a template for generation of Mad3p-TAP	Casparay et al, 1999
pBS1539	<i>URA</i> marked TAP plasmid used as a template for generation of Mad3p-TAP	Casparay et al, 1999

Table 2.9 Plasmids used in this study.

2.4.2 Phenol-chloroform extraction

Nucleic acids were purified away from protein in aqueous solution by adding an equal volume of phenol:chloroform:isoamyl alcohol (25:24:1) and vortexing for 10 seconds. The mixture was then centrifuged at 13,000 RPM for 5 minutes. The upper (aqueous) phase was then removed and placed in a new tube.

Reagents

Phenol:chloroform:isoamyl alcohol (24:25:1)

2.4.3 Precipitation of nucleic acids

Nucleic acids were precipitated from solution by the addition of 1/10th volume of solution containing nucleic acids to be purified 3M NaOAc, pH5.2 plus 2.5 volumes of 95% ethanol. The mixture was then placed on ice or at -20°C for 15 minutes. The nucleic acids were pelleted by centrifugation at 13,000 rpm for 15 minutes at 4°C. The ethanol/NaOAc mixture was then removed before the pellet was washed in 250µl 70% ethanol and centrifuged again at 13,000 rpm for 5 minutes at 4°C. The 70% ethanol was removed and the pellets left to air dry and resuspended in an appropriate volume of TE or Tris-Cl pH8.5.

Reagents

3M NaOAc, pH5.2

Ethanol – 95% and 70% ice-cold stocks

TE

2.4.4 Plasmid mini-prep by spin column

Plasmid DNA was prepared using a mini-prep kit (Qiagen™), following the manufacturer's instructions from 1.5ml of *E. coli*.

2.4.5 Agarose gel electrophoresis

Agarose gel electrophoresis of DNA fragments was typically performed with 0.8-1.5% (w/v) agarose gels with TBE buffer used as a diluent, 3µl/100ml ethidium bromide was added immediately before pouring. 'Blue juice' was added to approximately 10% of sample volume before loading. The gels were run in TBE buffer at 90 – 120 V, depending on gel size. A 1kb DNA ladder (Gibco BRL). Fragments were visualised using a UV transilluminator.

Reagents

Agarose – General purpose

Ethidium bromide – 10mg/ml

Blue Juice – 0.25% (w/v) bromophenol blue, 30% (v/v) sucrose

TBE buffer

2.4.6 Extraction of DNA from agarose gels

DNA was isolated from agarose using a gel purification kit (Qiagen™).

2.4.7 Restriction digestion of DNA

Digests were performed in volumes of 20-125µl in the buffers provided by the manufacturer to accompany the enzyme(s) used. 5 units of enzyme were used per 1µg

of DNA digested. The digest was incubated at the temperature recommended by the manufacturer, usually 37°C, for at least one hour.

Reactions were 'cleaned' prior to use in any subsequent enzymatic reaction using the QIAquick PCR purification kit (Qiagen) according to the manufacturer's instructions.

2.4.8 Amplification of DNA using the Polymerase Chain Reaction

2.4.8.1 Oligonucleotides used in this study

Primer Name	Primer Sequence (5' – 3')
IN1A	GCGAGTCGACATGAAAGCGTACGCAAAGAAACG
IN1B	CAGGAATTCTTGATTTGCAAGCTCTAGTCTATTGAC
IN32A	GCGAGTCGACATGAATGGCACATCAAGTGACGTC
3M3INTEIN	CAGGAATTCACGCTGTGGTGGGTACGATATG
3.16	TGGGTCGCTTAATGCAGGG
3.17	GAATACATAAAGTGGCTGAAC
3.18	GCCTTAGTCTCCAAGTCG
3.20	CTACCACCTTTAGATTCCTC
3.23	GTCTCAGTGCTTCGTCCCTT
3.34	GAAAAATTTCAATATGCCGTG
3.2	ATTCATTCATGGAAAGCAGAG
3.7	GACTTAAAGGCAGAAAGGAAC
M3S303A	GAAAACAACAACCTTCGAATAGCATTGCTAGAAGCAAATA CC
M3S303AR	GGTATTTGCTTCTAGCAATGCTATTCGAAGGTTGTTGTTTC
M3S337A	CTACCGATCTTTAGAGATGCTATAGGTAGAAGTGACCC
M3S380A	GGTGGTAGACTAGAATTTGCGCTAGAAGAAGTCTTGCCA

M3SS222/9A A	GCTAGGAAATGAAATAGCGATGGACTCATTAGAGTCTGCA GTACTTGGGAAAAC
M3S380D	GGTGGTAGACTAGAATTTGACCTAGAAGAAGTCTTGGCA
M3SS222/9D D	GCTAGGAAATGAAATAGACATGGACTCATTAGAGTCTGAC GTACTTGGGAAAAC
M3KEN30	GAAGAAATCGAAACTCAAGCAGCAGCCATTCTTCCCCTGAA GG
M3KEN296	CTTAAAGGCAGAAAGGAACGCAGCAGCCAACCTTCGAATA TCATTG
M3TAP1	AAAATTCTGAGATCATTTTCAGATGATGACAAGTCGAGTTC GTCTTTAATATCGTACCCACCACAGGCTTCCATGGAAAAGA GAAG
M3TAP2	AATAAAAAGTCGGCCGGTCGATGTGTTTACGATTGGCCAG TATACTTACTCATTTCATGGGATTAGTTTTATTTACGACTCAC TATAGGG

Oligonucleotide primers were synthesised by Sigma and stored at -20°C after resuspension in 1 ml dH_2O . Those to be used in SDM or multi-SDM reactions were PAGE purified and 5' phosphorylated. The oligonucleotides used in the generation of TAP-tagged Mad3p were HPLC purified.

2.4.8.2 Preparation of yeast genomic DNA

1ml of a 5ml overnight of yeast grown in liquid culture was harvested by centrifugation at 2,5000RPM for 2 minutes then resuspended in 200 μl of yeast 'crunch' buffer (2% v/v Triton X-100, 1% w/v SDS, 100 mM NaCl, 10mM Tris-Hcl pH8, 1mM EDTA), 200 μl of phenol:chloroform:isoamyl alcohol (25:24:1). Glass beads equal to pellet volume were added and samples were subject to bead-eating for 1 minute then

centrifuged for 5 minutes at 13,000 RPM. The upper, aqueous, phase was removed and the DNA recovered by ethanol precipitation. DNA pellets were resuspended in TE.

2.4.8.3 Polymerase Chain Reaction (PCR)

A typical PCR reaction mix was set up as follows:

Template DNA	10-30ng plasmid DNA/ 10-500ng yeast genomic DNA
Oligonucleotide primer 1	0.5 μ M
Oligonucleotide primer 2	0.5 μ M
1x dNTPs	
1x PCR buffer	
DNA polymerase	1 μ l/100 μ l reaction
Sterile distilled water	To desired final volume

Colony PCR from bacteria was possible by replacing 'template DNA' with cells added to the reaction mix.

dNTPs (2.5mM dATP, dCTP, dGTP, dTTP) and PCR buffer were stored until use as a 10x stock at -20°C. The polymerase used was dependent on the eventual use of the amplified product. For diagnostic purposes Taq DNA polymerase was used. For applications in which a higher fidelity was required, Pfu polymerase (Stratagene) was used.

PCR reactions were carried out in a PTC-200 gradient cycler (MJ Research).

A typical three-step program followed the cycling program below

Initial template denaturation 95°C for 1 minute

Typically followed by 30 cycles of:

Denaturation	95°C for 30 seconds
Annealment	Td°C (commonly 55°C) for 30 seconds
Extension	72°C for 1min/kb of product synthesised

One final step of 72°C for 5 minutes

2.4.8.4 PCR mediated cycle sequencing of DNA

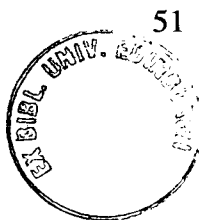
Reactions were performed using dRhodamine terminator cycle sequencing kit (Perkin Elmer). Reactions were set up as follows:

Template (plasmid) DN	50ng
Primer	1.6pmol
Terminator reaction mix	4µl
dH ₂ O	To 10µl final volume

25 cycles of the program below were performed

Step 1	96°C for 30 seconds
Step 2	50°C for 15 seconds
Step 3	60°C for 4 minutes

After PCR reactions were made up to 20µl total volume and given to the departmental sequencing service (ICMB, University of Edinburgh) where they were run on an ABI PRISM 377 DNA sequencer. Sequences produced were analysed using Sequencher Version 4.0 (Gene Codes Corporation, USA).



2.4.9 PCR mediated site directed mutagenesis

2.4.9.1 Single-site directed mutagenesis

A typical reaction was made up as follows:

Template DNA	10ng
Forward primer	125ng
Reverse primer	125ng
Buffer	5 μ l (of 10x stock)
dNTPs	5 μ l (of 10x stock)
QuikSolution (Stratagene)	3 μ l
PfU polymerase	1 μ l
dH ₂ O	To a final volume of 50 μ l

Cycling parameters were as follows:

Initial denaturation of template:

95°C 1 minute

18 cycles of:

95°C 50 seconds

60°C 50 seconds

68°C 2 minutes/kb of plasmid length

Final elongation:

68°C 7 minutes

2.4.9.2 Multi-site directed mutagenesis

Multi-site directed mutagenesis was performed using a kit provided by Stratagene.

A typical reaction was made up as follows:

Template DNA	100ng
Each primer	100ng
Buffer	5 μ l
dNTPs	5 μ l
Quik Solution	1.5 μ l
QuikChange™ Multi enzyme blend	2 μ l
dH ₂ O	To a final volume of 50 μ l

Cycling parameters were as follows:

Initial denaturation of template:

95°C 1 minute

30 cycles of:

95°C 1 minute

55°C 1 minute

65°C 2 minutes/kb of plasmid length

To the mutagenesis reactions (single and multi-SDM) 1 μ l of DpnI restriction enzyme was added and incubated at 37°C for four hours. The reactions were then ethanol precipitated and the cut DNA suspended in 5 μ l TE. 2.5 μ l of the digested DNA was

then transformed into XL-1 Blue electro-competent cells as per the manufacturers instructions.

The reactions were then digested and transformed as per single-site directed reactions.

2.4.10 Purification of PCR products

PCR products were purified from excess oligonucleotide primers, unincorporated dNTPs, polymerase and buffer salts using the QIAquick (Qiagen) PCR purification kit as per the manufacturers instructions. The purified product was typically eluted in 30 μ l of the elution buffer provided and stored at -20°C.

2.4.11 Ligation of DNA molecules

The total volume of ligation reactions was typically 20 μ l and set up as follows:

Vector DNA	100ng plus
Insert DNA	three times this amount (with respect to the number of moles)
Ligation buffer	2 μ l
ATP	1mM
T4 DNA ligase	2 arbitrary units
dH ₂ O	To a final volume of 20 μ l

Reactions were incubated at room temperature (approximately 24°C) overnight. Half the reaction was then transformed into XL1-blue bacteria (Stratagene) as per the manufacturers instructions.

2.5 Protein methods

2.5.1 Crude total cell lysate preparation

Crude samples for analysis by SDS-PAGE and Western blotting were prepared as follows. Cells were harvested by centrifugation at 2500 RPM for 2.5 minutes, washed once with water and pelleted again by centrifugation at 8000 RPM for 30 seconds. Pellet mass was determined by weight. 300-500 μ l (volume added to reflect pellet mass) of SDS sample buffer containing protease inhibitors, and phosphatase inhibitors if required, was added depending on pellet size. An equal volume (to pellet) of glass beads (425-600 μ m) was then added and samples were subjected to ribolysing for 20 seconds at setting 4 (Nybaid Ribolyser). Samples were then centrifuged at 13,000 RPM for 5 minutes at 4°C.

Reagents:

Reagent (stock concentration)	Final concentration
10% w/v SDS	2 %
1M Tris pH6.8	80 mM
70% v/v Glycerol	10 % v/v
0.5M EDTA	10 mM
Bromophenol blue	0.01g
Water	To final volume
1M DTT	0.1 M
1M NaF	0.05 M
0.1 M Pefabloc	0.05M
120 mM Na pyrophosphate	2 mM
0.1 mM Microcystein	0.1 μ M

2.5.2 Total cell lysate preparation for use in (co-) immunoprecipitation

Cells were harvested by centrifugation at 2500RPM for 2.5 minutes, washed once with water and pelleted again by centrifugation at 8000 RPM for 30 seconds. Pellet mass was determined by weight. 300-500 μ l (volume added to reflect pellet mass) of lysis buffer containing protease inhibitors, and phosphatase inhibitors if required, was added. An equal volume (to pellet) of glass beads (425-600 μ m) was then added and samples were subjected to ribolysing for 20seconds at setting 4 (Nybaid Ribolyser). Samples were then centrifuged at 13,000 RPM for 5 minutes at 4°C. The supernatant was removed and spun twice more to produce a clarified extract. DTT was added at this point to a final concentration of 1mM. A 50 μ l sample was removed to represent the input into the subsequent immunoprecipitation reaction.

Affinity matrix plus antibody were then added to the clarified extract as appropriate. Where pre-coupled antibodies were used they were pre-washed in lysis buffer and resuspended as a 1:1 slurry. 30 μ l of a 1:1 slurry was incubated in batch with up to 500 μ l of clarified extract for 2 hours at 4°C with rotation. After this period, the beads were pelleted by centrifugation (8000 RPM for 30 seconds) and a supernatant sample (50 μ l) was removed. The beads were subsequently washed 3 times in lysis buffer and finally twice in PBS.

An equal volume of SDS sample buffer was added to input and supernatant fractions and 30 μ l to bead fractions prior to further analysis.

2.5.3 Lambda phosphatase treatment

Following immunoprecipitation and washing, beads were resuspended in 50 μ l of Lambda phosphatase buffer (NEB) and 1 μ l of enzyme was added. The beads were then incubated at 30°C for 30 minutes.

2.5.4 SDS polyacrylamide gel electrophoresis (SDS-PAGE)

All SDS-PAGE gels were poured between 2 glass plates separated with spacers and assembled in a 'pouring rig' (Anachem). Resolving gel solutions were prepared, poured between the plates and overlaid with water-saturated butan-1-ol until polymerised after which it was washed off with an excess of tap water. A stacking gel was then poured in the presence of a plastic comb to produce wells for sample loading.

Resolving gel mixes

Volumes given are required for 12ml of the given acrylamide percentage gel or 5ml for the stacking gel. Polymerisation was induced by the addition of 1/10th volume of the gel of 10%APS and 1/100th volume of TEMED.

Reagent	10% gel	15% gel	Stacking gel
40% acrylamide	3ml	4.5ml	670µl
2% Bis-acrylamide	780µl	516µl	325µl
1.5M Tris pH8.8	3ml	3ml	-
1M Tris pH6.8	-	-	625µl
10% SDS	120µl	120µl	-
Water	5.1ml	3.9ml	3.38ml

Table 2.10 Resolving gel constituents.

Gels were run at 180V in running buffer until the loading dye had run off the bottom of the gel or if phosphorylation of Mad3p was being analysed the gels were run 30 minutes past when the loading dye ran off the bottom of the gel.

2.5.5 Coomassie staining

Gels were manipulated in plastic staining containers with lid. Stain solution was added to cover well the gel. Stain was done while rocking (up to ten minutes, strong staining is usually seen after 4 minutes; 2 minutes is good to just detect proteins). For de-staining, the Stain solution is poured out and is replaced with a large amount of Destain solution, and Kim Wipes. Results can be seen in a few minutes after adding destain; leave 2 hours to overnight for complete de-staining.

Reagents

Reagent	Constituents
Stain solution	40% methanol 10% acetic acid 50% water 0.1 % (w/v) Coomassie Brilliant Blue
Destain solution	40% methanol 10% acetic acid 50% water

Table 2.11 Reagents used in Coomassie staining

2.5.6 Western blotting

The protein was transferred from the polyacrylamide gel to Hybond PVDF membrane (Amersham) by wet transfer. The membrane was placed between 4 pieces of 3MM

paper adjacent to the membrane as per manufacturers instructions. Transfers were performed in Towbin buffer at 65V for 1.5 hours.

Transfer and equal loading of protein samples was confirmed by Ponceau staining.

Membranes were then blocked to reduce non-specific binding of antibody in 'blotto' for 30 minutes. Primary antibody incubations were typically performed overnight at 4°C in 'blotto'. The quantity of antibody used is given in table 2.5.6.1. Secondary antibody incubations were performed at room temperature for 1 hour in 'blotto'. Membranes were washed twice with PBST between, and following each incubation.

Reagents:

Towbin Buffer; 25mM Tris base, 192mM Glycine, 0.1% SDS, 20% methanol.

Blotto (50ml); 2.5g Marvel (dried skimmed milk powder), 45ml dH₂O, 5ml 10X PBS, 50µl 20% (v/v) Tween.

PBST (500ml); 50ml 10XPBS, 500ml dH₂O, 500µl 20% Tween

2.5.6.1 Antisera used in this study

Name	Working concentration	Source
Anti-Mad3p (Rb pAB)	1/1000	This study
Anti-C1b2p (Rb pAB)	1/1000	Kevin Hardwick
Anti-Mad1p (Rb pAB)	1/1000	Hardwick et al 1995
Anti-Myc (A14) (Rb pAB)	1/1000	Santa Cruz Laboratories
AntiMad2p (Sh pAB)	1/500	Hardwick et al 1995
Anti-Rabbit IgG-HRP (Dk)	1/5000	Amersham
Anti-sheep IgG-HRP (Gt)	1/10,000	SAPU

2.5.6.2 Enhanced chemi-luminescence (ECL)

Membranes were exposed to a mix of equal volumes of each solution provided in the ECL kit (Amersham) for 1 minute. Wrapped in saran wrap and exposed to Biomax Mr-Light film typically for 30 seconds, 5 minutes and 1 hour intervals.

2.6 Sister chromatid separation assay

Performed as described in Biggins et al., 2001.

2.6.1 Fixation of cells for visualisation of GFP-marked chromosomes

Performed as described by Indjeian et al., 2004

2.7 Mad3-intein fusion protein expression and purification

An 'intein' is an engineered protein splicing element that can undergo self-cleavage in the presence of a reducing agent e.g. DTT.

2.7.1 Soluble extract preparation

Cells were grown in selective media to mid-log phase. Mad3-intein-chitin binding domain (CBD) fusion protein expression was induced by the addition of IPTG (0.1M) and incubated overnight at 16°C

Cells were harvested by centrifugation at 5000g for 10 minutes at 4°C then resuspended in ice cold cell-lysis buffer (20mM HEPES pH8 (KOH), 500mM KCl, 1mM EDTA,

0.1% w/v Triton X-100, 0.2% w/v Tween 20, 20 μ M Pefabloc), sonicated for 25 seconds 10 times and centrifuged for 30 minutes at 10,000 RPM at 4°C.

2.7.2 Column preparation and incubation with soluble cell extract

The chitin beads were washed, prior to incubation with soluble extract, with 10 times the column volume of column buffer (as lysis buffer minus detergent and Pefabloc). The soluble extract was incubated with chitin beads recovered from the washed column in batch for 2 hours at 4°C. The column was then washed again with 10 column volumes of column buffer.

2.7.3 Cleavage induction and elution

Self-cleavage of an intein is induced by the presence of a reducing agent. The column was quickly flushed with 3 volumes of column buffer plus 50mM DTT to distribute the reducing agent uniformly through the column, then incubated for 96 hours at 4°C. Elution was performed using half-column volumes of column buffer. Eluted protein was subsequently dialysed overnight into 100mM KCl, 50mM Hepes (pH 7.6), 30% glycerol) for storage at -80°C until further use.

2.8 Tandem affinity purification (TAP) protocol

The TAP purification method (Rigaut et al., 1999) involves the fusion of the TAP tag to the target protein of interest and the introduction of the construct into the cognate host cell or organism. To purify protein complexes it is preferable to maintain expression of the fusion protein at, or close to, its natural level. The fusion protein present in extracts prepared from these cells, as well as associated components, are then recovered by Tandem Affinity Purification (TAP). Combined with the highly sensitive mass-spectrometry methods available nowadays, the TAP method is useful to characterize

protein complexes. In addition, the activity of the purified proteins can be analyzed.

2.8.1 Soluble extract preparation

Cells were harvested by centrifugation at 3000 RPM for 10 minutes then washed in Buffer A and frozen as droplets in liquid N₂. The frozen cells were lysed by grinding using a pestle and mortar in liquid N₂. The ground cells were then resuspended in buffer and thawed at 4°C by stirring. The total cell lysate was then centrifuged for 15 minutes 13,000 RPM, the supernatant removed (LSS) and centrifuged once more at 35,000 RPM for 150 minutes (HSS) following the addition of DTT to 2mM.

2.8.2 Bead preparation and purification of Mad3-TAP

IgG sepharose was washed thoroughly with Buffer IPP150 then incubated with the clarified cell extract in batch for 2 hours at 4°C. The beads were then drained in a column by gravity and washed with buffer IPP150 until no protein was detectable by Bradford Assay. Protein bound to the IgG sepharose was eluted using 0.5M acetic acid pH3.4. Protein was precipitated by the addition of an equal volume of 30% TCA, incubation on ice for 15mins, centrifugation at 13,000 RPM for 15 minutes then washing twice with acetone.

Reagents:

Buffer A; 10mM Hepes (pH7.6), 1.5mM MgCl₂, 150mM potassium acetate, 14% glycerol, 0.5mM PMSF, LPC 1µl/ml, 1 complete mini EDTA protease inhibitor tablet (Roche).

Buffer IPP150; 10mM Tris-Cl pH8.0, 150mM NaCl, 0.1% Triton X-100

2.9 TNT coupled transcription/translation system (Promega)

PCR products encoding the peptides synthesised, with the T7 promoter at their 5' end were added as templates to the TNT quick coupled transcription/translation reaction. Other components were added as per manufacturer's instructions (Promega) and incubated for 90 minutes at 30°.

2.10 *In vitro* binding assay

Radiolabelled peptides (synthesised using the TNT coupled transcription/translation system) were incubated with glutathione agarose-bound GST fusion proteins (or GST alone as a control) for 2 hours at 4°C. The beads were then washed thoroughly with PBST and resuspended in SDS-sample buffer.

Chapter 3

Analysis of Putative Mad3p Phosphorylation by Cdc5p and Ipl1p

3.1 Preliminary analysis of Mad3p modification

3.1.1 Mad3p is modified through an unperturbed cell cycle

The mammalian homologue of Mad3p, BubR1, is phosphorylated in a cell cycle dependent manner and upon spindle checkpoint activation (Chen, 2002; Li et al., 1999; Taylor et al., 2001; Yamaguchi et al., 2003). In yeast, this is also true of the checkpoint components Mad1p and Bub1p (Hardwick and Murray, 1995; Yamaguchi et al., 2003). For all the aforementioned proteins, phosphorylation is visualised by the presence of multiple species when subjected to SDS-PAGE and Western blotting. The slower migrating forms corresponded to phosphorylated forms and were sensitive to treatment with lambda phosphatase. Previously published work on Mad3p has only identified Mad3p as a single form of approximately 60kDa that did not appear to undergo any post-translational modification (Hardwick et al., 2000).

The modification of Mad3p through an unperturbed cell cycle was re-examined using a wild-type *bar⁻* strain (KH186), for ease of arrest by alpha-factor. Wild-type cells were grown to mid-log phase then arrested in G1 using alpha-factor to obtain a synchronous population. Cells were then washed and released into YPDA for continued synchronous growth. Samples were taken at 20 minute intervals for 120 minutes. Alpha-factor was added back to the cultures after cells had started to re-bud, 60 minutes after release, to arrest cells in G1 and prevent re-entry into the next cell cycle. Total protein lysate samples were prepared from the cells harvested for analysis by SDS-PAGE and Western blot. Mad3p was visualised using an affinity purified rabbit anti-Mad3p anti-body. Clb2p was visualised using an affinity purified rabbit anti-Clb2p antibody.

Figure 3.1A demonstrates a subtle band shift of Mad3p, suggestive of post-translational modification, at timepoints 40, 60, 80, 100 and 120 minutes. Clb2p (a B-type cyclin) levels were monitored to demonstrate the stage of the cell cycle from which samples were taken, as B-type cyclin levels peak in mitosis. Mad3p modification was greatest (i.e. maximum band-shift) at timepoints 60-80 minutes after alpha-factor release and corresponded with a peak in Clb2p levels giving an indication that Mad3p modification may be maximal during mitosis.

3.1.2 Arresting cells at various stages of the cell cycle confirms Mad3p modification is cell cycle dependent and peaks during mitosis

To confirm the result seen previously (section 3.1) cells were arrested at various stages of the cell cycle.

Wild-type cells (KH186) were grown to mid-log phase and arrested in G1 using alpha factor, S-phase by the addition of hydroxyurea or mitosis in the presence of nocodazole. A mitotic arrest independent of the spindle checkpoint was achieved by the utilisation of a temperature sensitive APC mutant, *cdc26Δ* (KH243) that at 37°C arrests at metaphase (Hwang and Murray, 1997). The *cdc26Δ* strain was grown to mid-log phase at 23°C, then shifted to 37°C and incubated for 2 hours. After growth and subsequent arrest under the pre-described conditions, cells were harvested and total protein lysates were prepared for analysis by SDS-PAGE and Western blot. Mad3p was detected using an anti-Mad3p rabbit antibody.

SDS-PAGE and Western blot analysis of samples revealed in Figure 3.1B that slower migrating forms of Mad3p were absent in an alpha-factor arrest, had been initiated in the presence of hydroxyurea and peaked following the addition of nocodazole or when *cdc26Δ* cells were grown at 37°C. Thus, Mad3p modification is absent in G1 but is present in S-phase and peaks in mitosis.

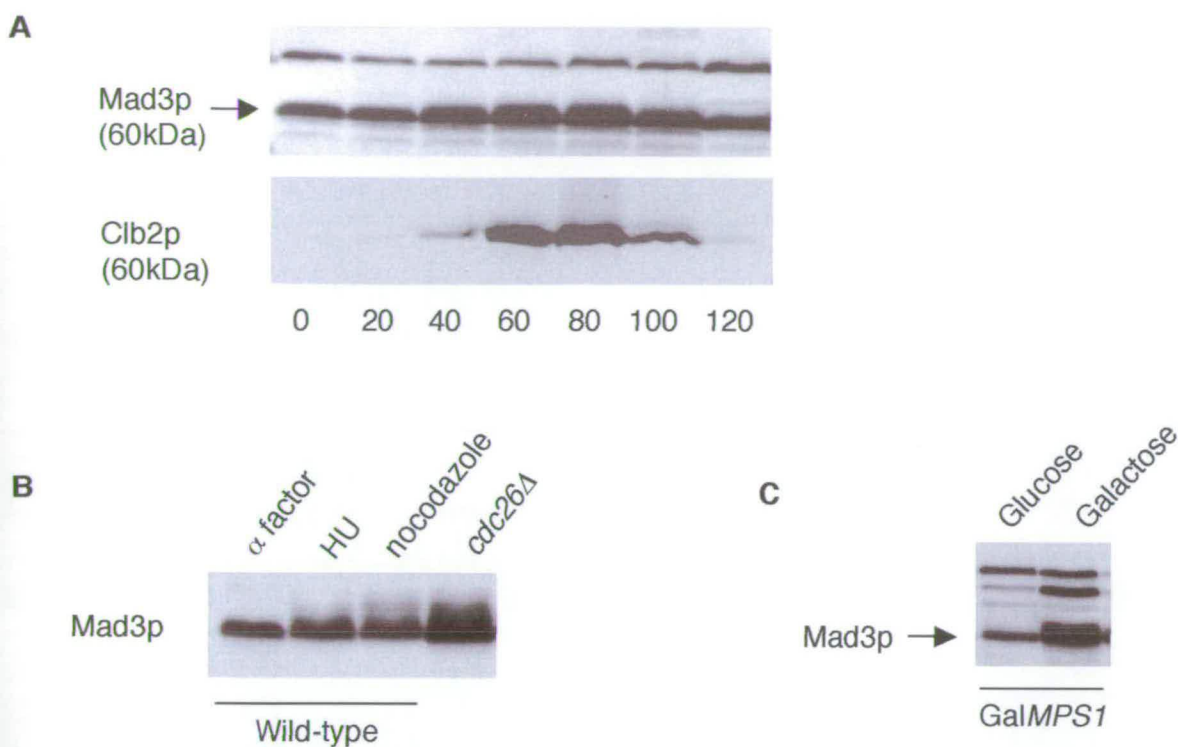


Figure 3.1 Mad3p is modified in a cell cycle dependent manner

A Cells were arrested in alpha-factor at time zero and released. Samples were taken every 20 minutes and analysed by SDS-PAGE and Western blotting with anti-Mad3p and anti-Clb2p antibodies. **B** Wild-type cells were arrested in alpha factor (G1), hydroxyurea (S-phase), nocodazole (mitosis), or at 37°C in a *cdc26Δ* (metaphase arrest). Samples were analysed by SDS-PAGE and Western blotting with anti-Mad3p antibody. **C** Cells were arrested in metaphase by overexpression of Mps1p under the control of a GAL promoter. Samples were analysed by SDS-PAGE and Western blotting with anti-Mad3p antibody.

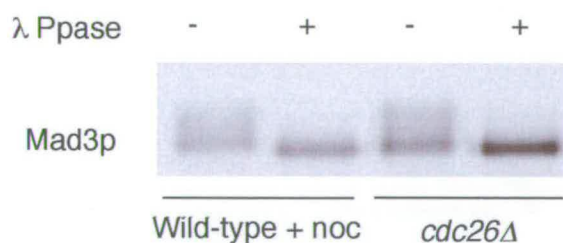


Figure 3.2 Mad3p modification is phosphorylation

Cells were arrested in metaphase by the addition of nocodazole to wild-type cells or growth at 37°C in a *cdc26Δ*. Mad3p was immunoprecipitated using anti-Mad3p antibody. Half the immunoprecipitate was subjected to treatment with lambda phosphatase. Samples were analysed by SDS-PAGE and Western blotting with anti-Mad3p antibody.

3.1.3 Over-expression of Mps1p induces modification of Mad3p

An alternative method to induce a metaphase arrest, with the characteristics of a spindle checkpoint arrest, is over-expression of the kinase Mps1p (Hardwick et al., 1996). Over-expression is induced in this experiment from the *GALI-10* promoter integrated into the genome upstream of the *MPS1* gene by growth in media containing galactose as a sugar source.

GALI-10MPS1 (KH153) cells were grown to mid-log phase in YPDA, in the absence of galactose. Cells were then washed thoroughly to remove any glucose present and re-suspended in YEP GAL/RAFF for incubation at 30°C for 6 hours to induce the over-expression of Mps1p through the activation of the *GALI-10* promoter. Cells were harvested and total protein lysates prepared for SDS-PAGE and Western blot analysis using a rabbit anti-Mad3p anti-body.

Figure 3.1C shows that Mad3p in cells grown in the presence of glucose (*GALI-10* promoter repressed) was visible as a single band. However, when cells were grown in the presence of galactose, several slower migrating forms of Mad3p were visible. It was therefore possible to conclude that Mad3p is modified following the over-expression of Mps1p and consequential arrest in metaphase.

3.1.4 The modification of Mad3p is phosphorylation

The following experiments were designed to determine the nature of the Mad3p modification. The slower migrating forms were predicted to be as a result of phosphorylation, and, if so, would therefore be sensitive to λ protein phosphatase.

Wild-type (KH186) cells were grown to mid-log phase and arrested at metaphase in the presence of nocodazole. *cdc26* Δ cells (KH243) were also grown to mid-log phase at

23°C, then shifted to 37°C for 2 hours to induce arrest in metaphase. Total cell lysates suitable for immunoprecipitation were prepared from cells arrested by both means. Mad3p was immunoprecipitated from each sample using an anti-Mad3p rabbit polyclonal antibody (see materials and methods). Half the immunoprecipitate was treated with λ protein phosphatase. The treated immunoprecipitates were subjected to SDS-PAGE and Western blotting using anti-Mad3p antibody.

Figure 3.2 reveals that the retarded forms of Mad3p, seen when wild-type cells were arrested using nocodazole or *cdc26* Δ cells were arrested at their restrictive temperature, were removed following treatment by λ protein phosphatase. The result demonstrates that the slower migrating forms of Mad3p seen in a metaphase arrest are due to phosphorylation.

3.1.5 The phosphorylation of Mad3p is unaffected in checkpoint mutants

Previous studies have shown that the formation of complexes involving Mad3p (or its mammalian homologue, BubR1) is important for its checkpoint function. Similarly, the importance of protein localisation to kinetochores upon checkpoint activation has been inferred. Mad3p is thought to act at the effector end of the checkpoint pathway by interacting with Mad2p and Cdc20p to inhibit APC activity (Hardwick et al., 2000). It is therefore possible that the absence of checkpoint components earlier in the cascade and subsequent interruption of complex formation or localisation of Mad3p may affect the protein's ability to be phosphorylated.

Though phosphorylation is visible in cells arrested in mitosis, the nature of this phosphorylation may be of a different source and have different requirements. If so, the absence of checkpoint components may have different effects under conditions of checkpoint arrest and a normal mitosis.

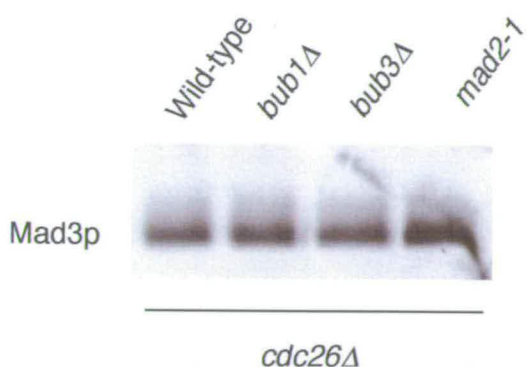
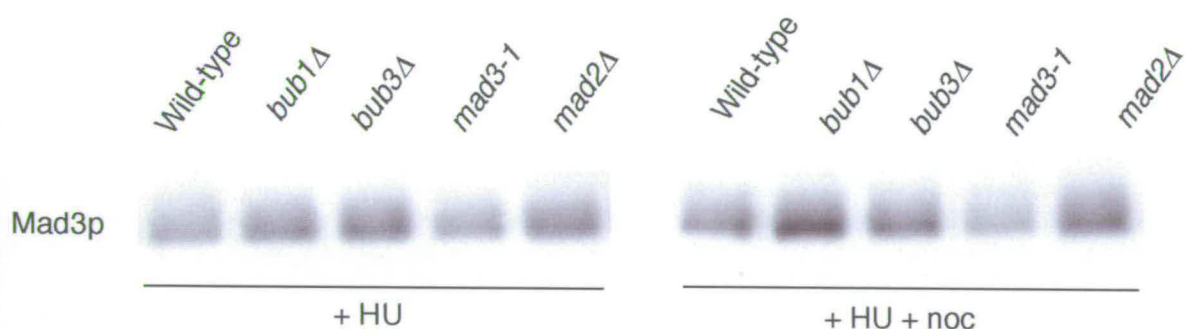
A**B**

Figure 3.3 Mad3p phosphorylation is unaffected in checkpoint mutants

A *cdc26Δ* cells with different checkpoint components absent were arrested at 37°C and analysed by SDS-PAGE and Western blotting with anti-Mad3p antibody. **B** Wild-type cells with different checkpoint components absent were arrested with Hydroxyurea +/- nocodazole and analysed by SDS-PAGE and Western blotting with anti-Mad3p antibody.

To assess the effect of the absence of checkpoint components during mitosis of an unperturbed cell cycle, strains with the checkpoint components *BUB1* (MB090) and *BUB3* (MB094) deleted or a checkpoint defective *mad2-1* allele (MB086) in conjunction with a *cdc26Δ* were utilised. The checkpoint components absent or non-functional in this experiment are not required for arrest in a *cdc26Δ* background. Each strain and a *cdc26Δ* (KH243) control was grown to mid-log phase at 23°C and then shifted to 37°C for 2 hours to induce a metaphase arrest. Cells were harvested and total protein lysates prepared for analysis by SDS-PAGE and Western blotting with anti-Mad3p antibody.

Figure 3.3A shows the band-shift of Mad3p seen in *cdc26Δ* cells arrested by this means was maintained in *bub1Δ*, *bub3Δ* and *mad2-1* strains. Therefore the mitotic phosphorylation of Mad3p seen in the absence of checkpoint activation does not require Bub1p, Bub3p or Mad2p function.

To investigate the effect of different checkpoint mutants on Mad3p phosphorylation upon checkpoint activation, strains with *MAD2*, *BUB1* and *BUB3* deleted (MB106, MB060, MB003 respectively) and the *mad3-1* allele (KH45), that cannot bind Bub3p, were grown to mid-log phase. Hydroxyurea was then added to pre-arrest cells in S-phase. This was necessary as a metaphase arrest following the addition of nocodazole is not possible in the absence of a functional checkpoint that is perturbed in the different mutants used in this experiment. Cultures were then split. Nocodazole was added to half the cultures to depolymerise microtubules and activate the spindle checkpoint. All cultures were then incubated at 23°C for a further 1 hour. Cells were harvested and total protein lysates prepared for analysis by SDS-PAGE and Western blotting with anti-Mad3p antibody.

The Mad3p band shift, indicative of phosphorylation, though reduced overall in strains arrested in hydroxyurea was present to the same degree in the *bub1Δ*, *bub3Δ*, *mad3-1*

and *mad2Δ* lanes as it was in the wild-type control. In cells that had nocodazole added, following a pre-arrest in hydroxyurea, the band-shift of Mad3p seen in wild-type cells remained present in the absence of Bub1p, Bub3p or Mad2p and in the *mad3-1* mutant (Figure 3.3B). In conclusion, none of Bub1p, Bub3p or Mad2p proteins is required for the phosphorylation of Mad3p seen during S-phase or that seen after the addition of nocodazole to cells pre-arrested in S-phase or when cells are arrested in metaphase of an un-perturbed cell cycle.

From this, one can conclude that neither complex formation (Mad3p-Bub3p or Mad3p-Mad2p-Cdc20p) nor kinetochore localisation (shown in other systems to be Bub1p and Bub3p dependent) is necessary for Mad3p modification.

3.2 The identification of putative phosphorylation sites within Mad3p

The large-scale purification of proteins using a TAP-tag has become a prevalent method of identifying phosphorylated sites of proteins *in vivo*. Mad3-TAP was generated but the purification on a scale necessary for the identification of sites by mass-spectrometry was unsuccessful (see Appendix).

As Mad3p phosphorylation has been shown to increase into mitosis and Mad3p's main function to date is concerned with a mitotic checkpoint it is sensible to suggest that a kinase with mitotic function may be physiologically relevant. Such kinases include Ipl1p, Cdc5p, Cdc28p (CDK) and Mps1p.

Unpublished data has suggested a role for Cdc5p in the phosphorylation of Mad3p *in vivo* (S. Piatti, per comm.) and kinase assays have shown that recombinant Mad3 can be phosphorylated by Cdc5p *in vitro* (N. Rachidi, per comm). Mammalian data has demonstrated a role for Aurora B, the mammalian homologue of Ipl1p, in phosphorylation of BubR1 (Ditchfield et al., 2003).

0 MKAYAKKRISYMPS^{*}SPSQNVINFEEIETQKENILPLKEGRSAAALSKAIH
 51 QPLVEINQVKSSFEQRLIDELPALS DPITLYLEYIKWLN NAYPQGGNSKQ
 101 SGMLTLLERCLSHLKD LERYRNDVRFLKIWFYIELFTRNSFMESRDIFM
 151 YMLRNGIGSELASFYEEFTNLLIQKEKFQYAVKILQLGIKNKARP NKVLE
 201 DRLNHLLRELGENNIQLGNEI^{*}S^{*}MDSLESTV LGKTRSEFVNRLELANQNGT
 251 SSDVNLTKNNVFVDGEE SDVELFETPNRGVYRDGWENFDLKAERNKENNL
 301 RI^{*}S^{*}LLEANTNLGELKQHEMLSQKKRPYDEKLP IFRD^{*}S^{*}IGRSDPVYQMINT
 351 KDQKPEKIDCNFKLIYCEDEESKGGRL E^{*}F^{*}S^{*}LEEVLAISRNVYKRVRTNRK
 401 HPREANLGQEE SANQKEAEAQSKRPKISRKALVSKSL^{*}T^{*}PSNQG RMFSGEE
 451 YINCPM^{*}TPKGRSTETSDI ISAVKPRQL^{*}T^{*}PILEMRESNSFSQSKNSEIISD
 501 DDKSSSSFISYPPQR^{*}

Figure 3.4 Identification of putative sites for phosphorylation within Mad3p

Sites were identified using published and derived consensus sequences (see text for details). Blue denotes phosphorylation by Cdc28p; green Cdc5p; red Ipl1p. * = residue predicted to be phosphorylated. No putative sites for phosphorylation by Mps1p are highlighted as no consensus sequence has as yet been derived.

Published work has led to the identification and inference of consensus amino acid sequences within proteins that indicate putative sites of phosphorylation.

Alexandru et al., 2001 demonstrated the preferential phosphorylation of serine residues adjacent to Scc1p (cohesin) cleavage sites. The sequence of amino acids upstream of sites of Scc1p cleavage is [D/E]X[S/T][I/L/M/V][D/E], including a residue phosphorylated by Cdc5p. From this we derived a consensus sequence for phosphorylation by Cdc5p. Three putative sites of phosphorylation by Cdc5p kinase were identified as serine 222, threonine 229 and serine 380. Interestingly, the consensus sequence surrounding serine 380 includes the glutamate residue that is mutated to a lysine residue in the original *mad3-1* allele. This allele of *mad3* is no longer checkpoint proficient and cannot bind Bub3p (Hardwick et al 2000).

Cheeseman et al., 2002 identified phosphorylation sites of kinetochore components Dam1p and Ask1p by Ipl1p kinase. The *in vivo* and *in vitro* results identified the motif [R/K]X[S/T][I/L/V] as a requirement for phosphorylation. Two consensus sequences for phosphorylation by Ipl1p kinase are present and include serine 303 and serine 337.

The main CDK in budding yeast, Cdc28p, is known to phosphorylate SP residues and has a broader consensus sequence [S/T]PXX. The simple [S/T]P motif indicating putative phosphorylation by Cdc28p is present five times in the Mad3p amino acid sequence at residues serine 35 and threonines 275, 438, 457 and 478.

Though one *in vivo* substrate, Spc110p, for the checkpoint kinase Mps1p has been identified by (Friedman et al., 2001) and Mad1p has been identified as a substrate *in vitro* (Hardwick and Murray, 1995), no consensus sequence for phosphorylation has been determined as yet.

As existing data suggested Ipl1p and Cdc5p kinases may have a role in Mad3p phosphorylation, each putative site of phosphorylation by these kinases was mutated to either an alanine or an aspartate. Phosphorylatable residues mutated to alanine can no longer be phosphorylated. Serines or threonines replaced by aspartate can mimic constitutive phosphorylation of the site as the result of adding a phosphate group, by phosphorylation, also generates an acidic residue. The results of mutating the Ipl1p consensus sites, serine 303 and serine 337, are discussed later in this work.

3.3 Analysis of Mad3p mutated at sites putatively phosphorylated by Cdc5p

3.3.1 A Mad3p mutant at putative sites of phosphorylation by Cdc5p is sensitive to microtubule depolymerising drugs

All identified residues identified as putative sites of phosphorylation by Cdc5p, serine 222, threonine 229 and serine 380, were mutated simultaneously by multi-site directed mutagenesis (multi-SDM) of wild-type vector pKH535 to create triple alanine phosphorylation site mutants or triple aspartate phosphorylation site mutants. In parallel, serine 380 was mutated independently to either alanine or aspartate as it is part of a conserved series of amino acids surrounding the glutamate to lysine mutation of the *mad3-1* allele.

The new plasmids, empty vector (YCpLac22) and wild-type control (pKH535) were then transformed into a *mad3Δ* strain, KH173 for further analysis.

The function of each mutant as a component of the spindle checkpoint was assessed by their ability to grow on YPDA solid media containing benomyl. A *mad3Δ* strain (KH173) transformed with each mutant plasmid (and controls) was spotted onto YPDA plates containing 0μg/ml, 10μg/ml, 12.5μg/ml and 15μg/ml benomyl in 10-fold dilutions. The growth of the triple alanine mutant S222/T229/S380A in the presence of

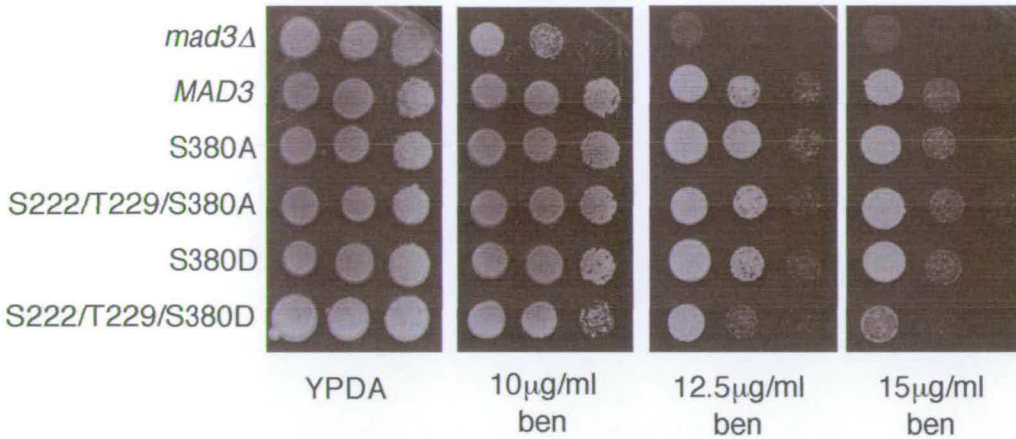


Figure 3.5 Mutation of residues within derived consensus sequences for phosphorylation by Cdc5p to aspartate generates a subtle benomyl sensitivity

Mad3 mutated to either alanine (S380A, S222/T229/S380A) or aspartate (S380D, S222/T229/S380D), plus controls, were plated on to media containing increased concentrations of benomyl in serial dilutions.

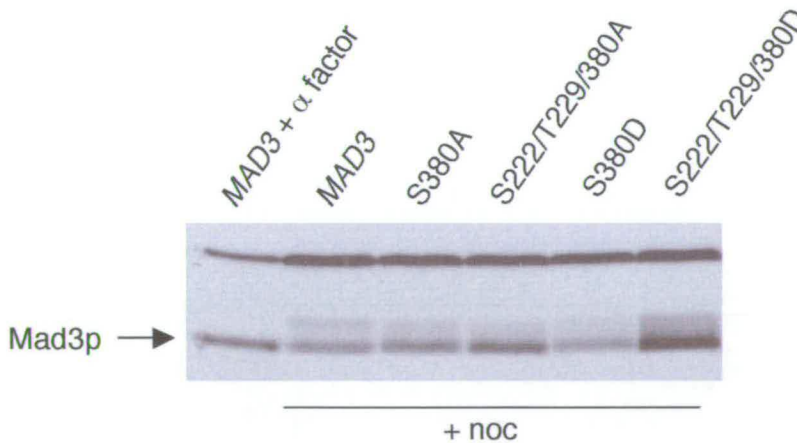


Figure 3.6 Mutation of residues within derived consensus sequences for phosphorylation by Cdc5p to aspartate stabilises *Mad3p* but does not affect its phosphorylation

Mad3 mutated to either alanine (S380A, S222/T229/S380A) or aspartate (S380D, S222/T229/S380D), plus controls, were grown in the presence of nocodazole for 2 hours. Samples were analysed by SDS-PAGE and Western blotting with an anti-*Mad3p* antibody.

benomyl was the same as seen in the wild-type control, suggesting that the phosphorylation of any of these sites is not important in spindle checkpoint function. However, the triple aspartate mutant S222/T229/S380D demonstrated reduced growth on all concentrations of benomyl, compared to that of wild-type, suggesting that it may be partially deficient in checkpoint function, but not as severely as seen in the *mad3Δ* control (Figure 3.5).

3.3.2 Mad3p phosphorylation is unaffected by mutation of putative sites of Cdc5p phosphorylation.

To assess the effect, if any, of the mutations on the phosphorylation of Mad3p, KH173 (*mad3Δ*) transformed with the alanine and aspartate versions of the mutants and a wild-type (pKH535) control were grown to mid-log phase and arrested in metaphase, with an activated spindle checkpoint, by the addition of nocodazole. Total cell lysates of each culture were prepared for analysis by SDS-PAGE and Western blotting with an anti-Mad3p antibody.

Figure 3.6 shows that the band shift and proportion of the retarded band, representing phosphorylation, was unaffected in all mutants. The results suggest that the phosphorylation of Mad3p at serine 222, threonine 229 and serine 380 is not responsible for the band shift seen in wild-type Mad3p. In mutants where these residues were mutated to alanine the band shift remained visible. In both varieties of aspartate mutant the band shift also remained unaffected. However, there was significantly more Mad3p present (quantified in Figure 3.11).

The results shown in Figures 3.5 and 3.6 suggest that mutation of Mad3p at putative sites of phosphorylation by Cdc5p led to an increase in protein stability and an increased sensitivity to benomyl.

3.4 Mad3p phosphorylation, in response to a lack of tension at kinetochores, requires Ipl1p kinase function *in vivo*

Mcd1p/Scc1p forms part of the cohesin complex responsible for sister chromatid cohesion (Guacci et al., 1997). Mcd1p/Scc1p is cleaved by separase at the metaphase to anaphase transition, permitting sister separation and progression through mitosis. However, in a *mcd1-1* mutant, grown at its restrictive temperature, though sisters are attached by their kinetochores to microtubules, the cohesion between them is perturbed and there is a lack of tension at kinetochores (Guacci et al., 1997). This lack of tension is sufficient to activate the spindle checkpoint. A similar lack of tension is apparent when the initiator of replication Cdc6p is absent. In this scenario, chromatids remain unreplicated but attached to a microtubule at their kinetochore. Due to the lack of a sister and no poleward pull of microtubules on the kinetochore, again the spindle checkpoint is activated. The arrest is Mad1p and Mad2p dependent (Biggins and Murray, 2001).

Ipl1p is required for spindle checkpoint function when there is a lack of tension at the kinetochore and when Mps1p kinase is over-expressed (Biggins and Murray, 2000; Stern and Murray, 2001). However, Ipl1p kinase activity is not required in *Saccharomyces cerevisiae* for the arrest seen when spindle microtubules are depolymerised.

3.4.1 Mad3p phosphorylation is reduced in response to reduced cohesion between sister chromatids in an *ipl1-321* mutant

In a *mcd1-1* mutant at a restrictive temperature (37°C) cohesion is lost between replicated sister chromatids and cells arrest in metaphase with stabilised levels of Pds1p (Biggins and Murray, 2001).

The phosphorylation of Mad3p was compared between two strains; *mcd1-1* (SBY870) and *mcd1-1 ipl1-321* (SBY871). Both strains were temperature sensitive and contained a myc epitope-tagged version of Pds1p to allow monitoring of cell cycle progression.

Each strain was grown to mid-log phase at 23°C and subsequently arrested in G1 using alpha-factor. Cells were then released from G1 at 37°C and samples were collected every 20 minutes for 3 hours. Samples were then prepared for and subjected to analysis by SDS-PAGE and Western blotting with anti-Mad3p and anti-myc antibodies.

Figure 3.7Ai shows that from 60-90 minutes after release from alpha factor in the *mcd1-1* strain retarded forms of Mad3p were visible, indicative of phosphorylation. Levels of Pds1p were near their peak at this point and remained stable for the remainder of the experiment as cells remained in metaphase and cell cycle progression was significantly delayed in response to the lack of tension at kinetochores encountered (data not shown).

However, in the *mcd1-1 ipl1-321* strain there was little evidence of a Mad3p band-shift at any point through the timecourse. Pds1p levels peaked after 90 minutes but degradation had occurred after 120 minutes as cells passed through the metaphase to anaphase transition (data not shown). Mad3p is usually phosphorylated during mitosis every cell cycle (Figure 3.1A) but these results suggest that this may not be the case during a cell cycle in a *mcd1-1 ipl1-321* mutant. It is therefore possible to conclude that complete Mad3p phosphorylation in response to a lack of tension between sister chromatids requires Ipl1p kinase activity.

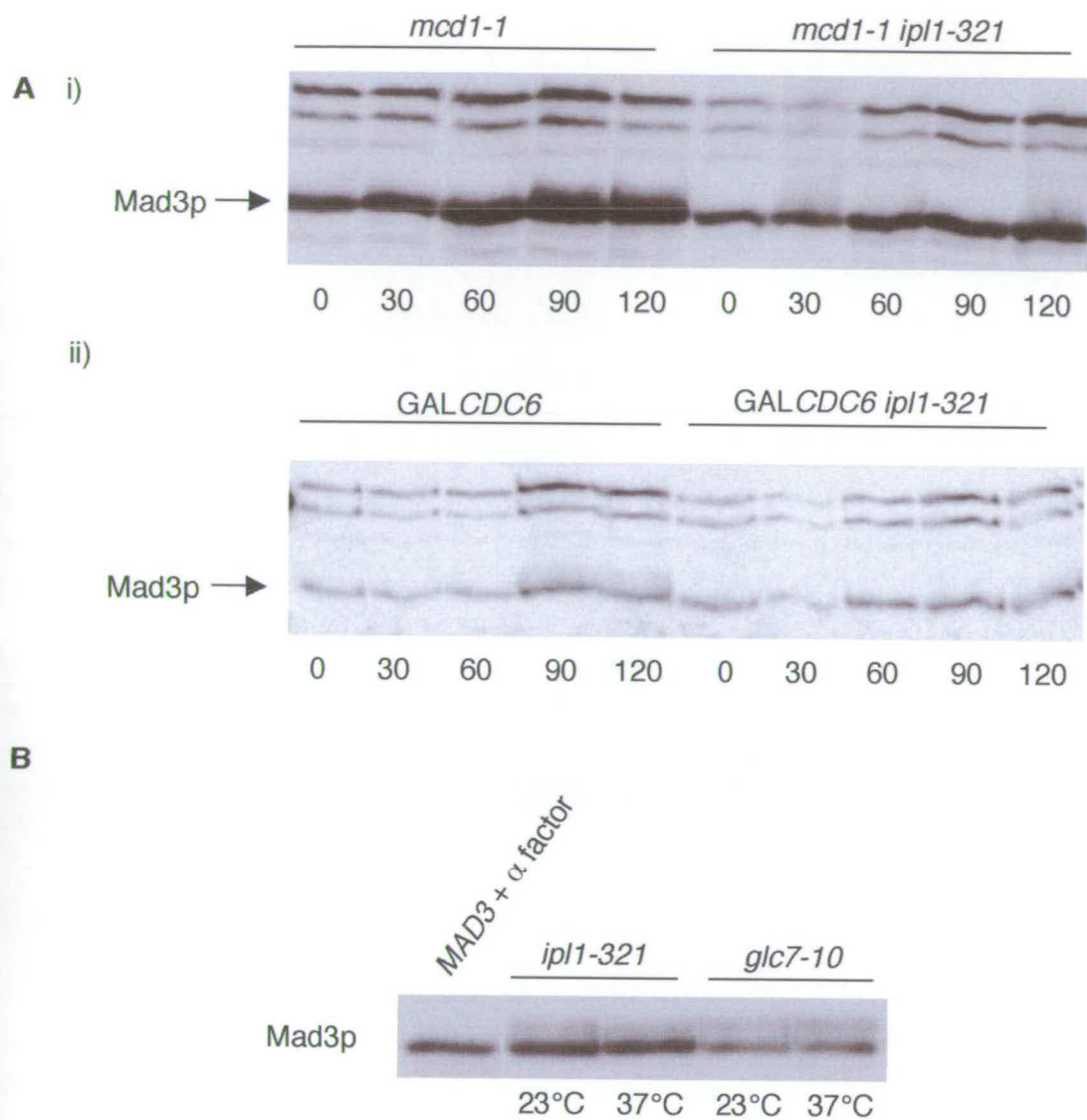


Figure 3.7 Mad3p phosphorylation in response to a lack of tension requires Ipl1p function but does not in the absence of kinetochore-microtubule attachment

A i) *mcd1-1* and *mcd1-1 ipl1-321* cells were arrested in G1 using alpha factor at their permissive temperature, then released at 37°C. Samples were taken every 30 minutes and analysed by SDS-PAGE and Western blotting with anti-Mad3p antibody. ii) *GALCDC6* and *GALCDC6 ipl1-321* were grown in the presence of glucose to inhibit DNA replication, then arrested in G1 using alpha-factor at 23°C and subsequently released at 37°C. Samples were taken every 30 minutes and analysed by SDS-PAGE and Western blotting with anti-Mad3p antibody. **B** *ipl1-321* and *glc7-10* cells were grown at 37°C in the presence of nocodazole to depolymerise microtubules. Samples were analysed by SDS-PAGE and Western blotting with anti-Mad3p antibody.

3.4.2 Mad3p phosphorylation in response to Cdc6p repression is reduced in an Ipl1p mutant

A strain containing *CDC6* under the control of the *GAL* promoter was utilised to control transcription of the gene. In the presence of galactose *CDC6* transcription is permitted, however, in the presence of glucose the promoter is repressed and transcription of *CDC6* is repressed.

The phosphorylation of Mad3p was compared between two strains, *GAL-CDC6* (SBY772) and *ipl1-321 GAL-CDC6* (SBY771), the presence of the allele *ipl1-321* rendering cells temperature sensitive. Each strain was grown under conditions that led to the attachment of mono-oriented, unreplicated chromatids to one pole, no Cdc6p present in the cell and cells synchronised at G1 (see Biggins and Murray, 2001). Cells were then released at 37°C with *CDC6* repressed. Samples were taken every 30 minutes for two hours. The samples were prepared for and subjected to analysis by SDS-PAGE and Western blotting with anti-Mad3p antibody.

Figure 3.7Aii shows that in the absence of Cdc6p the resulting arrest induces the phosphorylation of Mad3p seen as a band shift in samples from 90 minutes after release. However, in an *ipl1-321* mutant, in the absence of Cdc6p, little or no band shift of Mad3p was visible. This was not due to a lack of metaphase arrest as even though cells don't arrest in response to *CDC6* repression in *ipl1-321* cells it would have been expected to see phosphorylation of Mad3p due to progression through the cell cycle, but even this was absent. From these results it was possible to conclude that wild-type levels of Mad3p phosphorylation in response to repression of *CDC6* transcription requires Ipl1p kinase activity.

3.4.3 Mad3p phosphorylation is subtly reduced in an *ipl1* mutant when spindle microtubules are de-polymerised

Previous results in this thesis have shown that Mad3p is phosphorylated during mitosis and consequently phosphorylation is visible when cells are arrested in metaphase in response to microtubule depolymerisation (Figure 3.1B). Though it is known that Ipl1p function is not required for arrest in response to the addition of nocodazole, it is still possible that Mad3p phosphorylation may be affected in its absence. Unpublished data has also suggested a role for PP1, a phosphatase encoded by the *GLC7* gene, in checkpoint signalling (Sue Biggins poster, FASEB July, 2004) and this phosphatase is thought to work in opposition to Ipl1p (REF).

To address this question *ipl1-321* (NRY38a) and *glc7-10* (PAY007) were grown to mid-log phase (OD_{600} = 0.2–0.5) and arrested in metaphase by the addition of nocodazole at 37°C, the restrictive temperature. The cells were harvested, prepared for and subjected to SDS-PAGE analysis and Western blotting with an anti-Mad3p antibody.

The results presented in Figure 3.7B demonstrate a slight reduction in bandshift in the *ipl1-321* mutant sample arrested at its restrictive temperature, but it is not abolished. The *glc7-10* mutation samples demonstrate that even at 23°C (and at 37°C) the proportion of retarded (phosphorylated) Mad3p is increased and subsequently the amount of Mad3p that migrates fastest is reduced.

The combination of results shown in Figure 3.7 demonstrates a total requirement for Ipl1p function for Mad3p phosphorylation in the absence of tension at kinetochores but only a partial requirement for Mad3p phosphorylation in response to a lack of kinetochore – microtubule attachment. There is also the suggestion that PP1 phosphatase (through its regulatory subunit Glc7p) plays a role in the dephosphorylation of Mad3p.

3.4.4 Mad3p is required for the metaphase delay seen in a cohesin mutant

Lee and Spencer, 2004 have previously shown that Mad1p and Mad2p are required for the arrest seen when a lack of tension at the kinetochore is induced due to repression of *CDC6* transcription. The experiment described here assesses the requirement of Mad3p for the delay seen in a *mcd1-1* mutant.

mcd1-1 mad3Δ strain (EK12), *mcd1-1* (SBY870) and *mcd1-1 ipl1-321* (SBY871) strains, all containing Pds1-myc18, were grown to mid-log phase at 23°C and subsequently arrested in G1 using alpha-factor. Cells were then released at 37°C and samples were taken every 20 minutes for 3 hours. Samples were prepared for and analysed by SDS-PAGE and Western Blotting using an anti-myc (A14) antibody.

Figure 3.8 shows cell cycle progression of each strain by monitoring Pds1p levels at each time point. In the *mcd1-1* mutant Pds1 levels increased until 80-100 minutes after release and remained stable for the duration of the time course as cells arrested in response to a lack of tension at their kinetochores. In the *mcd1-1 ipl1-321* strain Pds1p levels peaked after 100 minutes from release and then dropped as there is no arrest in response to a lack of tension in the absence of Ipl1p kinase activity. Analysis of samples taken from the *mad3Δ mcd1-1* strain show that Pds1p levels increase to 120 minutes after release but drop from 140–180 minutes as the cell cycle progresses through metaphase to anaphase. This result demonstrates that the cell cycle delay seen in response to a *mcd1-1* defect requires Mad3p.

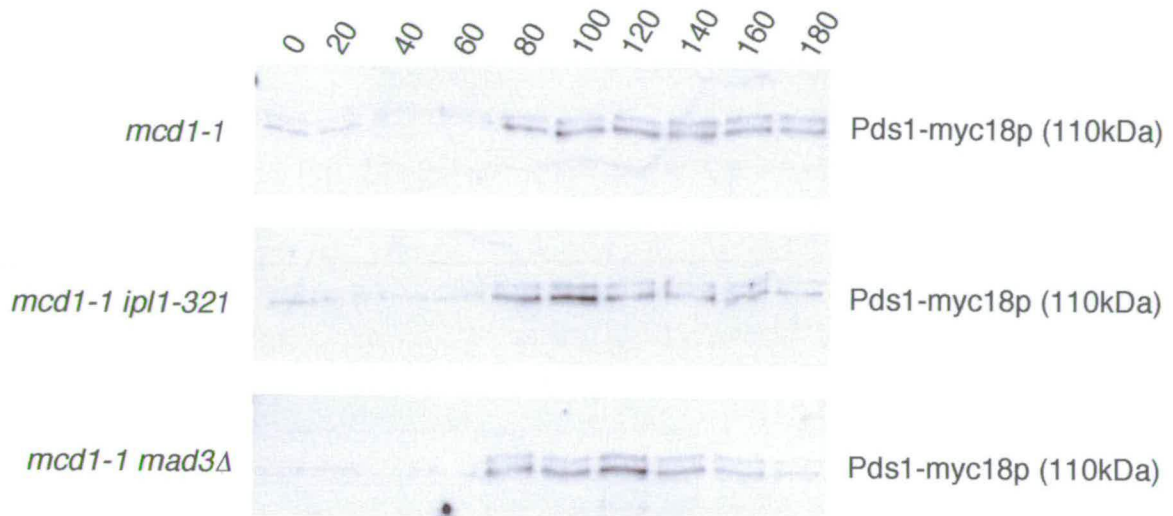


Figure 3.8 Mad3p is required for the delay in a *mcd1-1* mutant

mcd1-1, *mcd1-1 ipl1-321* and *mcd1-1 mad3Δ* cells containing Pds1-myc18 were arrested in alpha-factor at their permissive temperature then released at 37°C. Samples were taken every 20 minutes and analysed by SDS-PAGE and Western blotting using anti-myc (A14) antibody to monitor cell cycle progression.

3.5 Mad3p is Phosphorylated *In Vitro* by Ipl1 Kinase

3.5.1 Mad3-intein purification

Protein purified from *E. coli* can be used for *in vitro* experiments and as an antigen for antibody production. Many tagging systems and protocols exist to produce recombinant protein but we decided to utilise the IMPACT-CN (New England Biolabs) system where the target protein, in this case Mad3, is fused to a chitin binding domain separated from the target protein by an inducible self-cleavage protein splicing element, the intein, that allows release of the recombinant protein without the use of a protease. We also knew that proteins purified this way, though yield was reduced compared to a GST purification, suffered reduced degradation and gave rise to a very 'clean' prep (Stuart MacNeill pers. comm.).

Recombinant Mad3 was produced to allow the identification of sites phosphorylated by Ipl1p *in vitro* for further analysis *in vivo*.

3.5.1.1 Construction of the Mad3-Intein Fusion Protein Expression Plasmid

Mad3p contains two regions that are homologous to regions found in another checkpoint protein, Bub1p (Hardwick et al., 2000). PCR fragments encoding each region and surrounding amino acids, Region I comprising amino acids 1-247, Region II amino acids 248-516, and full length *MAD3* were ligated into the vector pKYB1 for expression and purification.

Positive transformants were selected on LB media containing kanamycin. Colony PCR was performed to detect the presence of an insert in the correct orientation. Mini-preps of clones positive by PCR were made and a BstEII/EcoR1 diagnostic digest was

performed to confirm the presence of the insert. Finally, positive clones were sequenced and subsequently transformed into the expression strain ER2566.

3.5.1.2 Extraction and purification of Mad3-intein

Expression of the fusion protein was induced from cultures grown to mid-log phase using 0.5mM IPTG at 17°C overnight (16 hrs). A soluble protein extract was prepared and incubated with chitin beads. The column was then washed and self-cleavage was induced by the addition of DTT. Initial experiments were disappointing with only a small yield of recombinant protein observed by coomassie blue staining of samples taken throughout the purification and subjected to SDS-PAGE analysis (data not shown). As different induction temperatures and durations had not shown significant effects upon recombinant protein expression, the cleavage step of the protocol was investigated further.

Figure 3.9A shows the effect of cleavage reaction duration on the recovery of recombinant protein. Equal amounts of sample were loaded in each lane, subjected to SDS-PAGE and gels were stained with coomassie blue. For both N-terminal and C-terminal fusion proteins, cleavage for 96 hours increased significantly the amount of target protein eluted - as seen in the lanes representing the elutions. The bead lanes after 96 hours also show much reduced fusion protein still bound to the beads and an increased amount of CBD-intein, from which the target protein had been cleaved when compared to the equivalent sample after 16 hours. As a result of this investigation in subsequent experiments the cleavage reaction was allowed to proceed for 96 hours.

The expression and purification of full-length Mad3p-intein was performed using 5 litres of culture to counteract reduced expression levels, whereas the N-terminal and C-terminal portions were expressed and purified from only 1 litre of culture.

A

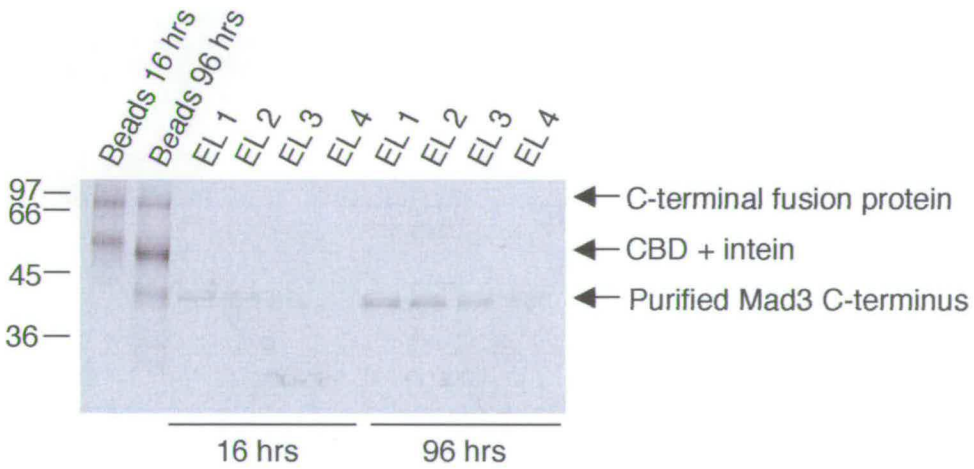
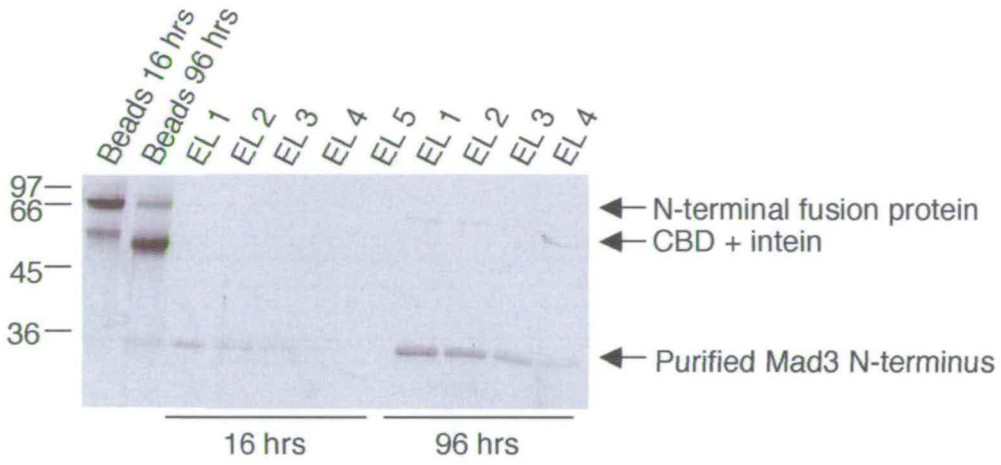


Figure 3.9 Mad3-intein purification

A Optimisation. Cleavage reactions of the two Mad3-intein portions were performed for either 16 hours or 96 hours at 4°C. Samples were taken and analysed by SDS-PAGE and stained with coomassie blue.

B

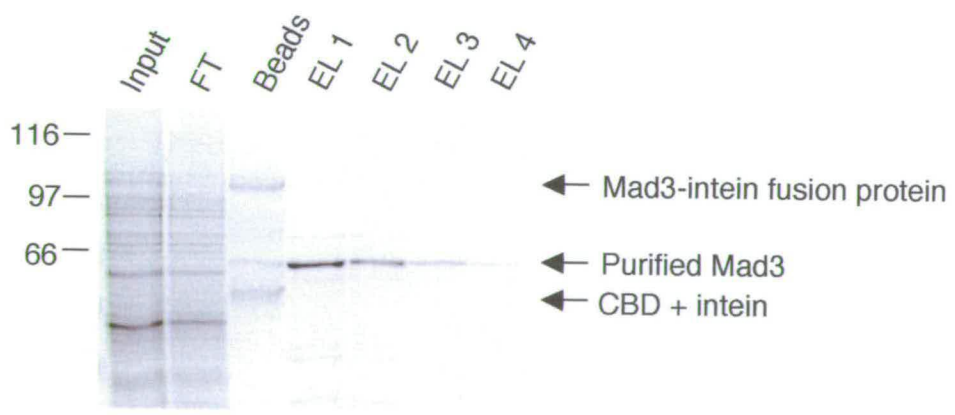
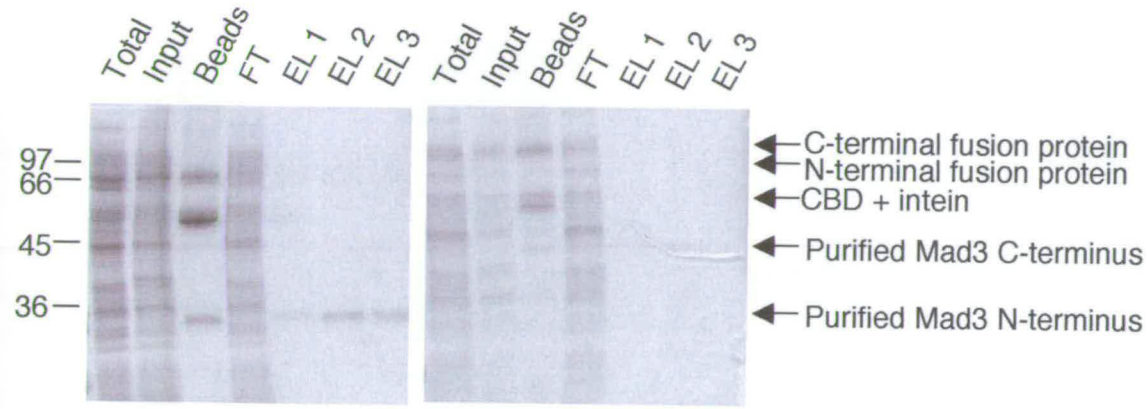


Figure 3.9 Mad3-intein purification continued

B Final purifications of Mad3-intein portions and full length. Samples were analysed by SDS-PAGE and stained with coomassie blue.

Samples of extracted protein and elutions from final purifications were analysed by coomassie blue staining of SDS PAGE gels and are presented in Figure 3.9B.

3.5.2 Mad3, but not the N-terminus of Bub1 or Mad1 is phosphorylated *in vitro* by Ipl1p

Recombinant Bub1 and Mad3 were used as substrates in an *in vitro* kinase assay using the kinase Ipl1p. A complex of the C-terminal portion of Mad1 in a complex with Mad2 was also utilised (donated by Michelle Brady).

The *in vitro* kinase assays were performed by Najma Rachidi of Mike Stark's laboratory, University of Dundee. The assays were performed using recombinant Ipl1 and Ipl1-GST purified from yeast.

The initial results showed that of all potential substrates assayed only full length Mad3 and the C-terminal portions of Mad3 were phosphorylated *in vitro* by Ipl1p.

The phosphorylated protein was then subjected to digestion by trypsin and peptides generated were separated by HPLC. The fraction containing ^{32}P was identified and subjected to analysis by mass-spectrometry to determine the mass of the phosphorylated peptide. The mass of the phosphopeptide was then compared to the predicted mass of peptides generated by tryptic digestion of Mad3p to predict the primary amino acid sequence. Solid phase Edman sequencing of the recovered phosphopeptide was used to identify which residue was phosphorylated. Released ^{32}P was plotted against the amino acid sequence determined/inferred by mass-spectrometry (Figure 3.10A). The residue on Mad3p was serine 337.

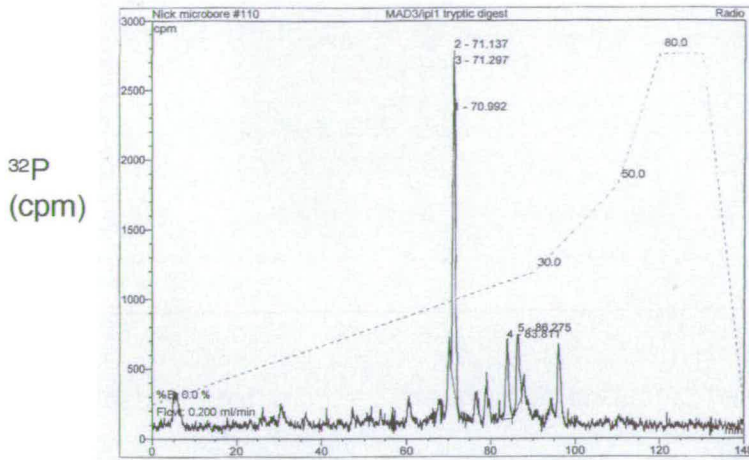
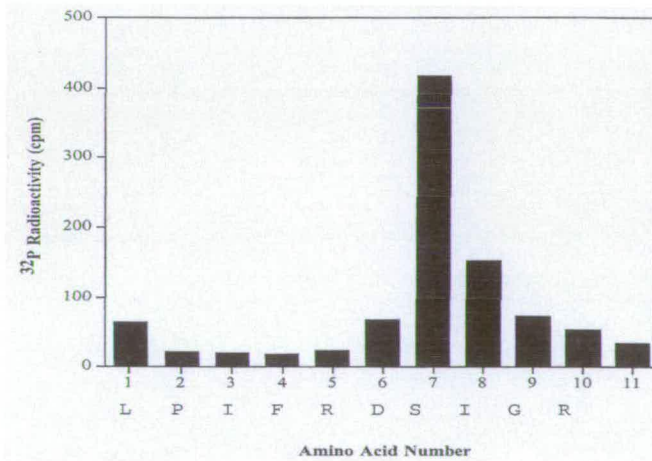
A**B**

Figure 3.10 Identification of serine 337 as the residue phosphorylated by lpl1p *in vitro*

A Peptides generated by tryptic digestion of phosphorylated Mad3 following the *in vitro* kinase assay using lpl1p were separated by HPLC and the ^{32}P containing fraction(4) was identified (and subsequently isolated for mass determination by MALDI-TOF MS). **B** Solid phase Edman sequencing of the recovered phosphopeptide was used to identify which residue was phosphorylated. Released ^{32}P was plotted against the primary amino acid sequence determined/inferred by mass-spectrometry (Najma Rachidi).

3.6 *In vivo* analysis of *mad3* mutants at putative sites of phosphorylation by Ipl1p

To assess the role of serines 303 and 337 (see figure 3.4) in Mad3p function in response to a lack of kinetochore-microtubule attachment, pKH535, created from the yeast centromere vector YcpLac22 (Hardwick and Murray, 1995) plus wild-type *MAD3* promoter and ORF, was mutated by site-directed mutagenesis to create S303 and S337 alanine and aspartate mutants independently, together and with the triple mutant at sites of putative phosphorylation by Cdc5p (S222/T229/S380). The mutants were transformed into a *mad3Δ* strain (KH173) for further analysis.

3.6.1 The mutation to aspartate of all putative Ipl1p phosphorylation sites and all Cdc5p phosphorylation sites within Mad3p renders cells sensitive to microtubule depolymerisation

The function of each mutant as a component of the spindle checkpoint was assessed by its ability to grow on YPDA solid medium containing benomyl. A *mad3Δ* strain (KH173) was separately transformed with each mutant plasmid (and controls) were spotted onto YPDA plates containing 0µg/ml, 10µg/ml, 12.5µg/ml and 15µg/ml benomyl in 10 fold dilutions.

The growth of the quintuple (S303/S337/S222/T229/S380D) aspartate mutant was slightly reduced on concentrations of benomyl equal to or higher than 12.5µg/ml compared to that of wild-type suggesting that it is partially deficient in spindle checkpoint function (Figure 3.11). All other varieties of mutant proved non-sensitive to the presence of benomyl, insinuating that phosphorylation of these residues is not important for Mad3p function as part of the spindle checkpoint response to microtubule depolymerisation.

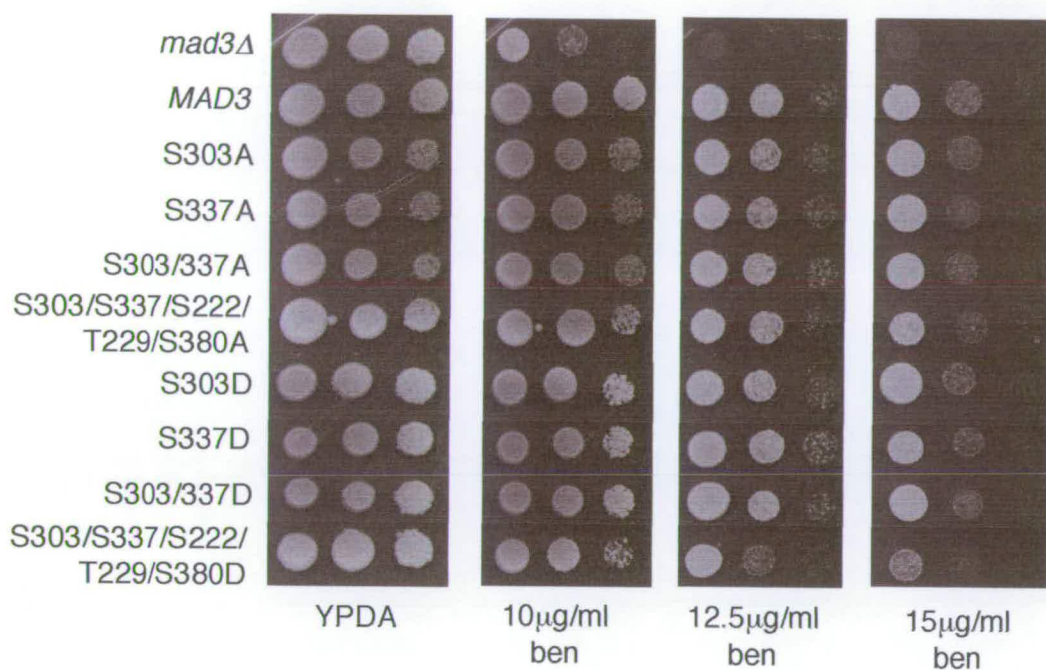


Figure 3.11 Analysis of Mad3p mutated at consensus sites for phosphorylation by Ipl1p and cdc5p

Serines 337 and 303 were mutated to either alanine (S303A, S337A, S303/337A) or aspartate (S303D, S337D, S303/337D) independently or in conjunction with S222, T229 or S380 (S303/S337/S222/T229/S380A or S303/S337/S222/T229/S380D respectively) were plated in serial dilutions onto media containing increased concentrations of benomyl.

3.6.2 Mad3p phosphorylation is not obviously affected by mutation of putative sites of Ipl1p and/or Cdc5p phosphorylation

The mutants and a wild-type (pKH535) control in a *mad3Δ* strain were grown to mid-log phase and arrested in metaphase, with an activated spindle checkpoint, by the addition of nocodazole. Total cell lysates of each culture were prepared for analysis by SDS-PAGE and Western blotting with an anti-Mad3p antibody.

Figure 3.12 shows that the band shift and proportion of the retarded band, representing phosphorylation, was unaffected in all alanine or aspartate mutants. From these results it is possible to deduce that the Mad3p band-shift seen was not due to phosphorylation at serines 303, 337, 222, 380 or threonine 229. Similarly, the proportion of phosphorylated Mad3p was not increased in the aspartate mutants. However, there was a subtle increase in the amount of S337D mutant protein and significantly more Mad3p in the quintuple aspartate mutant (quantified in Figure 3.13).

The results shown in Figures 3.11 and 3.12 suggest that mutation of Mad3p at putative sites of phosphorylation, to aspartate residues, by Ipl1p in combination with Cdc5p led to an increase in protein stability and caused increased sensitivity to benomyl.

3.6.3 Mad3p stability was increased in the quintuple S222/T229/S380/S303/S337D mutant

To quantify the amount by which Mad3p is stabilised in the 2 multiple aspartate mutant cells were grown to mid-log phase then arrested in nocodazole for 2 hours. Samples were prepared for analysis by SDS-PAGE. Samples from each mutant were loaded onto the gel in decreasing amounts for comparison with a wild-type control arrested under the same conditions.

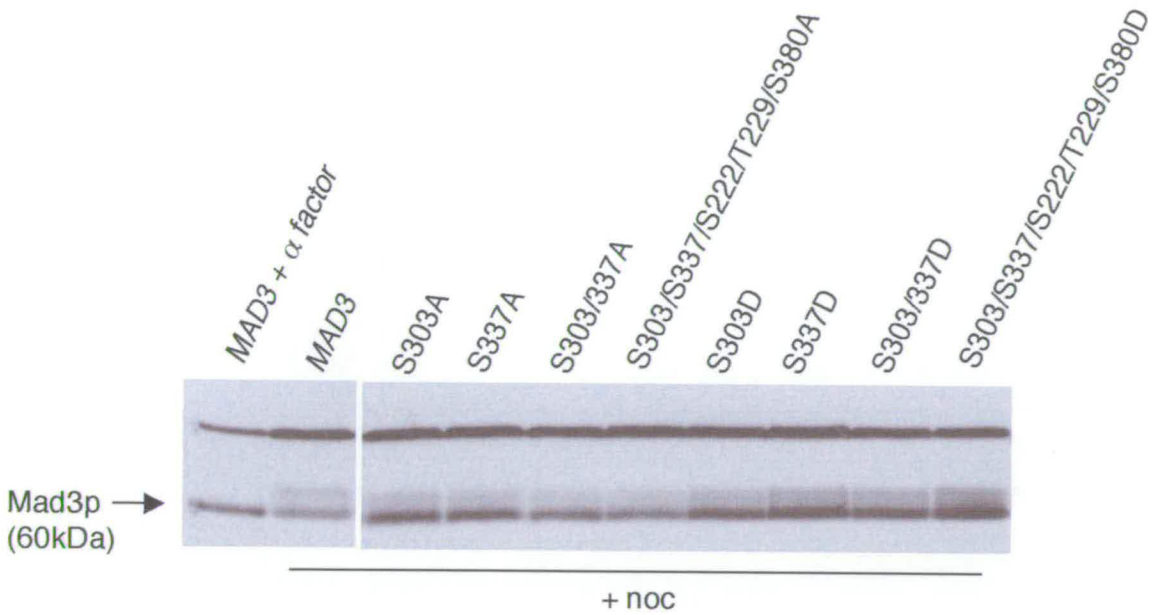


Figure 3.12 Mutation of serines within consensus sequences for phosphorylation by Ipl1p to aspartate slightly stabilise Mad3p. The effect is exaggerated when in combination with serines derived from consensus sequences for phosphorylation by Cdc5p.

Serines 337 and 303 were mutated to either alanine (S303A, S337A, S303/337A) or aspartate (S303D, S337D, S303/337D) independently or in conjunction with S222, T229 or S380 (S303/S337/S222/T229/S380A or S303/S337/S222/T229/S380D respectively) were grown in the presence of nocodazole for 2 hours. Samples were analysed by SDS-PAGE and Western blotting with anti-Mad3p antibody.

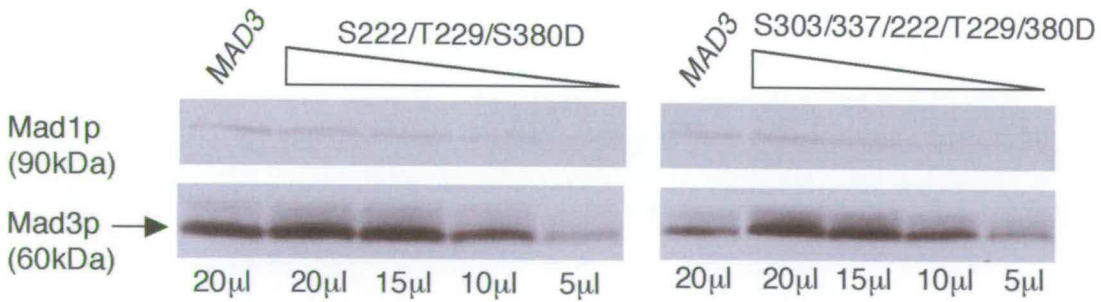


Figure 3.13 S222/T229/380D is approximately 1.5 fold and S303/337/222/T229/380D is approximately 3 fold more stable than wild-type Mad3p.

S222/229/380D and S303/337/222/229/380D mutants were grown in the presence of nocodazole and analysed by SDS-PAGE and Western blotting using anti-Mad3p antibody and anti-Mad1p antibody as a loading control. Serial dilutions were loaded to analyse the increase in stability seen.

Western blotting was performed using anti-Mad1p antibodies as a loading control and anti-Mad3p antibodies.

The levels of protein visualised in the mutants were compared to the amount of protein visible in the wild-type and the increase in stability was calculated from knowing how much of each mutant was loaded when the amount of Mad3p was similar to that of wild-type.

Protein levels of the triple S222/T229/S380D mutant mimicked wild-type levels when between 10 μ l and 15 μ l of the sample was loaded. Protein levels of the quintuple S222/T229/S380/S303/S337D mutant mimicked wild-type levels when between 5 μ l and 10 μ l of the sample was loaded (Figure 3.13).

It is therefore possible to conclude that the triple aspartate mutant at putative Cdc5p phosphorylation sites increased Mad3p stability approximately 1.5-fold and the combination quintuple mutant increased stability approximately 3-fold when compared to wild-type levels by eye. Subsequently, as the band-shift in these mutants remains unaffected (Figure 3.11 and 3.12) the phenotype may be attributed to the increase in protein stability.

3.7 Discussion

The initial experiments in this chapter described the post-translational modification of Mad3p in terms of its temporal regulation and nature.

Careful analysis of the Mad3p profile following visualisation by SDS-PAGE and Western blotting revealed that retarded forms of the protein were visible through an unperturbed cell cycle and in specific cell cycle arrests. The nature of the modification

was determined to be phosphorylation as the retarded forms of Mad3p were removed following treatment with Lambda phosphatase.

Mad3p phosphorylation increased gradually through the cell cycle and peaked at a point that corresponded to high levels of Clb2 in the cell, indicative of mitosis. In the yeast cell cycle S phase and mitosis occur concurrently though modification present in an HU-induced S-phase arrest was increased in either a nocodazole induced, or APC/C mutant arrest, suggesting that modification continues through until at least metaphase. However, in a G1 arrest (following the addition of alpha-factor), no modification was visible suggesting that Mad3p is abruptly de-phosphorylated between the metaphase to anaphase transition and G1, which is consistent with unpublished data that demonstrates a reduction in Mad3p phosphorylation when the phosphatase Cdc14p is overexpressed (Simonetta Piatti, *pers comm.*). Comparison of the two metaphase arrests, one with and the other without checkpoint activation, revealed no specific modification visibly induced in response to checkpoint activation. Though without performing 2D gel analysis of the two phosphorylated species or gaining better resolution of the gel shift, it is impossible to tell if the same species of modified protein are present under both conditions. The result also gives no indication as to the kinase responsible.

Though present in a normal cell cycle, the post-translational regulation of Mad3p may play a role in checkpoint function. Mad3p forms a constitutive complex with Bub3p and upon checkpoint activation is a component of the MCC that also contains Bub3p, Mad2p and Cdc20p (Hardwick et al., 2000). In higher eukaryotes and *S. pombe*, it has also been shown to localise to kinetochores in a Bub1p/Bub3p dependent manner. Bub1p is also a kinase. To address the influence of complex formation and inferred localisation to kinetochores, the degree of phosphorylation was analysed in mutants lacking several checkpoint components or a *mad2-1* allele encoding a truncated version of Mad2p, that behaves as a null mutant, and using a *mad3-1* allele that can no longer

bind Bub3p (Hardwick et al., 2000). Three different conditions (HU, nocodazole and a *cdc26Δ* mutant) under which Mad3p phosphorylation is visible, were used to ensure that different checkpoint components were not required for phosphorylation at different cell cycle stages or in the presence/absence of different modes of checkpoint activation. From the results it was possible to conclude that under all conditions Mad3p phosphorylation is unaffected by its complex formation, localisation and is not phosphorylated by Bub1p.

At this point the evidence suggests that the modification of Mad3p seen in a normal mitosis is akin to that experienced upon checkpoint activation as the same retarded forms of Mad3p are visible and their dependency upon other checkpoint components is identical and does not require the kinase activity of Bub1p.

The subsequent experiments were designed to identify sites within Mad3p are phosphorylated and to determine or infer the kinase responsible. Though large-scale TAP purifications have proved an invaluable tool in other studies for identifying phosphorylation sites *in vivo*, unfortunately the approach was unsuccessful in this project as the purification protocol rendered Mad3-TAP unstable. However, future experiments using TAP-tagged Bub3p to pull-down associated Mad3p may elucidate more information should it prove successful. The temporal, mitotic nature of Mad3p phosphorylation and its function in a mitotic checkpoint led me to analyse the primary amino acid sequence of Mad3p for the presence of consensus sequences for phosphorylation by several important mitotic kinases: Cdc28p, Cdc5p and Ipl1p. Though Mps1p has a role in the spindle checkpoint there was little information available to allow a consensus sequence for phosphorylation to be derived. In the future it may be interesting to analyse the effect of Mps1p on Mad3p phosphorylation through the use of a strain sensitive to an analogue of ATP that acts as competitive inhibitor and represses Mps1p kinase activity.

This approach was implemented as it had recently been demonstrated that Mad3p was a substrate for Cdc5p and Ipl1p *in vitro* (Najma Rachidi *pers. com.*) though no sites had yet been identified. The role of these kinases is known to include regulating other kinases that may be involved in Mad3p phosphorylation. Therefore, the use of non-functional alleles and the subsequent analysis of any effect on Mad3p phosphorylation may only elucidate an indication of gross requirement for a specific kinase. In contrast, mutational analysis of predicted phosphorylation sites within Mad3p allowed direct effects to be analysed.

The preferential phosphorylation of sequences surrounding Scc1p cleavage sites by Cdc5p (Alexandru et al., 2001) led us to the derivation of a consensus sequence for phosphorylation by Cdc5p as [D/E] X [S/T] [I/L/V/M] [D/E]. Interestingly, one such sequence is conserved between Mad3p/BubR1s in different species and the final glutamate residue when mutated to lysine abrogates Mad3p-Bub3p binding in budding yeast and subsequently gives rise to a benomyl sensitive phenotype. As a result, analysis of serine 380 within this sequence was analysed independently and in conjunction with the two other identified sites (serine 222 and threonine 229).

While mutation of all the phosphorylatable residues within these sequences simultaneously or serine 380 independently to alanine did not obviously affect protein function or alter the gel mobility of Mad3p, when changed to aspartate the triple mutant cells become sensitive to benomyl and the amount of the protein appeared to be increased by approximately 1.5-fold over the wild-type protein. No effect was seen in the serine 380 mutant on its own. The simplest explanation for these results would be that the triple aspartate mutant was no longer checkpoint proficient. However, only one criterion for checkpoint deficiency has been assayed. Complete analysis would require biochemical determination or microscopy analysis of premature sister chromatid separation and rapid death upon exposure to nocodazole and microcolony analysis. At the time of writing it is not possible to exclude the possibility that these cells arrest

competently but cannot exit this arrest or that they re-attach their microtubules following microtubule depolymerisation. If either of these scenarios were the case, one would expect sister chromatids to remain cohesed and cells may recover from short-term microtubule depolymerisation. If there were a problem in re-attachment of microtubules following the removal of a microtubule depolymerising agent, it would be detected using a biorientation assay that can identify sufficient tension across kinetochores. Further analysis may also include mutating sites that putatively confer phosphorylation by Cdc28p. Mutation of such residues would need to be carefully analysed as the motif required within a substrate for binding and subsequent phosphorylation by Cdc5p minimally requires the consensus sequence and phospho-residue generated by Cdc28p activity for POLO box binding and subsequent phosphorylation.

Ipl1p is required for the spindle checkpoint response to a lack of tension at kinetochores (Biggins and Murray, 2001; Stern and Murray, 2001) though it is not required for an arrest in response to a lack of kinetochore-microtubule attachment. Analysis of the Mad3p primary amino acid sequence revealed two sites that fit the consensus sequence for Ipl1p phosphorylation, [R/K] X [S/T] [I/L/V/M] published by Cheeseman *et al.*, (2002). The experiments performed here demonstrate that Ipl1p kinase activity is required for phosphorylation of Mad3p upon a reduction of tension at the kinetochore but did not greatly affect the band shift seen in a mitotic arrest following the addition of nocodazole. Interestingly, the abolition of Ipl1p function removed all phosphorylation of Mad3p under these conditions, suggesting a possible role of Ipl1p in global kinase activity regulation. The effect of Glc7p, a regulatory subunit of the PP1 phosphatase, was also analysed as it has been described to work in opposition to Ipl1p kinase. In a *glc7-10* mutant the slowest migrating band of Mad3p was enriched slightly and in turn the fastest migrating band had reduced intensity. These results suggest that PP1 is in part responsible for Mad3p dephosphorylation, but though its role with respect to Ipl1p has been characterised, it is still possible that it dephosphorylates sites

phosphorylated by other kinases. For an indication of whether the phosphorylation of Mad3p is important for a tension-induced cell cycle delay, it was first determined that Mad3p was required for the delay seen in a *mcd1-1* mutant. In parallel, kinase assays were utilised to determine that Mad3p is a direct substrate of Ipl1p *in vitro* (Najma Rachidi).

Subsequently *in vivo* analysis of *mad3* mutants at the two Ipl1p sites within consensus sequences sufficient for phosphorylation was undertaken. This included serine 337 identified as a site phosphorylated *in vitro*. To date, work has focused on the function and analysis of these mutants in the absence of microtubule – kinetochore attachment. Though a phenotype was only seen when both putative Ipl1p sites and the three putative Cdc5p sites within Mad3p were mutated to aspartate, the single mutation of serine 337 to aspartate did appear to slightly increase the stability of Mad3p even though a phenotype was not apparent in the assays performed. The combination of aspartate mutants, however, greatly increased the stability of Mad3p so it was now approximately 3-fold more stable than the wild-type protein (compared with the triple mutant of putative Cdc5 sites that increases stability approximately 1.5-fold). Future experiments to characterise the quintuple mutant phenotype further would be as described for the triple aspartate mutant discussed earlier.

The major focus of further investigations would be the function of the serine 337 mutants *in vivo* when the spindle checkpoint is activated by a lack of tension at kinetochores. Through the analysis of cell cycle progression or delay when wild-type Mad3p is replaced with alanine or aspartate versions of serine 337, the importance of Mad3p phosphorylation or de-phosphorylation will be addressed in the *mcd1-1* mutant or a strain, recently received, that allows transcription of *MCD1* to be shut off (*GALMCD1*). It is also our intention to confirm the *in vitro* kinase assay result that highlighted serine 337 as the only residue phosphorylated by Ipl1p. It is possible that

in a Mad3-intein S337A mutant Ipl1p would alternatively phosphorylate serine 303 within the other consensus sequence.

In addition, Najma Rachidi has purified phospho-Mad3p specific antibodies that have been preliminarily tested and shown to be specific for Mad3p phosphorylated at serine 337 *in vitro*. Application of these antibodies will allow the confirmation of phosphorylation at this residue *in vivo* and the conditions under which it occurs.

The increase in stability viewed in putative phosphorylation sites mutated to aspartate suggests complex post-translational regulation of Mad3p by at least two different processes that are intricately linked. The effect of stabilising Mad3p, potentially by mutation of two conserved KEN boxes, is addressed and discussed in the following chapter.

Chapter 4

The role of KEN boxes in Mad3p

It has been demonstrated that KEN boxes within a protein can act as a recognition signal for ubiquitination the APC/C, that targets it for destruction via the 26S proteasome (Pfleger and Kirschner, 2000). Substrates that contain a KEN box are thought to be specifically recognised by APC/C^{Cdh1}. In support of this theory, direct binding between Cdh1p and the KEN box motif and the motif's requirement for degradation of the substrate protein in an APC/C dependent manner has also been shown (Burton et al., 2005).

4.1 Mad3p contains conserved KEN boxes

A common and distinguishing feature of all Mad3 and BubR1s is the presence of a conserved KEN box near the N-terminus. In addition, Mad3 in yeasts contain a conserved KEN box towards their C-terminus that upon alignment using Clustal-X does not align directly with a second KEN box found in higher eukaryotic Mad3/BubR1 sequences (Figure 4.1). BubR1s also contain a sequence similar to that of a destruction box RSSLAEKLS.

4.1.1 Mutagenesis to make pKH535 KEN mutants

To assess the role of the KEN boxes in Mad3p stability and function, pKH535, created from the yeast centromere vector YcpLac22 plus wildtype *MAD3* promoter and ORF, was mutated by site-directed mutagenesis to create KEN30AAA, KEN296AAA and a double KEN30/296AAA mutant.


```

ScMad3  MKAYAKKRISYMPSSPSQNVINFEETQKENILPLKEGRSAAALSK-----AIHQ  51
SpMad3  -----MEPLDAGKNVWVHMDVIEQSKENIEPRKAGHSASALAK-----SSSR  41
AnSLDA  -----MAATGDLIDFDIIENQKENIQSLPGRSARELARIFSPRDPDKLSS  47
MmBub1B -----MAEASEAMCLEGAEWELSKENIQPLRHGRVMSTLQG-----ALAK  40
HsBubR1 ----MAAVKKEGGALSEAMSLEGDEWELSKENVQPLRQGRIMSTLQG-----ALAQ  47

ScMad3  P-----LVEINQVKSSFQRLIDELPALSDPITLYLEYIKWLNAYPQGGNSKQSGMLTL  106
SpMad3  NHTEKEVAGLQKERMGHERK-IETSESLDDPLQVWIDYIKWTLDNFPQGE-TKTSGLVTL  99
AnSLDA  PSPNDTRTLNDAIRQEEAE-LQAIGESDDPLDIYDRYVKWALNAYPTAQATPESGLLPL  106
MmBub1B QESAGHTALQQQKR-AFESE-IRFYSG-DDPLDVWDRYINWTEQNYPPQGG--KESNMSAL  96
HsBubR1 ESACNNT--LQQQKRAFYE-IRFYTG-NDPLDVWDRYISWTEQNYPPQGG--KESNMSTL  101

ScMad3  LERCLSHLKDLEERYNDVRFKLIWFYIELFTRNSFMESRDIFMYMLRNGIGSELASFYE  166
SpMad3  LERCREFVRNPLYKDDVRYLRIMWQVYNYID----EPVELFSFLAHHHIGQESSIFYE  154
AnSLDA  LERAVKSFLLSSPHYKNDPRYLKWLWHYIRLFS----SPRETFAFMARHHVGEGLALFYE  162
MmBub1B VERAIEALQGETRYNDPRFLSLWIKLGHLCN----EPLDMYSYLQSQGIGVSLAQFYI  151
HsBubR1 LERAVEALQGEKRYYS DPRFLNLWLKLGRLCN----EPLDMYSYLHNQIGVSLAQFYI  156

ScMad3  EFTNLLIQKEKFQYAVKILQLGKIKNKARPKNVLEDRLNHLREL-----  210
SpMad3  EYANYFESRGLFQKADEVYQKGRMKAKPFLRFQQKYQQFTHR-----  198
AnSLDA  EFAAWLESVGRWTOADEVYRLGIDREARPTERLIRKYGEFQRRY-----EQQ  209
MmBub1B SWAEEYEARENFKKADII FQEGIERKAEPLDRLQSQHRQFQSRVSRQAFALG-NEEEEA  210
HsBubR1 SWAEEYEARENFRKADAI FQEGIQQKAEPLERLQSQHRQFQARVSRQTLLEKEKEEEEV  216

ScMad3  -----GENNIQLGNEISMSLESTVLGKTRSEFVNR-LELANQNGTSSDVNLTKNN  260
SpMad3  -LEFAPQSFSSN-----TNSVNPLQTFESTNIQEISQSRTKISKPKFKFS  243
AnSLDA  PQDNGPSSPALPAVRPALAAKVPDFASSAAAPTDPQSQQGSRTTAPKTKSGKP--KMA  267
MmBub1B LEPSEPQRSSLAELKSRGKMARAPISRVGSALKAPGQSRGFLNAVQPVHGNRRITVFD  270
HsBubR1 FESSVPQRSTLAELKSKGKKTARAPIIRVGGALKAPSQNRGLQNPFPQMQNNSRITVFD  276

ScMad3  VFVD-----GEESDVELFETPNRGVYRDG-----WENFDLKAERNKENNLRISLLEA-  307
SpMad3  VYSD-----ADSGKDG-QPGTWQTLGTVDQRRKENN-----ISA-  277
AnSLDA  IFTD-----TEPAA----NQPALGAQTKG-----WDSLESRHDRRKENQ-----IEA-  305
MmBub1B ENADTASRPELSKPVAQPWMAAPPVPRAKENELQPGPWSTDRPVGRRPHDNPASVTSIPSV  330
HsBubR1 ENADEASTAELSKPTVQPWIAPPMPRAKENELQAGPWNTGRSLEHRPRGNTASLIAVPAV  336

ScMad3  ----NTNLGELKQHEMLSQKKRPYDEKLPIFRDSIG-----RSDPVYQMINTKD  352
SpMad3  ----TSWVGE--KLPLKSPRKLDPGLGKFQV-----  301
AnSLDA  ----KPWAGE----TLKAGRKAPPEKLAVFRDESKSDLPTKEEMQSNPVPEHRIEAVN  357
MmBub1B LPSFPTYVEESAQQTVMTPCKIEPSINHVLSTRKPG-----REEGDPLQRVQSHQQ  381
HsBubR1 LPSFPTYVEETAQQPVMTPCKIEPSINHILSTRKPG-----KEEGDPLQRVQSHQQ  387

ScMad3  QKPEKIDCNFKLIYCEDEES---KGRLEFSLEEVLAISRNVYKR-----  394
SpMad3  -----HCDEEVS-----  308
AnSLDA  PRTGRRE---RVFVDLDAVYPDYKNPSIEVSFEELRAMKRGWMDRDWRKKGPLKQISGNA  414
MmBub1B GCEEKKE---KMMYCKEKIY---AGVGEFSFEEIRA---EVFRKCLKERR-----  422
HsBubR1 ASEEKKE---KMMYCKEKIY---AGVGEFSFEEIRA---EVFRKCLKEQR-----  428

```

Figure 4.1 Alignment of Mad3p/BubR1 across species reveals conserved KEN boxes and D-boxes

Alignment of Mad3p/BubR1 across species using Clustal-X. KEN boxes are highlighted in red, D-boxes in blue. Sc=*S. cerevisiae*; Sp=*S. pombe*; An=*Aspergillus niger*; Mm=*M. musculus*; Hs=*H. sapiens*.

4.2 *mad3* KEN mutants are sensitive to microtubule depolymerisation

For the following experiments a *mad3Δ* (KH173) strain was transformed with either an empty vector (YCpLac22), wild-type *MAD3* (pKH535), KEN30AAA, KEN296AAA or the double KEN30/296AAA.

4.2.1 *mad3* KEN mutants do not grow on medium containing benomyl

To assess the sensitivity of the mutants to benomyl, a microtubule depolymerising drug *mad3Δ*, *MAD3*, KEN30AAA, KEN296AAA and KEN30/296AAA strains were spotted in 10-fold dilutions onto YPDA plates containing 0μg/ml, 10μg/ml 12.5μg/ml and 15μg/ml benomyl.

Figure 4.2A shows that KEN30AAA, KEN296AAA and KEN30/296AAA are sensitive to the presence of benomyl. Equal growth of all strains on plates containing 0μg/ml benomyl showed that the mutants have no obvious growth defect and equal amounts of cells are assayed throughout the experiment. The *MAD3* strain grew well on all concentrations of benomyl. The growth of strains expressing KEN30AAA, KEN296AAA and KEN30/296AAA on plates containing increasing amounts of benomyl was similar to that of the *mad3Δ* strain and was reduced compared to the strain expressing wild-type Mad3p.

4.2.2 Microcolony analysis of KEN30AAA reveals a classic checkpoint phenotype

To analyse further the growth of KEN30AAA and KEN296AAA mutants in the presence of benomyl, microcolony assays were performed.

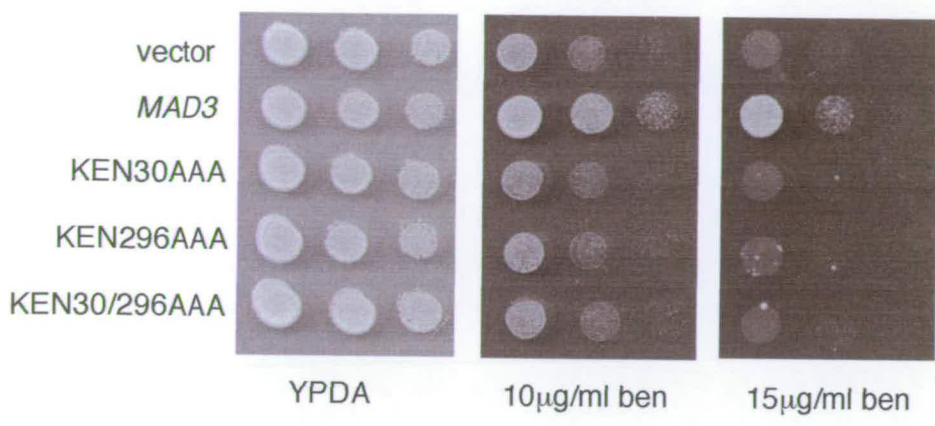
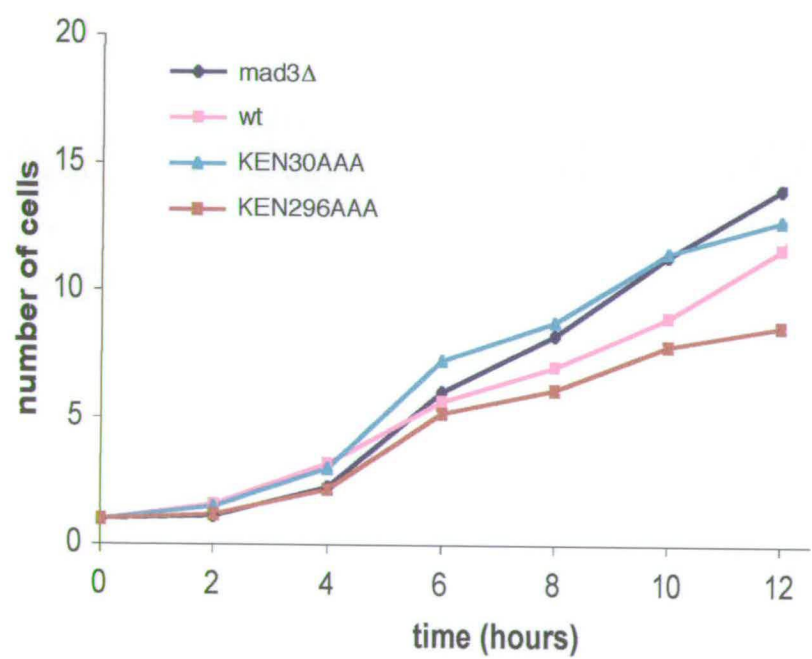
A**B**

Figure 4.2 Mad3 KEN box mutants are sensitive to benomyl and KEN30AAA displays a checkpoint defective phenotype

A *Mad3* mutated at KEN30, KEN296 and both KEN30 and 296 to alanine, plus controls, were transformed in to a *mad3Δ* strain (KH173) and plated on to media containing increasing concentrations of benomyl in serial dilutions. **B** A microcolony assay was performed, using the same strains as in A, to assess their division in the presence of 12.5 µg/ml benomyl over 12 hours.

The cell division rate in the presence of benomyl of KEN30AAA and KEN296AAA was compared to *MAD3* and *mad3Δ* controls. Previous studies have demonstrated that checkpoint mutants, including *mad3Δ* mutants, continue to divide in the presence of benomyl, but subsequently die (Li and Murray, 1991). *MAD3* cells however detect the presence of benomyl and delay division until the checkpoint is satisfied and accurate chromosome segregation can be achieved.

Individual *mad3Δ*, *MAD3*, KEN30AAA and KEN296AAA cells were picked onto YPDA plates containing 12.5μg/ml benomyl. Cell divisions were monitored over 12 hours. Approximately 40 representatives of each genotype were analysed, an average of the results collected is shown in Figure 4.2B.

The *mad3Δ* and KEN30AAA cells divided at a similar rate, indicative of a checkpoint deficient phenotype. They experienced faster cell division; reflected in the increased cell number seen, when compared to wild-type, after 8 and 10 hours.

MAD3 and KEN296AAA cells divided slower than the *mad3Δ* and KEN30AAA cells. After 12 hours KEN296AAA almost stopped dividing at a micro-colony cell number average of 8.5 cells and only reached an average of 9.9 cells after 14 hours. In contrast, *MAD3* cells continued to divide slowly and by 14 hours had an average microcolony cell number of 13.5.

From these results it was concluded that the KEN30AAA mutant behaved as a classic spindle checkpoint mutant but the KEN296AAA mutant had a different phenotype and did not behave as a typical checkpoint mutant or as wild-type.

4.2.3 All KEN box mutants die rapidly following exposure to the microtubule depolymerising drug nocodazole

For the following experiments a *mad3Δ* strain with GFP-marked chromosome III (EK13) strain was transformed with either an empty vector (YCpLac22), wild-type *MAD3* (pKH535), KEN30AAA, KEN296AAA or the double KEN30/296AAA. The GFP-marked chromosome III has a tandem array of *lacO* integrated at its centromere, to which GFP-tagged *lacI* is bound, thus 'marking' the chromosome with GFP.

Strains were grown to mid-log phase and arrested in G1 using alpha-factor. Cells were counted using a hemacytometer so approximately 500 cells were plated out at time zero, when alpha factor was removed and nocodazole was added. The same volume of cells was then plated at 2 hour intervals for 6 hours onto YPDA. At time zero and after 4 hours, cells were also collected and fixed to allow visualisation of GFP-marked chromosome III and determination of whether sister chromatids remained cohesed or had separated (see section 4.2.4). Plates were incubated at 30°C for 2 days until colonies were visible and could be counted.

Figure 4.3A shows the percentage of cells that were still viable (no. of cells on the plate/total number of cells on plate from time zero x 100) after the said time of exposure to nocodazole. All mutant strains experienced rapid cell death at the same rate as a *mad3Δ* strain, and by 4 hours viability had dropped to approximately 1%.

4.2.4 All KEN box mutants experience premature separation of sister chromatids in the presence of nocodazole

A characteristic of spindle checkpoint deficient strains is premature separation of sister chromatids when challenged with a microtubule depolymerising agent.

Cells collected from the rate of death assay performed in the previous section were examined using fluorescence microscopy to visualise GFP marked chromosome III.

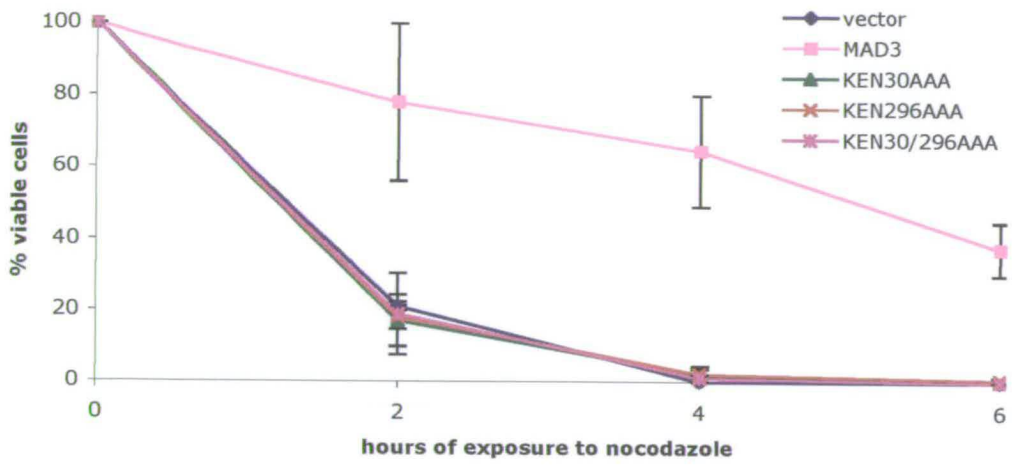
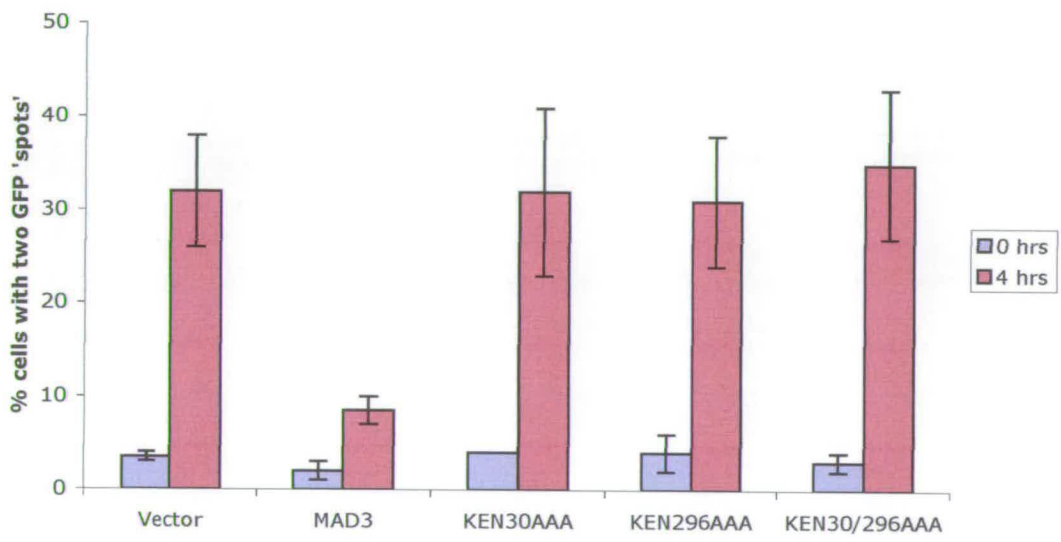
A**B**

Figure 4.3 Mad3 KEN box mutants die rapidly following exposure to nocodazole and precociously separate sister chromatids

A Mad3 mutated at KEN30, KEN296 and both KEN30 and 296 to alanine, plus controls in a *mad3Δ* GFP marked chromosome strain (EK13) were grown in the presence of nocodazole for 6 hours. Samples were taken every two hours and plated onto nocodazole-free media. Colonies were counted and viability is represented as a percentage of the total number of original cells plated without exposure to nocodazole. **B** Separation of sister chromatids was assessed in the different strains after 4 hours in nocodazole. 2 dots represents cells with separated sisters, represented as a percentage of the total number of cells.

Un-separated sister chromatids showed one GFP ‘spot’ whereas separated sister chromatids had two GFP spots visible per cell.

After four hours in nocodazole the wild type strain demonstrated only a small percentage of cells with separated sister chromatids (~8%). However, *mad3Δ* cells and all mutants experienced sister separation of approximately 32% (Figure 4.3B).

The combined result of the rate of death assay presented in Figure 4.3A and the increased sister separation seen in the mutants (Figure 4.3B) suggests that none of the mutants can arrest in the presence of nocodazole and subsequently die from resulting chromosome segregation defects.

4.3 KEN296AAA displays a phenotype that is dominant

For the experiments in this section a wild-type strain (KH186) was transformed with either an empty vector (YCpLac22), wild-type *MAD3*, KEN30AAA, KEN296AAA and KEN30/296AAA. These transformations resulted in strains that contained one wild-type copy of *MAD3* plus any extra plasmid borne-copy that had been introduced.

4.3.1 KEN296AAA mutants remain sensitive to benomyl in the presence of wildtype Mad3p

To assess the sensitivity of the mutants to benomyl in the presence of a wild-type copy of *MAD3*, the empty vector, *MAD3*, KEN30AAA, KEN296AAA and KEN30/296AAA strains were spotted onto YPDA plates, in ten-fold dilutions, containing 0μg/ml, 10μg/ml, 12.5μg/ml and 15μg/ml benomyl.

Figure 4.4A demonstrates the subtle dominant effect of KEN296AAA on an otherwise wild-type strain in the presence of benomyl. Equal growth of all strains on plates containing 0μg/ml benomyl showed that the mutants have no obvious growth defect

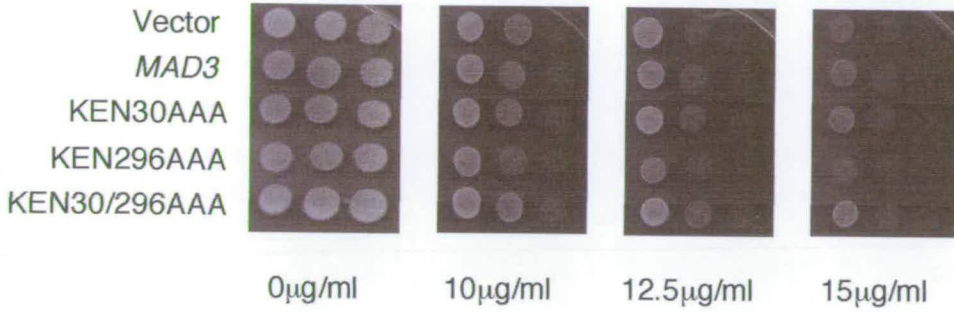
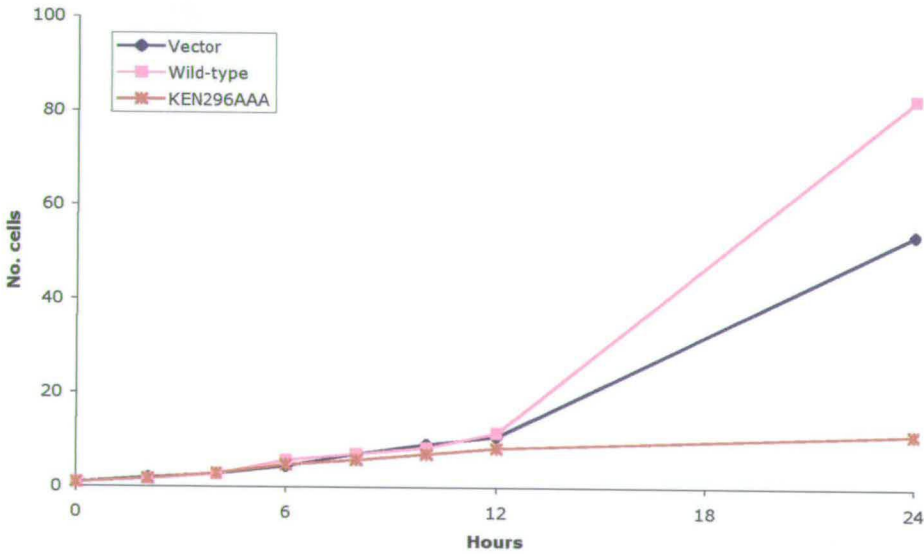
A**B**

Figure 4.4 KEN296AAA demonstrates a subtle increase in sensitivity to microtubule depolymerisation

A Mad3 mutated at KEN30, KEN296 and both KEN30 and 296 to alanine in a *MAD3* strain (KH186) were plated on to medium containing increasing concentrations of benomyl in serial dilutions. **B** A microcolony assay was performed on KEN296AAA to assess its division in the presence of 15 μg/ml benomyl in a *MAD3* background over 24 hours.

and equal amounts of cells were assayed throughout the experiment. Interestingly, cells that expressed KEN296AAA demonstrated subtly reduced growth on plates containing 10-15µg/ml benomyl in comparison to strains that expressed only endogenous Mad3p or endogenous Mad3p plus extra copy of wild-type *MAD3* or KEN30AAA. Thus, expression of KEN296AAA, even in the presence of wild-type Mad3p, rendered cells with a small increase in sensitivity to the presence of benomyl.

4.3.2 KEN296AAA in the presence of wildtype Mad3p cannot divide beyond 3 divisions on medium containing benomyl

To analyse further the growth of KEN296AAA mutants in the presence of benomyl, a microcolony assay was performed.

The cell division rate in the presence of benomyl and endogenous Mad3p of KEN296AAA was compared to strains containing an extra copy of *MAD3* or the empty vector.

Individual cells were picked onto YPDA plates containing 15µg/ml benomyl. Cell divisions were monitored over 24 hours. Approximately 40 representatives of each genotype were analysed, an average of the results collected is shown in Figure 4.4B. In the wild-type *MAD3* strain plus empty vector, *MAD3* or KEN296AAA, cells divided at a similar rate initially. However, after 8-10 hours KEN296AAA growth slowed at an average of 8 cells per micro-colony whereas the other strains continued to divide. The KEN296AAA mutants did not appear to divide further as the average number of cells per colony was (nearly) the same after 24 hours.

4.3.3 KEN296AAA dies rapidly following exposure to the microtubule depolymerising drug nocodazole with endogenous Mad3p present

For this experiment a *MAD3* strain with GFP-marked chromosome III (SBY215) was transformed with either an empty vector (YCpLac22), wildtype *MAD3* or KEN296AAA. These transformations resulted in strains that contained one wild-type copy of *MAD3* plus any extra plasmid-borne copy that had been introduced.

Strains were grown to mid-log phase and arrested in G1 using alpha-factor. Cells were counted using a hemacytometer so approximately 500 cells were plated at time zero, when alpha factor was removed and nocodazole was added. The same volume of cells was then plated out at 2 hour intervals for 6 hours onto YPDA. At time zero and after 6 hours, cells were also collected and fixed to allow visualisation of GFP-marked chromosome III and determination of whether sister chromatids remained cohesed or had separated (see section 4.3.4). Plates were incubated at 30°C for 2 days until colonies were visible and could be counted.

Figure 4.5A shows the percentage of cells that were still viable (number of cells on the plate/total number of cells on plate from time zero x 100) after the said time of exposure to nocodazole.

Cells with one or two copies of *MAD3* maintained at least 75% cell viability at all timepoints but KEN296AAA displayed reduced viability compared to the controls immediately. After 6 hours of exposure to nocodazole, viability in cells expressing KEN296AAA had dropped to only 20% (Figure 4.5A).

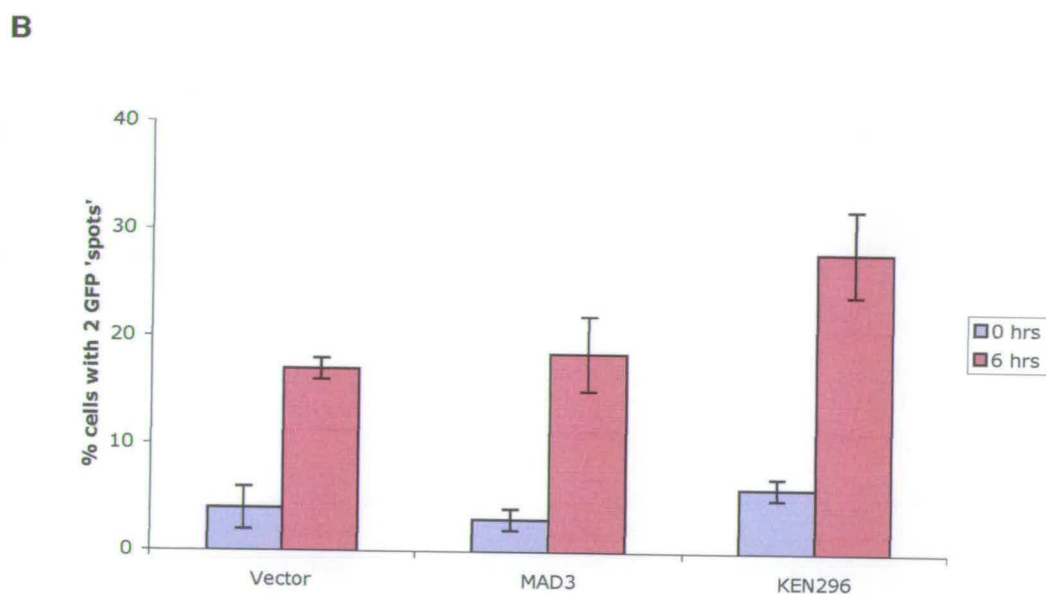
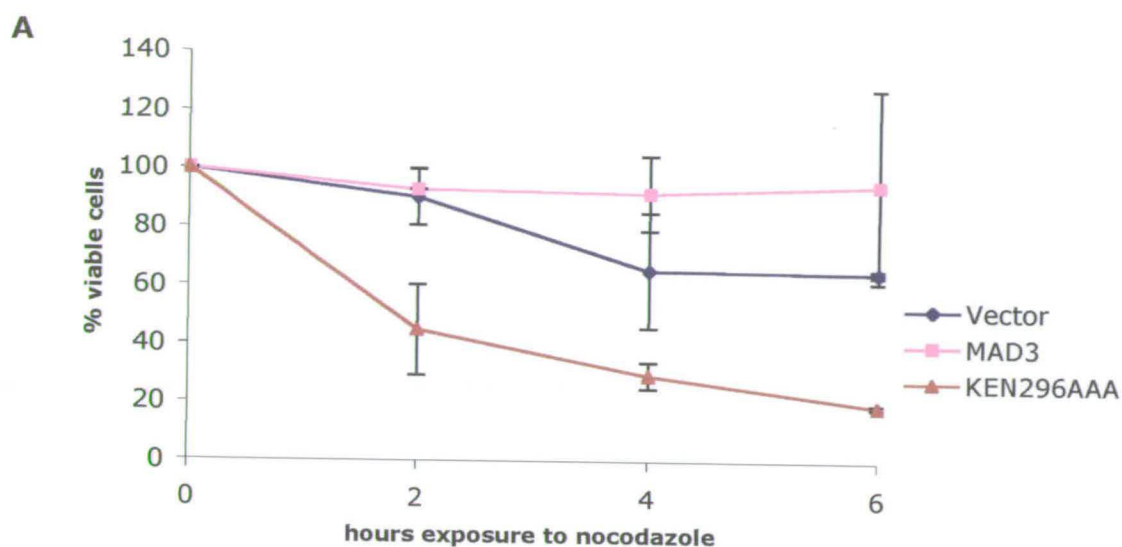


Figure 4.5 KEN296AAA dies rapidly following exposure to nocodazole and precociously separates its sister chromatids in the presence of *MAD3*

A Mad3 KEN296 mutated to alanine in a *MAD3* strain with GFP-marked chromosomes (SBY215) was grown in the presence of nocodazole for 6 hours. Samples were taken every two hours and plated onto nocodazole-free media. Colonies were counted and viability is represented as a percentage of the total number of original cells plated without exposure to nocodazole. **B** Separation of sister chromatids was assessed in KEN296AAA after 6 hours in nocodazole. 2 dots represents cells with separated sisters, represented as a percentage of the total number of cells.

4.3.4 KEN296AAA experiences premature separation of sister chromatids in the presence of nocodazole and endogenous Mad3p

Cells collected from the rate of death assay performed in the previous section were examined using fluorescence microscopy to visualise GFP-marked chromosome III. Unseparated sister chromatids showed one GFP 'spot' whereas separated sister chromatids had two GFP 'spots' visible per cell.

After six hours in nocodazole, strains transformed with an empty vector or extra copy of *MAD3* only approximately 18% of cells demonstrated separated sister chromatids. However, cells expressing KEN296AAA and endogenous Mad3p experienced sister separation of approximately 28% (Figure 4.5B).

The combination of results show that KEN296AAA displays a dominant phenotype in wildtype cells that is similar to that seen in a *mad3Δ* background, though not as severe.

4.4 Role of APC/C and its activators, Cdc20p and Cdh1p, in Mad3p stability

4.4.1 Mad3p is stabilised in APC/C mutants

APC/C mutants *cdc23-1* and *cdc16-1* are temperature sensitive alleles of two essential APC/C components. At the restrictive temperature (37°C), the mutants arrest in mitosis at the metaphase-anaphase transition.

cdc23-1 (ADR719A) and *cdc16-1* (ADR34) were grown to mid-log phase at 23°C when nocodazole was added. Half the cells were then grown at 23°C and half shifted to 37°C for 2 hours to inactivate the APC/C components. Nocodazole was added to ensure that cells grown at both temperatures were arrested at the same point of the cell cycle for analysis. Total protein lysate samples were prepared from harvested cells for

analysis by SDS-PAGE and Western blotting to assess the stability of Mad3p in these mutants using an anti-Mad3p antibody.

Visualisation of the samples, shown in Figure 4.6A, demonstrates that Mad3p is enriched in each of the APC/C mutants when grown at their restrictive temperature.

4.4.2 Mad3p stability is unaffected by Cdh1p and Cdc20p mutants

Cdc20p and Cdh1p are thought to confer substrate specificity for proteins degraded by the APC/C. It is possible that Mad3p requires the function of either or both of these proteins for degradation mediated by the APC/C.

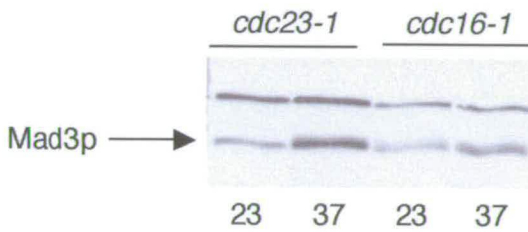
Cdh1p is non-essential for cell viability or a mitotic arrest induced by the addition of a microtubule depolymerising agent, but is required for the destruction of the cyclin Clb2p during anaphase (Schwab et al., 1997). To address the role, if any, of Cdh1p in Mad3p stability, Mad3p levels were compared between a *cdh1Δ* strain and a *CDH1* strain arrested in mitosis.

cdh1Δ (331) and wild-type (KH186) cells were grown to mid-log phase. Nocodazole was then added to arrest both strains in mitosis. Cells were harvested and prepared for analysis by SDS-PAGE and Western blotting with an anti-Mad3p antibody.

Visualisation of Mad3p revealed that levels of Mad3p were unaffected in the absence of Cdh1p (Figure 4.6B).

The role of Cdc20p was addressed in two ways: First using a temperature sensitive allele, *cdc20-1*; second, using a strain containing *GALCDC20* to allow shut off of transcription when cultured in medium containing glucose.

A



B

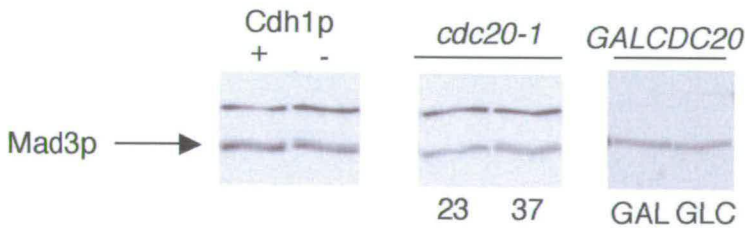


Figure 4.6 Mad3p is stabilised in APC mutants, but its stability seems to be unaffected by Cdc20p or Cdh1p

A Temperature sensitive *cdc23-1* and *cdc16-1* mutants were grown at 37°C and 23°C. Samples were analysed by SDS-PAGE and Western blotting with anti-Mad3p antibody. **B** *cdh1Δ* and *CDH1* cells were grown in the presence of nocodazole, temperature sensitive *cdc20-1* cells were grown at 37°C and 23°C and *GALCDC20* cells were grown in the presence or absence of glucose (to shut off *CDC20* transcription). Samples were analysed by SDS-PAGE and Western blotting using anti-Mad3p antibody.

cdc20-1 is a temperature sensitive allele of the gene encoding Cdc20p that at its restrictive temperature (37°C) arrests in mitosis at the metaphase-anaphase transition as APC/C activity required for progression into anaphase is inhibited.

cdc20-1 cells were grown to mid-log phase at 23°C. Half the cells were then grown at 23°C and half shifted to 37°C for 2 hours to inactivate Cdc20p at the restrictive temperature. Nocodazole was added to ensure that cells grown at both temperatures were arrested at the same point of the cell cycle for analysis. Total protein lysate samples were prepared from harvested cells for analysis by SDS-PAGE and Western blotting to assess the stability of Mad3p in these mutants using an anti-Mad3p antibody.

Figure 4.6B reveals that Mad3p levels are the same in cells grown at both the restrictive (37°C) and the permissive temperature (23°C).

Secondly, *GALCDC20* was grown to mid-log phase in medium containing galactose (2% w/v), then arrested in G1 using alpha-factor. Cells were then released into medium containing glucose to inhibit *CDC20* expression (or galactose as a control) for 2 hours. Cells were harvested and samples prepared for and subjected to analysis by SDS-PAGE. Western blotting was performed with anti-Mad3p antibody.

Figure 4.6B reveals that Mad3p levels are the same in cells grown with (in galactose) and without (in glucose) *CDC20* transcription (and subsequently translation).

From these results it is possible to conclude that Mad3p levels are not regulated by the activity of Cdc20p and are independent of Cdh1p function.

4.5 Biochemical analysis of KEN mutants

4.5.1 *mad3* KEN box mutants can still bind Bub3p

Mad3p is known to form a constitutive complex with Bub3p (Hardwick et al., 2000). The original *mad3-1* mutant, that could not arrest in response to the addition of a microtubule poison, could not bind Bub3p. On this basis, as the KEN mutants were sensitive to benomyl, it was possible that the interaction between Mad3p and Bub3p was perturbed. To address this possibility the ability of each mutant to co-immunoprecipitate with Bub3p was analysed.

In the following experiment, a *mad3Δ* strain containing myc-tagged Bub3p (RJ10) was transformed with either an empty vector (YCpLac22), wild-type *MAD3*, KEN30AAA or KEN296AAA.

Each strain was grown to mid-log phase, cells were harvested and total cell lysates suitable for use in co-immunoprecipitation reactions were prepared. The lysates were split and incubated with either anti-myc (mouse 9E10) antibody-coated beads or Protein-A sepharose with anti-Mad3p antibodies bound. Samples were prepared of the total lysates and beads (post-incubation) for analysis by SDS-PAGE and Western blotting with anti-myc (A14 rabbit) and anti-Mad3p antibodies.

Figure 4.7A shows that KEN30AAA and KEN296AAA co-immunoprecipitated with Bub3p-myc in both an anti-Mad3p and anti-myc co-immunoprecipitations at wild-type levels. Therefore, mutation of the KEN motifs does not perturb the Mad3p-Bub3p complex.

4.5.2 *mad3* KEN box mutants have reduced Cdc20p binding

Mad3p is also known to be a component of the MCC, with Mad2p and Cdc20p. (Hardwick et al., 2000) showed that Mad3p can be co-immunoprecipitated with Cdc20p upon checkpoint activation and in mitosis. As (Pfleger and Kirschner, 2000) demonstrated that KEN motifs can mediate an interaction between Cdc20p and other proteins, it was deemed of great interest to assess the effect of mutating the KEN boxes in Mad3p on their ability to bind Cdc20p under the conditions described.

In the following experiment a *mad3Δ* strain containing *myc-18CDC20* and (LB4) was transformed with either an empty vector (YCpLac22), wild-type *MAD3*, KEN30AAA, KEN296AAA or KEN30/296AAA. As strain not expressing *myc-18CDC20* was included as a control.

Strains were grown to mid-log phase and then arrested in S-phase with hydroxyurea for 2 hours (as the mutant cells would not arrest in the presence of nocodazole alone). Nocodazole was then added for a further 1 hour to depolymerise microtubules and activate the spindle checkpoint. Total cell lysates suitable for use in co-immunoprecipitation reactions were prepared. The lysates were incubated with anti-myc (mouse 9E10) antibody-coated beads. Samples were prepared of the total lysates and beads (post-incubation) and subjected to analysis by SDS-PAGE and Western blotting with anti-myc (A14 rabbit) and anti-Mad3p antibodies.

Figure 4.7B *myc-18Cdc20* specifically binds Mad3p but not any of the KEN mutants in the exposure shown (30 seconds). Upon long exposure (1 hour +) it is possible to see a very faint band in the KEN296AAA lane. The figure also confirms the ability of Cdc20p to interact with Mad2p in the absence of Mad3p binding (Hardwick et al., 2000).

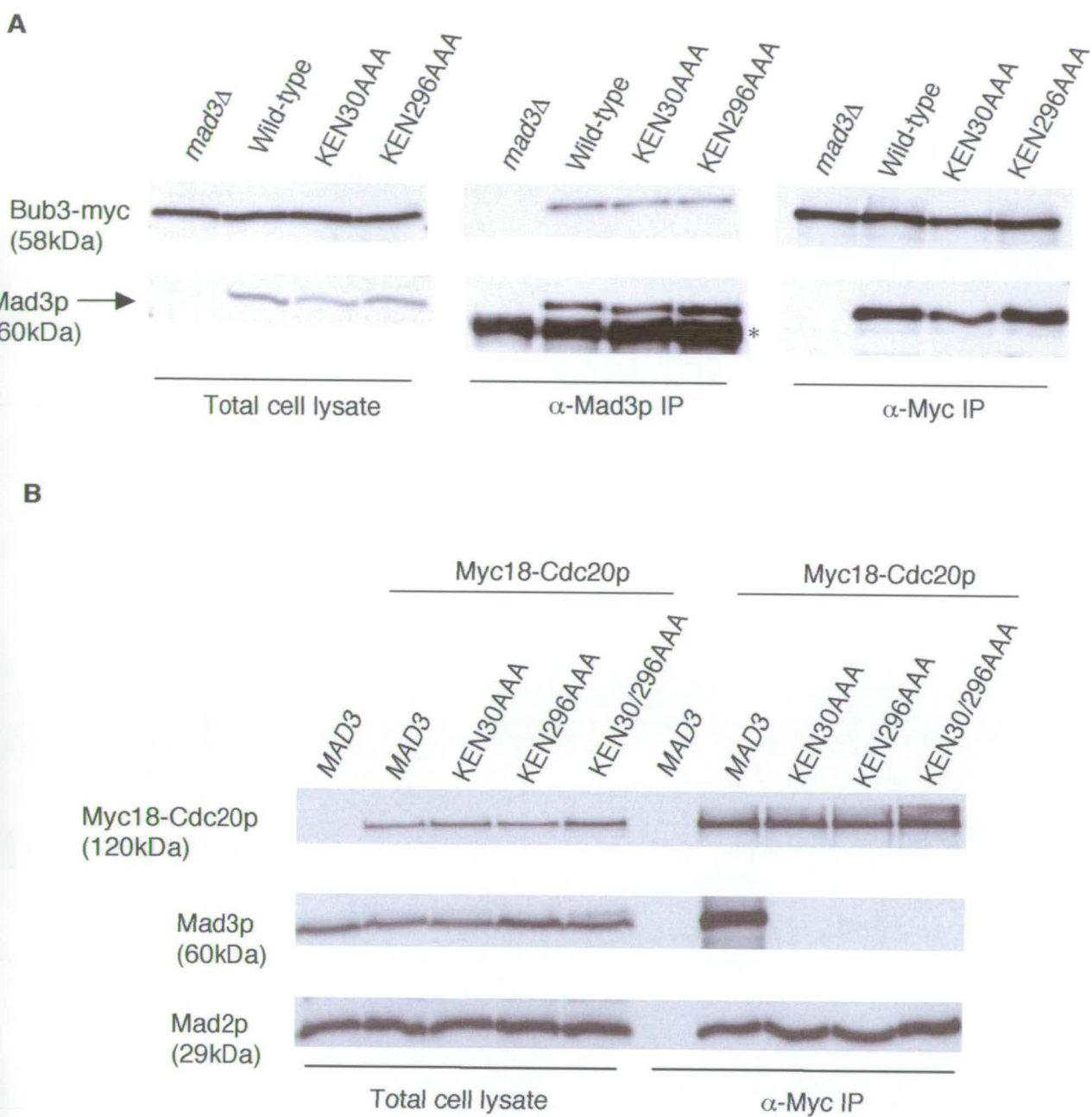


Figure 4.7 Mad3p KEN box mutants bind can bind Bub3p but Cdc20p binding is abolished in KEN30AAA and the double mutant and severely reduced in KEN296AAA

A Immunoprecipitations of Bub3p-myc were subjected to SDS-PAGE and Western blotted with anti-myc and anti-Mad3p antibodies **B** Immunoprecipitation of myc18-Cdc20 were subjected to SDS-PAGE and Western blotted with anti-myc, anti-Mad3p antibodies and anti-Mad2p antibodies

In summary, biochemical co-immunoprecipitation results show that none of the KEN mutants affect Bub3p binding to Mad3p, but the interaction between Mad3p and Cdc20p is severely abrogated.

4.6 The spindle checkpoint and Mad3 KEN mutants have a role in Cdc20p turnover

Recent findings have demonstrated a role for Mad1p, Mad2p and Mad3p in regulating Cdc20p levels in the cell (Pan and Chen, 2004) The roles of Bub1p and Bub3p are assessed here. Experiments were designed to analyse the turnover of Cdc20p in the absence of the checkpoint components. Reduced turnover increases the overall level of Cdc20p in the cell.

4.6.1 The role of spindle checkpoint components in Cdc20p turnover

Strains containing *myc18-CDC20* with the checkpoint genes *MAD1* (KH302), *MAD2* (KH340), *MAD3* (LB4), *BUB1* (LB1) and *BUB3* (KH345) deleted, respectively, and a wild-type control were grown to mid-log phase and arrested with hydroxyurea. Nocodazole was then added to activate the spindle checkpoint. Cycloheximide was subsequently added to the arrested cells to inhibit translation. Samples were taken every 10 minutes for 30 minutes and prepared for analysis by SDS-PAGE and Western blotting with anti-myc (A14, rabbit) antibody.

Figure 4.8 demonstrates that the absence of Bub1p or Bub3p reduced the turnover of Cdc20p in a similar fashion to that seen in the absence of Mad1p or Mad2p. The turnover of Cdc20p in all mutants was decreased with respect to wild-type where published data states it has a half life of approximately 6 minutes. The experiment also confirmed the effect of a *mad3Δ* where Cdc20p was stabilised with a half-life of over 30 minutes (Pan and Chen, 2004).

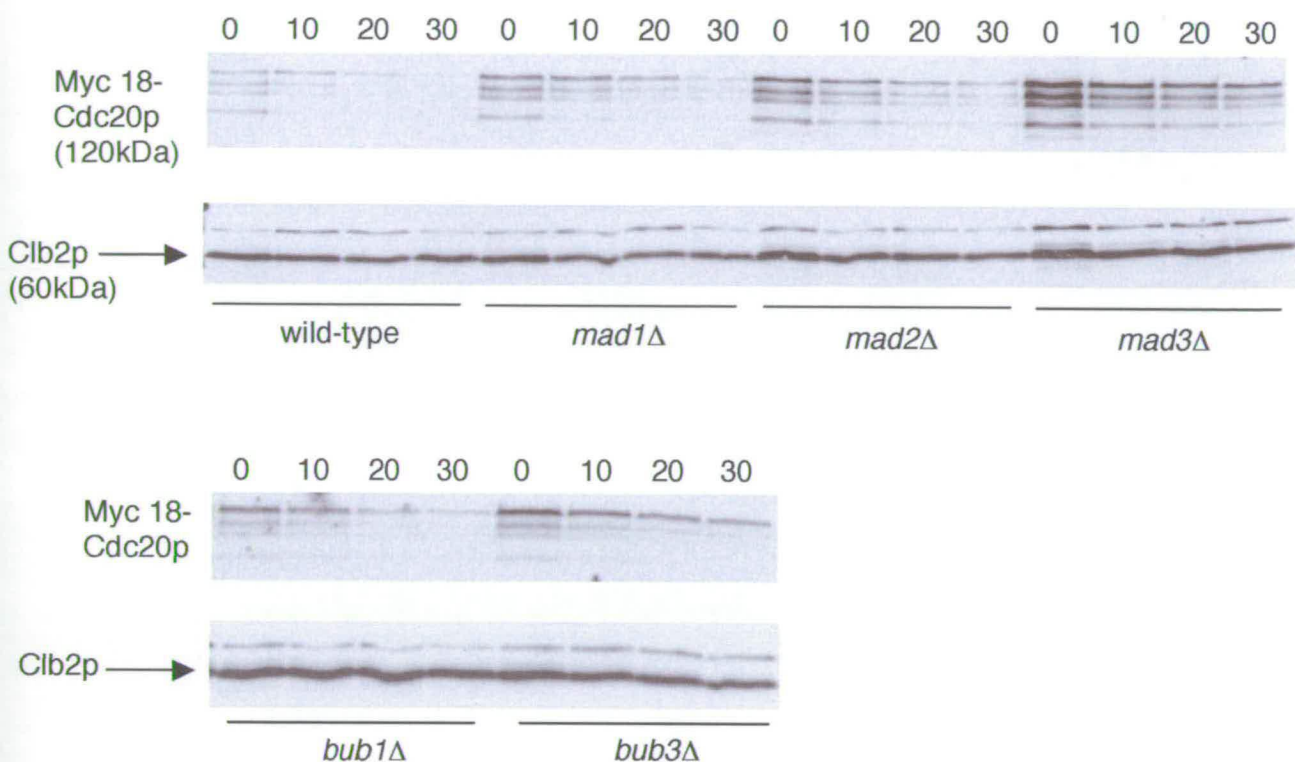


Figure 4.8 Spindle Checkpoint components have a role in Cdc20p turnover

Strains expressing myc18-Cdc20p with different checkpoint genes deleted were arrested in hydroxyurea and nocodazole. Cycloheximide was added at time 0 to inhibit translation. Samples were taken every 10 minutes for 30 minutes to assess Cdc20p turnover. Samples were then subjected to SDS-PAGE and Western blotted with anti-myc and anti-Clb2 (as a control) antibodies.

4.6.2 KEN30AAA and KEN30/296AAA but not KEN296AAA increase Cdc20p stability as seen in a *mad3Δ*

The absence of Mad3p has the most profound effect of all checkpoint mutants on Cdc20p turnover (Figure 4.8). The following experiment was designed to assess the effect of each KEN mutant on Cdc20p turnover.

A *mad3Δ* strain containing *myc18-CDC20* was transformed with either an empty vector (YCpLac22), wildtype *MAD3*, KEN30AAA, KEN296AAA or KEN30/296AAA.

Cells were grown to mid-log phase and arrested with hydroxyurea. Cycloheximide was subsequently added to the arrested cells to inhibit translation. Samples were taken every 10 minutes for 30 minutes and prepared for analysis by SDS-PAGE and Western blotting with anti-myc (A14, rabbit) antibody.

The single KEN30AAA or double KEN30/296AAA mutants stabilised Cdc20p to levels seen in the strain transformed only with an empty vector that behaved as a *mad3Δ*. However, the KEN296AAA mutant did not stabilise Cdc20p as the *mad3Δ* strain or destabilise to the extent seen in wild-type. The result suggests that KEN296AAA has a similar effect as other spindle checkpoint mutants (Figure 4.9).

4.7 Discussion

Mad3p is present throughout the cell cycle and its levels do not appear to grossly fluctuate. It does contain, however, two conserved KEN boxes that, in other proteins, have been shown to target them for destruction via the APC/C. The analysis in this chapter focussed on the role of the KEN boxes identified in Mad3p.

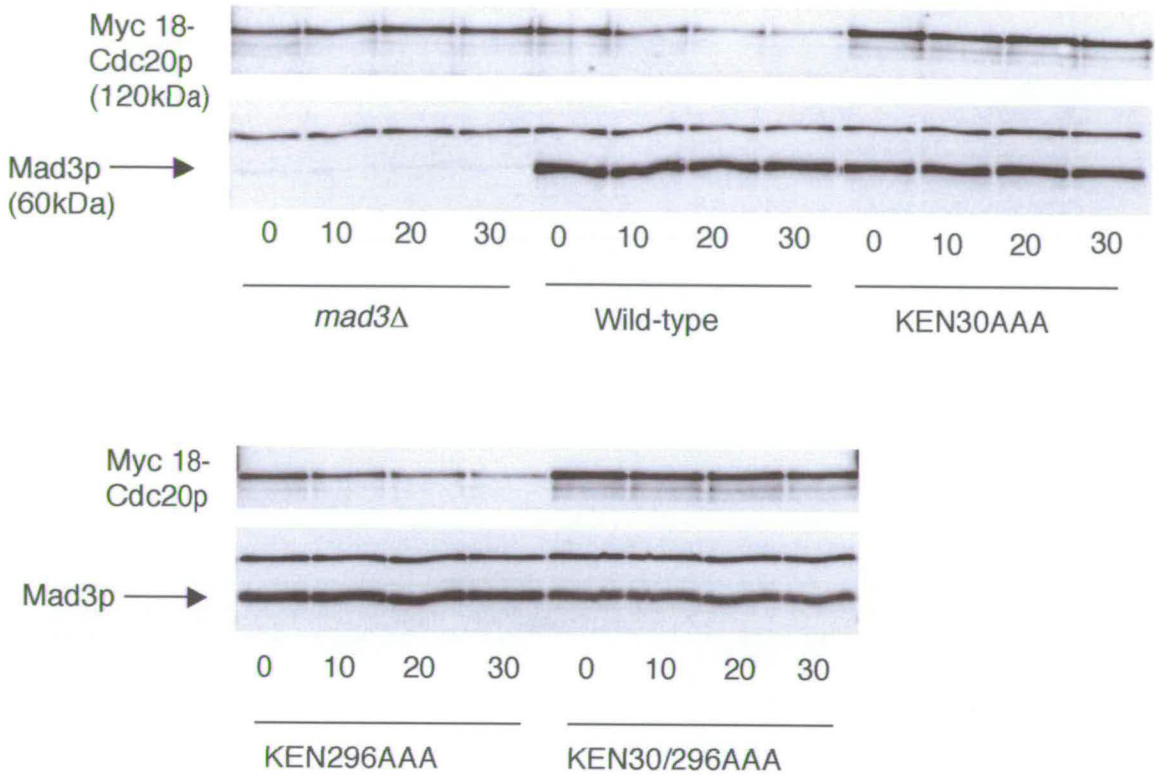


Figure 4.9 KEN30 of Mad3p regulates Cdc20p turnover

Strains expressing myc18-Cdc20p in combination with the different *mad3* KEN mutants were arrested in hydroxyurea. Cycloheximide was added at time 0 to inhibit translation. Samples were taken every 10 minutes for 30 minutes to assess Cdc20p turnover. Samples were then subjected to SDS-PAGE and Western blotted with anti-myc and anti-Mad3p antibodies.

Mutation of each KEN box to alanine independently and together rendered cells sensitive to benomyl, though only the double and KEN30AAA mutant displayed a typical checkpoint defective phenotype upon microcolony analysis. KEN296AAA, though benomyl sensitive, through microcolony analysis appeared to grow with similar morphology and division as wildtype initially, but failed to divide after approximately 3 divisions. This initially led to the hypothesis that this mutant could establish a mitotic arrest in the presence of benomyl but was struggling to exit such an arrest and Mad3p degradation was required for switching off a checkpoint response.

Upon closer examination, all mutants demonstrated rapid death following exposure to nocodazole and displayed premature sister chromatid separation in the presence of nocodazole. Thus, in these assays KEN296AAA behaved as a classic *mad3Δ* mutant and therefore, the possibility of being 'stuck' in a mitotic arrest could be ruled out.

Interestingly, the mutation of KEN296 to alanine residues in the presence of wildtype Mad3p invoked a similar, but less severe, phenotype as seen in a *mad3Δ* background, therefore KEN296AAA is dominant. No other dominant *mad3* mutants have been identified or analysed to date. After 6 hours in nocodazole, 20% of cells remained viable and assessment of sister chromatid separation revealed that (when compared to the controls) 10% more (27% in total) of wildtype cells expressing KEN296AAA had separated sister chromatids. Though this difference is significant and reproducible, it is unlikely to be the sole cause of the dominant phenotype. It would be useful to determine the destination of prematurely separated sisters through DAPI staining of total cellular DNA and comparing that to the location of separated sister chromatids to detect any defects in chromosome segregation. It would also be useful to assay the ability of this mutant to generate proper biorientation of kinetochores on the mitotic spindle following the removal of nocodazole. Massive chromosome segregation defects, as a result of a lack of ability to biorient chromosomes properly, are lethal to the cell and may explain the extreme phenotype seen.

Biochemical analysis of wild-type Mad3p revealed an increase in stability in the absence of APC/C function though this did not appear to depend on either Cdc20p or Cdh1p. Further careful analysis of the lack of dependency on Cdc20p and Cdh1p needs to be carried out. At present it is not known when, or if, turnover of Mad3p occurs. Knowing this would give a good indication of which of these proteins is important in its degradation due to the strict temporal nature of Cdc20p and Cdh1p activity with regard to APC/C activation, during S-phase/early mitosis and late mitosis/G1 respectively (Kramer et al., 2000). It would also become possible to assess the effect, if any, of the KEN mutants upon Mad3p turnover under conditions identified for the wild-type protein.

Mad3p is part of the MCC upon checkpoint activation (Hardwick et al., 2000; Millband and Hardwick, 2002; Sudakin et al., 2001; Sudakin and Yen, 2004) - a complex also containing Bub3p, Mad2p and Cdc20p. The ability of each mutant to co-immunoprecipitate with myc18-Cdc20p and consequently Mad2p was assessed. None of the KEN mutants were able to bind myc18-Cdc20 to wild type levels. Binding in the KEN30AAA and double mutants was totally absent though the KEN296AAA mutant demonstrated binding upon long exposure of the film. The presence of this binding may be significant. The biochemical result supports the phenotypic analysis performed. It infers Cdc20p is no longer bound to Mad3p and subsequently still capable of activating the APC, leading to premature sister separation and cell cycle progression under conditions that should inhibit such processes. A useful further experiment would be to determine if KEN296AAA is capable of abrogating the complex significantly in the presence of wild-type Mad3p, thus furthering the analysis of the dominant phenotype.

A recently identified form of checkpoint control is through the regulation of Cdc20p turnover. Pan *et al* (2004) demonstrated that while all Mad proteins are required for the

destabilisation of Cdc20p, Mad3p had the most important role. The work presented in this chapter demonstrated that Bub1p and Bub3p are required for the destabilisation to a similar degree as Mad1p and Mad2p. The KEN mutants displayed varying effects on Cdc20p turnover. KEN30AAA and the double mutant caused stabilisation of Cdc20p to the extent seen in a *mad3Δ*. However, KEN296AAA only increased stabilisation of Cdc20p to levels seen in other checkpoint mutants. It is my interpretation that KEN30 mediates an interaction between Mad3p and Cdc20p that is required for the destabilisation of Cdc20p. Consequently, though KEN296 demonstrates a subtle increase in Cdc20p stability the KEN30 remains intact and so can perform its function sufficiently.

The mutants analysed in this chapter display both common and differing characteristics. I would interpret the results of KEN30AAA and the double mutant as affecting the known roles of Mad3p in the spindle checkpoint. In addition, as the gross phenotype of KEN30AAA is seen in the double mutant, it can be inferred that the function of KEN296 is dependent upon the interactions and actions of KEN30. Consequently it is possible to predict that KEN30 may be temporally required before KEN296. This conclusion is in part supported by data from Pan *et al.*, 2004 demonstrating that Cdc20p turnover during S-phase requires Mad3p.

KEN296 has proved most interesting, highlighting an as yet unknown influence of Mad3p on the checkpoint. It is possible that KEN296 mediates an alternative inhibitory function that is also required for a successful checkpoint arrest. Unpublished data has purified Mad3p in *S. pombe* with an inactive APC/C (Kathy Gould, *pers. comm.*) and co-immunoprecipitation experiments utilising human cell extracts (Chan *et al.*, 1999) have demonstrated a potential interaction between Mad3p/BubR1 and APC/C subunits. It is possible therefore that KEN296 mediates an interaction with the APC/C that can inhibit its action directly.

The described results and conclusions are presented together as a current working model in Figure 4.10.

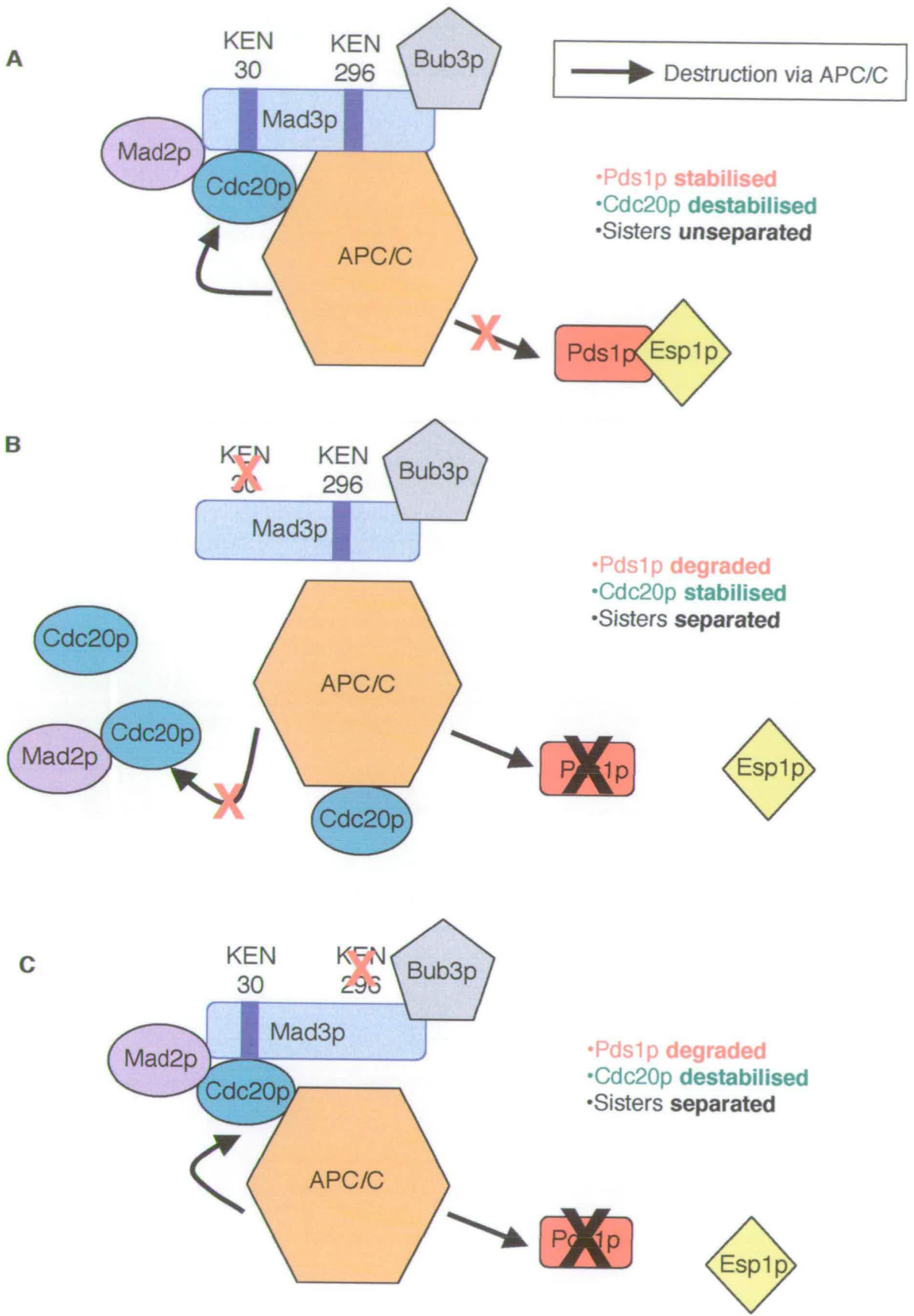


Figure 4.10 Proposed model for the role of KEN30 and KEN296 in Mad3p function

A Complex formation and APC/C regulation in a checkpoint arrest. **B** Complex formation and APC/C regulation in KEN30AAA. **C** Complex formation and APC/C regulation in KEN296AAA

Chapter 5

Final Discussion

In this thesis a preliminary analysis of Mad3p post-translational regulation has been presented.

Data has suggested that Mad3p is phosphorylated in a cell cycle-dependent manner and in response to spindle damage, consistent with observations made on its vertebrate orthologue, BubR1 (Chan et al., 1999; Ditchfield et al., 2003; Frascini et al., 2001a; Taylor et al., 2001).

The phosphorylation of Mad3p does not appear to require the presence of other checkpoint proteins, with or without checkpoint activation. As such, the results infer that the kinetochore localisation of Mad3p is also not of importance for this modification. This is interesting as many models place the kinetochore as the catalytic centre of the checkpoint and in the absence of an intact kinetochore, spindle checkpoint activation cannot be achieved (reviewed in (Musacchio and Hardwick, 2002)). It may therefore be argued that either phosphorylation of Mad3p occurs post-kinetochore localisation or the kinetochore is not required for Mad3p activity.

The spindle checkpoint can be activated by two means; a lack of kinetochore-microtubule attachment or a lack of tension. Data presented from experiments in metazoans suggests a role for Aurora B (Ipl1p) and BubR1 in both scenarios (Ditchfield et al., 2003): Hauf et al., 2003; Murata-Hori and Wang, 2002). Similarly Ark1 function in fission yeast is required for a checkpoint response to microtubule depolymerisation and formation of the MCC (Petersen and Hagan, 2003). Data presented here have supported the published role of Ipl1p, in budding yeast, in detecting a lack of tension at kinetochores but not in response to microtubule depolymerising drugs (Biggins and Murray, 2001; Stern and Murray, 2001). Mad3p phosphorylation is abolished in an

ipl1-321 mcd1-1 mutant, but is still largely present when an *ipl1-321* mutant is exposed to nocodazole. In addition, mutation of a serine residue to alanine, identified as phosphorylated by Ipl1p *in vitro*, does not appear to abrogate checkpoint function when nocodazole is added. Assessment of the *in vivo* phenotype of this mutant in response to a lack of tension and the use of antibodies purified to specifically recognise this residue when it is phosphorylated will be vital in furthering our knowledge. Until these analyses are performed, it is only possible to speculate that Mad3p phosphorylation by Ipl1p is of significance only when there is a lack of tension at the kinetochore but may prove to be unimportant or not present when there is a lack of attachment.

The role of Cdc5p in Mad3p phosphorylation is also not clear. Though *cdc5-1* mutants can arrest in metaphase in response to microtubule polymerisation, they fail to exit mitosis (E. King, unpublished data). Cdc5p/Plk1 has been shown to have a variety of roles in the cell and it regulates key cell cycle transitions (reviewed in (Barr et al., 2004)). The benomyl-sensitive phenotype of *mad3* mutants that have putative serine and threonine Cdc5p phosphorylation sites altered to aspartate indicates that they are of importance to Mad3p function. Biochemical data presented in this work demonstrated an increase in stability of these mutants. The effect seen may be a result of mimicking constitutive phosphorylation, but mutation of the residues to alanine did not affect the gel mobility in a way that could suggest the absence of phosphorylation. Again, identification of Mad3 phosphorylation sites *in vivo* will allow us to elucidate whether these mutations are indeed at phospho-residues or whether they are simply important in Mad3p turnover.

Though no gross turnover of Mad3p has been presented in this study, mutation of two KEN boxes found within Mad3p renders cells sensitive to the microtubule depolymerising agent, benomyl.

KEN30AAA behaves phenotypically as a *mad3Δ* mutant with regards to its benomyl sensitivity, premature sister separation, complex formation (Hardwick et al., 2000) and the lack of Cdc20p turnover (Pan and Chen, 2004). KEN296AAA however, has demonstrated a provocative phenotype. Though sensitive to benomyl, it does not initially grow as quickly as a *mad3Δ* in a microcolony assay (Hardwick et al., 2000). The mutant can still participate significantly in Cdc20p turnover and sister chromatid separation still occurs, indicating that the APC/C remains partially active. The model presented and discussed in section 4.7 suggests that KEN296 mediates a direct inhibitory interaction between Mad3p and the APC/C. It was recently demonstrated that the D-box motif of Cyclin B can interact directly with the APC/C (Yamano et al., 2004) suggesting that substrate interactions with the APC/C can be independent of the activator proteins Cdc20p or Cdh1p. Published data (Chan et al., 1999) and preliminary data suggests that Mad3/BubR1 can interact directly with the APC/C (Kathy Gould, *pers. Comm.*) though this has yet to be tested in budding yeast and the role of KEN296 to be assessed.

Sgo1p has been identified as a tension specific sensory protein in budding yeast (Indjeian et al., 2005). In addition *sgo1Δ* cells fail to biorient their chromosomes following the addition and subsequent removal of nocodazole. The result is massive chromosome segregation defects that confer a high level of lethality to cells. There is also data in press that BubR1 plays an important role in kinetochore-microtubule attachment in human cells, mediated through the regulation of Aurora B (Lampson et al., 2004). It is possible the severe phenotype seen in KEN296 is as a result of perturbed microtubule-kinetochore attachments.

Previously published data has demonstrated a link between BubR1 phosphorylation and Aurora B activity (Ditchfield et al., 2003). The data presented in this thesis supports this result, as Mad3p phosphorylation requires Ipl1p function under conditions that

induce a lack of tension at kinetochores *in vivo* and has gone on to identify serine 337 of Mad3p as a direct substrate of Ipl1p *in vitro*.

The identification of conserved putative KEN boxes in Mad3p and subsequent examination of their function has shown they are integral for Mad3p function as a component of the spindle checkpoint. Both published roles of Mad3p; MCC formation (Hardwick et al., 2000; Millband and Hardwick, 2002; Sudakin et al., 2001; Sudakin and Yen, 2004) and Cdc20p turnover (Pan and Yen, 2004) are compromised in KEN30AAA. While the second KEN296AAA mutant has a more complicated and less typical checkpoint mutant phenotype, it may prove to elucidate alternative roles for Mad3p in the checkpoint that are, as yet, uncharacterised.

Overall, the data strongly suggest a significant role for the post-translational modification of Mad3p in its function as a component of the spindle checkpoint.

Appendix

A.1 Affinity Purified Anti-Mad3p Antibody Production

Purified Mad3 in combination with Mad3-GST (from Kevin Hardwick) was injected in to rabbits as an antigen to provoke anti-Mad3p anti-body synthesis. The rabbit was boosted and bled monthly for three months and subsequently exanguinated. Serum from the rabbit was pumped slowly through a column containing purified Mad3 coupled covalently to affigel for 3 hours at 4°C. The affinity-purified antibodies were eluted from the column using 0.1M glycine (pH2.5) or 0.1M TEA (pH11.5) and subsequently dialysed for further use.

Each antibody was tested on total yeast extracts for specificity. Total protein extracts were prepared from a *mad3Δ* (KH173) and *MAD3* (KH34) separated by SDS-PAGE.

Figure A.1 shows antibodies eluted under both conditions recognise a protein of approximately 60kD, the correct size for Mad3p, in the *MAD3* extract that is absent in the extract prepared from the *mad3Δ* strain.

These antibodies were subsequently used throughout this study for Western blotting and immunoprecipitations of Mad3p.

A.2 TAP-tagging Mad3p

The large-scale purification of proteins from yeast has become an increasingly useful tool for the analysis of protein-protein interactions and the identification of phosphorylated residues *in vivo*. The TAP tag and strategy is one such tool.

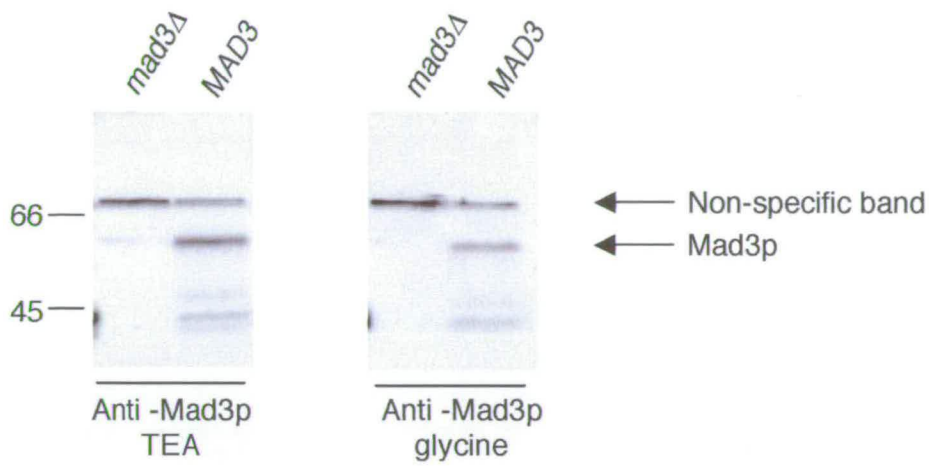


Figure A.1 Purification of anti-Mad3p Antibodies

Purified anti-Mad3p antibodies (section A.1) were checked for specificity on total cell lysates prepared from *mad3Δ* and *MAD3* cells.

The TAP tag consists of a calmodulin binding domain (CBD) and Protein A separated by a TEV protease cleavage site. The cassette is integrated in to the host chromosome at the C-terminus of the protein to be tagged, maintaining expression of the fusion protein at its normal level as it remains under the control of its endogenous promoter. The initial purification step binds the fusion protein to IgG beads via the Protein A portion of the tag. Cleavage by TEV protease between the Protein A and CBD domains of the tag then releases the target protein plus CBD. The second purification step comprises incubation of the remaining fusion protein with calmodulin beads in the presence of Calcium ions. Native elution from calmodulin beads is possible using EGTA, potentiating the maintenance of interactions between proteins.

A.2.1 Strain generation

The TAP tag was amplified from pBS1539 (URA+) for integration into a wild-type background strain (KH34) or pBS1479 (TRP+) for integration into a BM13 background, where Bub3p is tagged with 13 myc epitopes (MB143). The resulting PCR fragments had sequence complimentary to the integration site, downstream of *MAD3* at both their 5' and 3' end to mediate recombination and in-frame integration.

A PCR screen of genomic DNA prepared from yeast colonies that had grown successfully on selective media initially detected integration of the TAP tag. The 3' end of *MAD3* through in to the TAP tag was then sequenced to confirm correct integration and sequence of the integrated fragment.

Expression of TAP tagged Mad3p was established by Western blotting. Total cell lysates were prepared from strains identified as positive for integration by PCR and sequencing and subjected to analysis by SDS-PAGE and Western blotting with an anti-Mad3p antibody. Figure A.2A shows the expression and size of endogenous Mad3p (in KH34) as approximately 60 KDa and that of TAP-tagged Mad3p in strains EK001 and EK002 as approximately 95 KDa.

The function of the TAP tagged Mad3p in strains EK001 and EK002 as a component of the spindle checkpoint was assessed by their ability to grow on YPDA containing benomyl.

A wild-type strain (34a), *mad3Δ* strain (KH173) and strains EK001 and EK002 were spotted on to YPDA plates containing 0μg/ml and 15μg/ml benomyl in 10 fold dilutions.

Figure A.2B illustrates equal growth of all strains on plates containing 0μg/ml benomyl suggesting that the TAP-tagged Mad3p strains have no obvious growth defect and equal amounts of cells were assayed throughout the experiment. The strain expressing wild-type Mad3p grew well on the plate containing 15μg/ml benomyl as did strains expressing TAP-tagged Mad3p. Growth of the *mad3Δ* strain was reduced compared to the strain expressing wild-type Mad3p, demonstrating the effect of a compromised spindle checkpoint. As strains EK001 and EK002 grew as wild-type on plates containing 15μg/ml benomyl it can be concluded that they possess a functional spindle checkpoint and would be suitable for use in further experiments.

1

A.2.2 Extraction and purification of TAP-tagged Mad3p

Initial experiments followed the TAP protocol (see materials and methods) until incubation with IgG sepharose. From this point half the beads were subject to the calmodulin binding step and elution whilst protein was eluted from the other half using 0.5M acetic acid. Silver stain analysis (data not shown) showed no protein present following the complete tandem purification whereas acetic acid elution of protein from IgG beads revealed several bands.

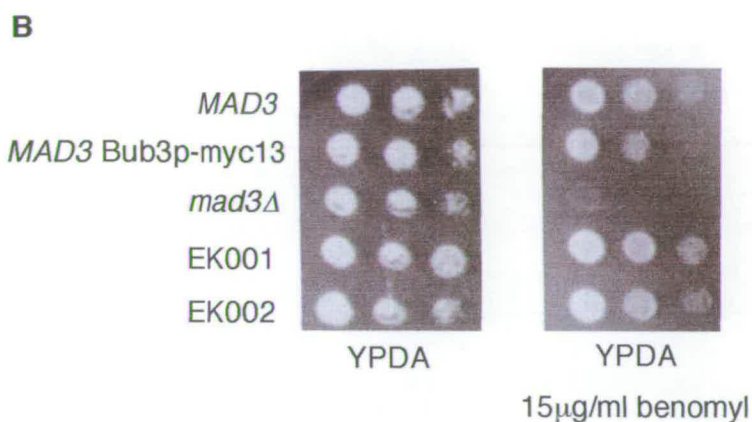
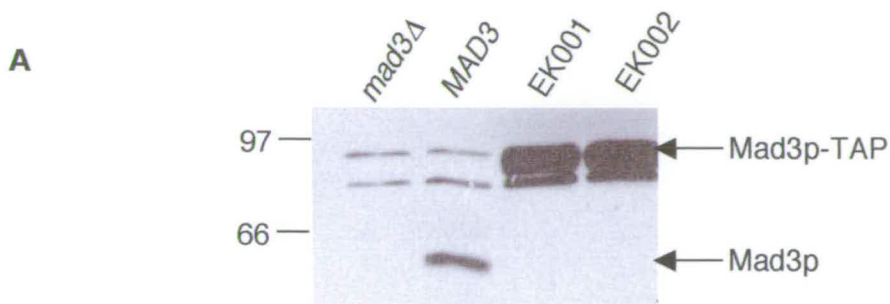


Figure A.2 Mad3p-TAP is Expressed and is Checkpoint Proficient

A The expression of TAP-tagged Mad3p was checked by SDS-PAGE and Western blotting with anti-Mad3p antibody. **B** The new TAP-tagged strains were tested for spindle checkpoint proficiency by plating on media containing benomyl.

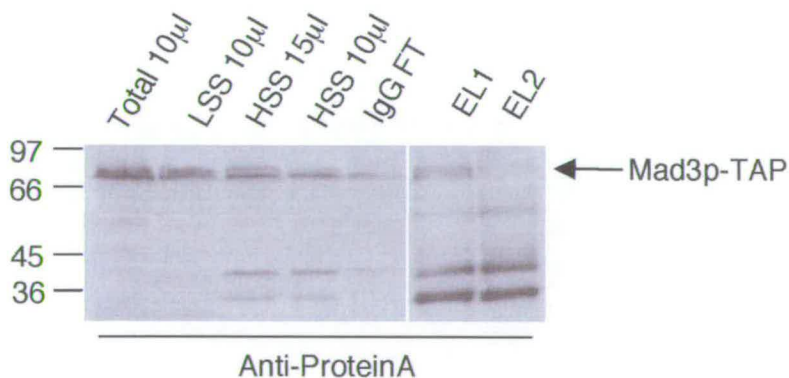


Figure A.3 Mad3p-TAP is Degraded through the Purification Protocol

Samples taken from stages of the TAP-purification of Mad3p-TAP were subjected to SDS-PAGE and analysed using an anti-Protein A antibody to track Mad3p-TAP through the protocol.

Subsequently, large scale experiments were performed and only elutions from the IgG beads were analysed. Samples taken through the purification and of the elution were prepared for analysis by SDS PAGE and Western blotting with anti-Protein A antibody.

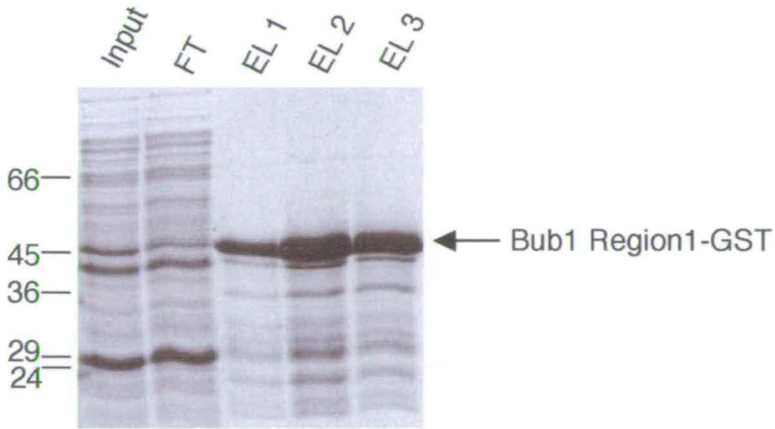
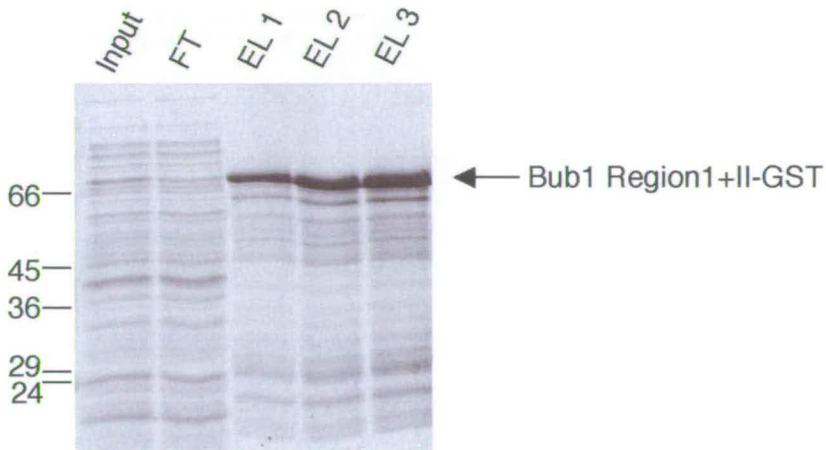
Figure A.3 follows Mad3p-TAP through the purification protocol. It can be seen that though Mad3p-TAP is present in the final elution lanes, there are also an increasing number of peptides through the gel recognised by the anti-Protein A antibody. The presence of these signals suggests that Mad3p-TAP is being degraded throughout the purification.

Though significant quantities of protease inhibitors were used throughout, (see materials and methods) and the protocol was performed at 4°C the extent of Mad3p degradation was enough to decide that under these purification conditions insufficient amounts of intact Mad3p-TAP could be purified and analysed by mass-spectrometry for the identification of phosphorylated residues or interacting proteins. If this method of purification were to be pursued in the future it would be advisable to use a protease deficient strain background, such as JB811.

A.3 Expression and Purification of Bub1-GST

Two N-terminal portions of *BUB1* were cloned in to pGEX6p (by Kevin Hardwick) for expression as a GST fusion protein. *N1* encoded amino acids 1-217 and *N2* amino acids 1-460 of Bub1p.

Expression of the recombinant proteins was induced by the addition of IPTG to a final concentration of 0.1mM to mid-log phase cultures of BL21 cells transformed with the expression plasmids. Induction was performed overnight at 18°C. A soluble extract was prepared and incubated in batch with glutathione sepharose. After washing the

A**B****Figure A.4 Purification of Bub1-GST**

A Bub1 Region I was expressed as a fusion protein with GST. Samples from the purification were analysed by SDS-PAGE and coomassie staining. **B** Bub1 Region I + II was expressed as a fusion protein with GST. Samples from the purification were analysed by SDS-PAGE and coomassie staining.

resin, recombinant proteins were eluted from the glutathione sepharose using a buffer that contained reduced glutathione.

Samples from the expression and purification were analysed by SDS-PAGE and gels were stained with coomassie, the results of which are presented in Figure A.4.

Unlike the intein purification of Mad3, Bub1-GST does not purify as one peptide but appears to suffer a considerable amount of degradation throughout the protocol as seen by the presence of several bands, smaller than the recombinant protein, in Figure A.6. However, the desired full-length recombinant protein was clearly the major band and the yield was in excess of 6.5mg/ml (as determined by Bradford Assay). It was concluded that sufficient full-length recombinant protein was present for use in further experiments.

A.4 Bub1p N-terminal Analysis

The N-terminus of Bub1, as yet, has no known function. Bub1p is known to form a constitutive complex with Bub3p and with Mad1p upon checkpoint activation (Brady and Hardwick, 2000). In the absence of Mad3p or when Bub1p is over-expressed an interaction with Cdc20p can be identified (Laura Boyes, Kevin Hardwick pers. comm.). The GIG motif, found in the N-terminus, conserved between Bub1p and Mad3p is required in *S. cerevisiae* for Cdc20p binding. The conserved region of amino acids found at the N-terminus of Bub1p and Mad3p is referred to as Region I.

The following experiments were designed to determine the function of Bub1p Region I.


```

      . . . . .10 . . . . .20 . . . . .30 . . . . .40 . . . . .50 . . . . .60
ScBublRegion1 1:MNLDLGSTVVRGYESDKDFFPQSKGVSSSQKEQHSQLNQTAKIAYEQRLNDLEDMDPPLDL: 60
SpBublRegion1 1:.....MSDWRLTENVLQDNIPEKTPRESKTRLEEIQRLLALFQEELDIEELDPPVDV: 52
DmBublRegion1 1:MDFDNAKENIQPLASGRNVSLQLQASLSQDSTHGQELLAQRKQMEEEVITYKG..ADPLGA: 58
XlBublRegion1 1:.....MD.LQSQAQMFEAHHQGYKG..DPLDL: 25
MmBublRegion1 1:.....MDNLENVFRMFEAHHQSYTG..NDPLGE: 26
HsBublRegion1 1:.....MDTPENVLQMLEAHHQSYKG..NDPLGE: 26

      . . . . .70 . . . . .80 . . . . .90 . . . . .100 . . . . .110 . . . . .120
ScBublRegion1 61:FLDYMIWISTSYIEVDSSESGQEVLRSTMERCIIYIQDMETFRNDPRFLKIWIWYINL..F:118
SpBublRegion1 53:WYRCIEWLETRF....LGMETVNKMLDDALQYLERCFALNDVRLIQLAKIKQSYE:107
DmBublRegion1 59:WYTFICWIEQSYYPAG...GSGSGLQTVLHQCTKFEDDERYRQDKRLTKLFIKFM.....110
XlBublRegion1 26:WDRYVVLWAEALPP...QEKQNFCLLERLVRNFIGDKRYCNDERTIKYCIKIFA.....: 76
MmBublRegion1 27:WESFIKWVEENFP....DNKEYLMLLEHLWREFLHKKNYHNDSPRFINYCLKFA.....: 76
HsBublRegion1 27:WERYIQWVEENFP....ENKEYLMLLEHLWREFLDKKRYHNDSPRISYCLKFA.....: 76

      . . . . .130 . . . . .140 . . . . .150 . . . . .160 . . . . .170 . . . . .180
ScBublRegion1 119:LSNNFHESENTFKYMFNKGIGTKLSLFYEEFKLLENAQFFLEAKVFLLELGAENNCRPYN:178
SpBublRegion1 108:TPDELQQAQKQFYQLASKGIGLELALFYEEYCSLLIRMQRWKEASEVHAIVSREARPLV:167
DmBublRegion1 110:..EKQKDKIEFYQQMYNNGIGTMLADFYIAWAYSYDLSGNVRKADEIFRLGLECRAEPL:168
XlBublRegion1 76:..DTINPGQYFEYLYNQGIGHQSAALHVTWAQLLETQGLQSASALYQKAIHSNAKPM:134
MmBublRegion1 76:..EYNSDRHQFFFLYNQGIGTKSSYIYMSWAGHLEAQGLQHASALPQTGIHNEAPE:134
HsBublRegion1 76:..EYNSDLHQFFFLYNHGIGTLSSPLYLAWAGHLEAQGLQHASALVLRGIQNQAEPRE:134

      . . . . .190 . . . . .200 . . . . .210 . . . . .220 . . . . .230 . . . . .240
ScBublRegion1 179:RLRSLSNVEDRLREMNIVENQNSVPDSRERLKGRLIYRDPAPFFIRKFLTSSLMTDDKEN:238
SpBublRegion1 168:RLRNAAEFSTRAYDLHNAHPSIHDAPYSSPFPPIVLSKPVSSSTLPSKPKSFQVFS:227
DmBublRegion1 169:DKAEAHHFGYTVGQRMITYSTGEANAVNQELNERRIALQSLHGRRQQISNSITVGSIRT:228
XlBublRegion1 135:IDQHYRTPQIRNSQANLANRGAPVEPLGNSQILNQMNPTASSNVQDLSVAKESSTPS:194
MmBublRegion1 135:LDQQYRLFQARLTGIHLPQAATTSEPLHSAQILNQVMMNNSPEKNSACVPKSQGSECS:194
HsBublRegion1 135:FDQQYRLFQARLTETHLPQAATTSEPLHNVQVLNQMITKSNPGNMMAKISKNGSELS:194

      . . . . .250 . . . . .260 . . . . .270 . . . . .280 . . . . .290
ScBublRegion1 239:R.....:239
SpBublRegion1 228:AS.....SSRDS...Q..NASDL.....:240
DmBublRegion1 229:G.....AAVKSG.....LPGVV.....:240
XlBublRegion1 195:ENHPSQESACNVD.RSGNKWVTISKSAVVPQPVKCVGVVVKQVPMYC...:240
MmBublRegion1 195:G...VASTCDEKSNMEQRVIMISKSECSVSSSVAPKPEAQQ.VMYCKEK:240
HsBublRegion1 195:G...VISSACDKESNMERRVITISKSEYSVHSSLASKVDVEQVVMYCKE.:240

```

Figure A.5 Bub1p Region I multiple-alignment across species

Clustal X was used to create a multiple-alignment of Bub1 Region I across species to identify highly conserved residues

A.4.1 Alignment of Bub1p across species reveals several conserved residues in the N-terminus

Alignment of Bub1p and Mad3p (BUBR1) across species reveals highly conserved amino acids in Region I (Figure A.5). The approach taken in the following experiments was to mutate several of these residues and assess their importance in Bub1p function.

A.4.2 Generation and Integration of Bub1p Region I mutants

A vector designed to integrate at the N-terminus of Bub1p was derived from the vector pRS604. The *CEN* sequence was removed by restriction digest using *SalI* and *BamHI*. Following this, nucleotides 1 – 1425 of the *BUB1* ORF were cloned in to the vector 3' of the *HIS* gene using *EcoRI* and *BglII* (from pKH5.2) and 500 nucleotides of sequence upstream of *BUB1* ORF (amplified from genomic DNA) were introduced 5' of the *HIS* gene to mediate integration at the *BUB1* locus. The vector was linearised prior to transformation for integration using *NotI*.

Positive integrants were first detected by selection on media lacking histidine. A PCR screen was then performed on genomic DNA prepared from such yeast colonies to confirm integration. *BUB1* ORF was subsequently sequenced to confirm the presence of the desired mutation.

Eight different mutants were generated by SDM of the vector as required (see materials and methods) for further analysis (Figure A.5).

A.4.3 Bub1p Region I Mutants have a benomyl sensitive phenotype

The function of each mutant as a component of the spindle checkpoint was assessed by their ability to grow on YPDA solid media containing benomyl. Each mutant, an unmutated wildtype *BUB1* integrant, wildtype, *mad1Δ*, *mad3Δ* and a *bub1Δ* were spotted on to YPDA plates containing 0μg/ml (data not shown) and 15μg/ml benomyl in 10 fold dilutions. The growth of DP56/57AA and RP175/176AA was similar to that of a *bub1Δ* and the growth of D56A was similar to *mad1Δ* or a *mad3Δ* on plates containing 15μg/ml benomyl, suggesting that they are deficient in spindle checkpoint function, but to varying degrees (Figure A.6A).

A.4.4 Several *bub1* region I mutants are unstable, reflecting their benomyl sensitive phenotype

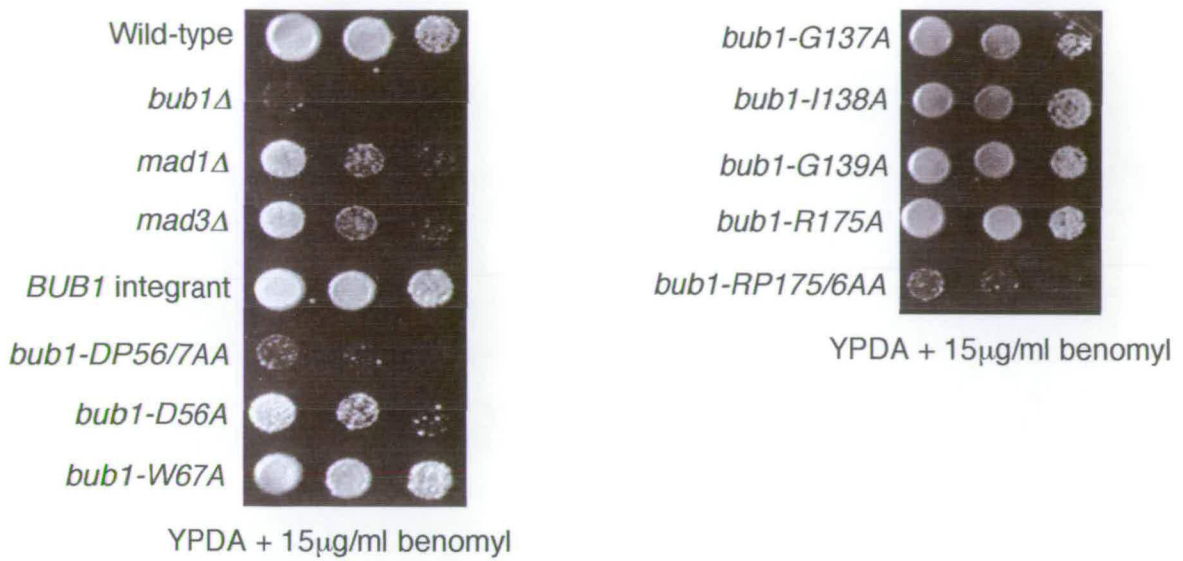
As part of the initial analysis of each mutant their integration and expression was confirmed by Western blot analysis of total cell lysates.

Each mutant, an unmutated wildtype *BUB1* integrant, wildtype, and a *bub1Δ* cells were harvested, prepared for, and analysed by SDS-PAGE. Western blotting was then performed with anti-Bub1p antibody.

Figure A.6B demonstrates the total instability of DP56/57AA and RP175/176AA and the partial stability of D56A and I138A.

Together, the result presented in Figure A.6 suggest that the benomyl sensitive mutants generated may be checkpoint deficient as they are not present to sufficient levels in the cell. As a result the *in vivo* analysis of Bub1p Region I was not pursued.

A



B

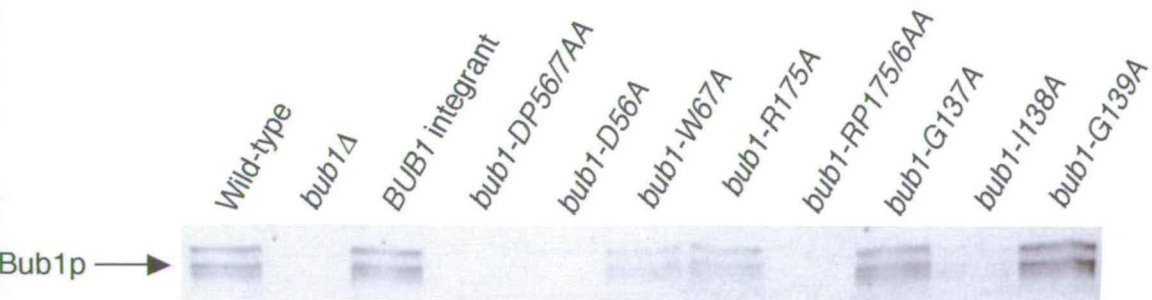


Figure A.6 Bub1 Region I mutants' sensitivity to benomyl reflects their stability

A The checkpoint proficiency of each mutant was crudely analysed by plating on media containing benomyl. **B** The expression of each mutant was assessed by SDS-PAGE and Western blotting with an anti-Bub1 antibody.

A.4.5 Portions of Bub1p and Cdc20p can be expressed *in vitro* using the reticulocyte lysate method of coupled transcription and translation

PCR generated fragments of *BUB1* and *CDC20* with the T7 promoter encoded at their 5' end (refer to materials and methods for details) were used as templates in the TNT[®] Quick Coupled Transcription/Translation System, that incorporates ³⁵S in to the translated peptides.

Region I (amino acids 1-219), Region II (220-465) Region I + II (1-465) and amino acids 1-300 (including region required for Mad2p binding) were expressed and the products were subjected to analysis by SDS-PAGE. The gels were stained with coomassie, dried and exposed to XR-film.

Figure A.6A shows the successful expression of each peptide as products of the coupled transcription/translation reactions.

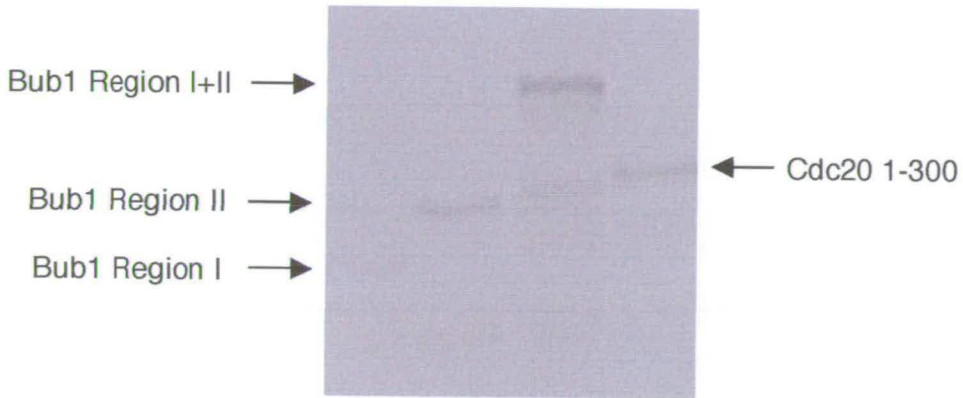
A.4.6 Region I of Bub1p is sufficient for binding the N-terminus of Cdc20p *in vitro*

In a *mad3Δ* strain or when Bub1p is overexpressed Cdc20p can be co-immunoprecipitated with Bub1p (Laura Boyes, *pers. comm.*).

The reticulolysate expressed, ³⁵S labelled N-terminus of Cdc20p (see previous section) was used in an *in vitro* binding assay with purified Bub1 Region I-GST and Bub1 Region I + II-GST (see section A3) to assess their ability to bind *in vitro* (see materials and methods for details). GST on its own was used as a control.

Bead samples from the assay were prepared for and subjected to analysis by SDS-PAGE. The gels were coomassie stained, dried and exposed to XR-film.

A



B

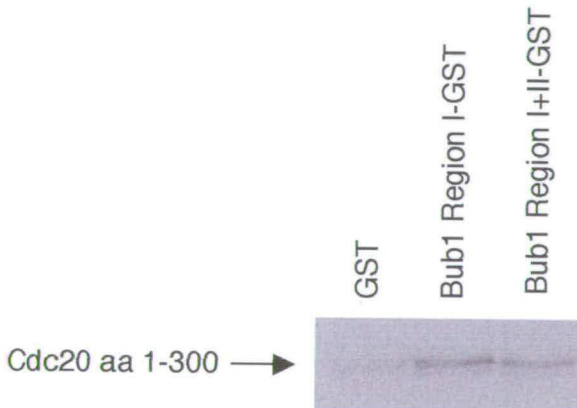


Figure A.7 Bub1 Region I can bind the N-terminus of Cdc20 *in vitro*

A ^{35}S labelled Bub1 Regions and Cdc20 amino acids 1-300 were expressed *in vitro* using reticulocyte lysate system. **B** ^{35}S labelled N-terminus of Cdc20 was used in an *in vitro* binding assay with purified Bub1-GST fusion proteins and was found to specifically bind Bub1 Region I.

Figure A.6B shows that though there is a some Cdc20 present in the GST control lane, the amount of Cdc20 present is enriched in both the Bub1 Region I and Bub1 Region I + Region II lanes and there is no difference between the amount of Cdc20p bound.

The results strongly suggest that Region I of Bub1p is sufficient for binding of the N-terminus of Cdc20 *in vitro*.

Bibliography

- Adams, R.R., M. Carmena, and W.C. Earnshaw. 2001. Chromosomal passengers and the (aurora) ABCs of mitosis. *Trends Cell Biol.* 11:49-54.
- Alexandru, G., F. Uhlmann, K. Mechtler, M.A. Poupard, and K. Nasmyth. 2001. Phosphorylation of the cohesin subunit Scc1 by Polo/Cdc5 kinase regulates sister chromatid separation in yeast. *Cell.* 105:459-72.
- Anderson, D.E., A. Losada, H.P. Erickson, and T. Hirano. 2002. Condensin and cohesin display different arm conformations with characteristic hinge angles. *J Cell Biol.* 156:419-24.
- Andrews, P.D., Y. Ovechkina, N. Morrice, M. Wagenbach, K. Duncan, L. Wordeman, and J.R. Swedlow. 2004. Aurora B regulates MCAK at the mitotic centromere. *Dev Cell.* 6:253-68.
- Andrews, P.D., and M.J. Stark. 2000. Type 1 protein phosphatase is required for maintenance of cell wall integrity, morphogenesis and cell cycle progression in *Saccharomyces cerevisiae*. *J Cell Sci.* 113 (Pt 3):507-20.
- Aono, N., T. Sutani, T. Tomonaga, S. Mochida, and M. Yanagida. 2002. Cnd2 has dual roles in mitotic condensation and interphase. *Nature.* 417:197-202.
- Barr, F.A., H.H. Sillje, and E.A. Nigg. 2004. Polo-like kinases and the orchestration of cell division. *Nat Rev Mol Cell Biol.* 5:429-40.
- Basrai, M.A., and P. Hieter. 1995. Is there a unique form of chromatin at the *Saccharomyces cerevisiae* centromeres? *Bioessays.* 17:669-72.
- Basto, R., R. Gomes, and R.E. Karess. 2000. Rough deal and Zw10 are required for the metaphase checkpoint in *Drosophila*. *Nat Cell Biol.* 2:939-43.
- Bernard, P., J.F. Maure, J.F. Partridge, S. Genier, J.P. Javerzat, and R.C. Allshire. 2001. Requirement of heterochromatin for cohesion at centromeres. *Science.* 294:2539-42.
- Biggins, S., and A.W. Murray. 2001. The budding yeast protein kinase Ipl1/Aurora allows the absence of tension to activate the spindle checkpoint. *Genes Dev.* 15:3118-29.
- Biggins, S., F.F. Severin, N. Bhalla, I. Sassoon, A.A. Hyman, and A.W. Murray. 1999. The conserved protein kinase Ipl1 regulates microtubule binding to kinetochores in budding yeast. *Genes Dev.* 13:532-44.
- Bishop, J.D., and J.M. Schumacher. 2002. Phosphorylation of the carboxy-terminus of INCENP by the Aurora B kinase stimulates Aurora B kinase activity. *Journal of Biological Chemistry.*
- Bloecher, A., and K. Tatchell. 1999. Defects in *Saccharomyces cerevisiae* protein phosphatase type I activate the spindle/kinetochore checkpoint. *Genes Dev.* 13:517-22.
- Bloecher, A., G.M. Venturi, and K. Tatchell. 2000. Anaphase spindle position is monitored by the BUB2 checkpoint. *Nat Cell Biol.* 2:556-8.

- Brady, D.M., and K.G. Hardwick. 2000. Complex formation between Mad1p, Bub1p and Bub3p is crucial for spindle checkpoint function. *Curr Biol.* 10:675-8.
- Burke, D.J. 2000. Complexity in the spindle checkpoint. *Curr Opin Genet Dev.* 10:26-31.
- Burton, J.L., V. Tsakraklides, and M.J. Solomon. 2005. Assembly of an APC-Cdh1-substrate complex is stimulated by engagement of a destruction box. *Mol Cell.* 18:533-42.
- Buvelot, S., S.Y. Tatsutani, D. Vermaak, and S. Biggins. 2003. The budding yeast Ipl1/Aurora protein kinase regulates mitotic spindle disassembly. *J Cell Biol.* 160:329-39.
- Campbell, M.S., G.K. Chan, and T.J. Yen. 2001. Mitotic checkpoint proteins HsMAD1 and HsMAD2 are associated with nuclear pore complexes in interphase. *J Cell Sci.* 114:953-63.
- Carmena, M., and W.C. Earnshaw. 2003. The cellular geography of aurora kinases. *Nat Rev Mol Cell Biol.* 4:842-54.
- Chan, G.K., S.A. Jablonski, D.A. Starr, M.L. Goldberg, and T.J. Yen. 2000. Human Zw10 and ROD are mitotic checkpoint proteins that bind to kinetochores. *Nat Cell Biol.* 2:944-7.
- Chan, G.K., S.A. Jablonski, V. Sudakin, J.C. Hittle, and T.J. Yen. 1999. Human BUBR1 is a mitotic checkpoint kinase that monitors CENP-E functions at kinetochores and binds the cyclosome/APC. *J Cell Biol.* 146:941-54.
- Charles, J.F., S.L. Jaspersen, R.L. Tinker-Kulberg, L. Hwang, A. Szidon, and D.O. Morgan. 1998. The Polo-related kinase Cdc5 activates and is destroyed by the mitotic cyclin destruction machinery in *S. cerevisiae*. *Curr Biol.* 8:497-507.
- Cheeseman, I.M., S. Anderson, M. Jwa, E.M. Green, J. Kang, J.R. Yates, 3rd, C.S. Chan, D.G. Drubin, and G. Barnes. 2002. Phospho-regulation of kinetochore-microtubule attachments by the Aurora kinase Ipl1p. *Cell.* 111:163-72.
- Cheeseman, I.M., M. Enquist-Newman, T. Muller-Reichert, D.G. Drubin, and G. Barnes. 2001. Mitotic spindle integrity and kinetochore function linked by the Duo1p/Dam1p complex. *J Cell Biol.* 152:197-212.
- Cheeseman, I.M., S. Niessen, S. Anderson, F. Hyndman, J.R. Yates, 3rd, K. Oegema, and A. Desai. 2004. A conserved protein network controls assembly of the outer kinetochore and its ability to sustain tension. *Genes Dev.* 18:2255-68.
- Chen, R.H. 2002. BubR1 is essential for kinetochore localization of other spindle checkpoint proteins and its phosphorylation requires Mad1. *J Cell Biol.* 158:487-96.
- Chung, E., and R.H. Chen. 2003. Phosphorylation of Cdc20 is required for its inhibition by the spindle checkpoint. *Nat Cell Biol.*
- Cohen-Fix, O. 2003. Meiosis: polo, FEAR and the art of dividing reductionally. *Curr Biol.* 13:R603-5.
- Cohen-Fix, O., and D. Koshland. 1997. The anaphase inhibitor of *Saccharomyces cerevisiae* Pds1p is a target of the DNA damage checkpoint pathway. *Proc Natl Acad Sci U S A.* 94:14361-6.

- Connelly, C., and P. Hieter. 1996. Budding yeast SKP1 encodes an evolutionarily conserved kinetochore protein required for cell cycle progression. *Cell*. 86:275-85.
- Courtwright, A.M., and X. He. 2002. Dam1 is the right one: phosphoregulation of kinetochore biorientation. *Dev Cell*. 3:610-1.
- D'Amours, D., and A. Amon. 2004. At the interface between signaling and executing anaphase--Cdc14 and the FEAR network. *Genes Dev*. 18:2581-95.
- De Wulf, P., A.D. McAinsh, and P.K. Sorger. 2003. Hierarchical assembly of the budding yeast kinetochore from multiple subcomplexes. *Genes Dev*. 17:2902-21.
- DeLuca, J.G., B.J. Howell, J.C. Canman, J.M. Hickey, G. Fang, and E.D. Salmon. 2003. Nuf2 and Hec1 are required for retention of the checkpoint proteins Mad1 and Mad2 to kinetochores. *Curr Biol*. 13:2103-9.
- Ditchfield, C., V.L. Johnson, A. Tighe, R. Ellston, C. Haworth, T. Johnson, A. Mortlock, N. Keen, and S.S. Taylor. 2003. Aurora B couples chromosome alignment with anaphase by targeting BubR1, Mad2, and Cenp-E to kinetochores. *J Cell Biol*. 161:267-80.
- Elia, A.E., L.C. Cantley, and M.B. Yaffe. 2003a. Proteomic screen finds pSer/pThr-binding domain localizing Plk1 to mitotic substrates. *Science*. 299:1228-31.
- Elia, A.E., P. Rellos, L.F. Haire, J.W. Chao, F.J. Ivins, K. Hoepker, D. Mohammad, L.C. Cantley, S.J. Smerdon, and M.B. Yaffe. 2003b. The molecular basis for phosphodependent substrate targeting and regulation of Plks by the Polo-box domain. *Cell*. 115:83-95.
- Elledge, S.J. 1996. Cell cycle checkpoints: preventing an identity crisis. *Science*. 274:1664-72.
- Enquist-Newman, M., I.M. Cheeseman, D. Van Goor, D.G. Drubin, P.B. Meluh, and G. Barnes. 2001. Dad1p, third component of the duo1p/dam1p complex involved in kinetochore function and mitotic spindle integrity. *Mol Biol Cell*. 12:2601-13.
- Fang, G. 2002. Checkpoint protein BubR1 acts synergistically with Mad2 to inhibit anaphase-promoting complex. *Mol Biol Cell*. 13:755-66.
- Feng, Z.H., S.E. Wilson, Z.Y. Peng, K.K. Schlender, E.M. Reimann, and R.J. Trumbly. 1991. The yeast GLC7 gene required for glycogen accumulation encodes a type 1 protein phosphatase. *J Biol Chem*. 266:23796-801.
- Francisco, L., W. Wang, and C.S. Chan. 1994. Type 1 protein phosphatase acts in opposition to IpL1 protein kinase in regulating yeast chromosome segregation. *Mol Cell Biol*. 14:4731-40.
- Fraschini, R., A. Beretta, G. Lucchini, and S. Piatti. 2001a. Role of the kinetochore protein Ndc10 in mitotic checkpoint activation in *Saccharomyces cerevisiae*. *Mol Genet Genomics*. 266:115-25.
- Fraschini, R., A. Beretta, L. Sironi, A. Musacchio, G. Lucchini, and S. Piatti. 2001b. Bub3 interaction with Mad2, Mad3 and Cdc20 is mediated by WD40 repeats and does not require intact kinetochores. *Embo J*. 20:6648-59.

- Fraschini, R., E. Formenti, G. Lucchini, and S. Piatti. 1999. Budding yeast Bub2 is localized at spindle pole bodies and activates the mitotic checkpoint via a different pathway from Mad2. *J Cell Biol.* 145:979-91.
- Friedman, D.B., J.W. Kern, B.J. Huneycutt, D.B. Vinh, D.K. Crawford, E. Steiner, D. Scheiltz, J. Yates, 3rd, K.A. Resing, N.G. Ahn, M. Winey, and T.N. Davis. 2001. Yeast Mps1p phosphorylates the spindle pole component Spc110p in the N-terminal domain. *J Biol Chem.* 276:17958-67.
- Gachet, Y., S. Tournier, J.B. Millar, and J.S. Hyams. 2001. A MAP kinase-dependent actin checkpoint ensures proper spindle orientation in fission yeast. *Nature.* 412:352-5.
- Gachet, Y., S. Tournier, J.B. Millar, and J.S. Hyams. 2004. Mechanism controlling perpendicular alignment of the spindle to the axis of cell division in fission yeast. *Embo J.* 23:1289-300.
- Gardner, R.D., A. Poddar, C. Yellman, P.A. Tavormina, M.C. Monteagudo, and D.J. Burke. 2001. The spindle checkpoint of the yeast *Saccharomyces cerevisiae* requires kinetochore function and maps to the CBF3 domain. *Genetics.* 157:1493-502.
- Gassmann, R., A. Carvalho, A.J. Henzing, S. Ruchaud, D.F. Hudson, R. Honda, E.A. Nigg, D.L. Gerloff, and W.C. Earnshaw. 2004a. Borealin: a novel chromosomal passenger required for stability of the bipolar mitotic spindle. *J Cell Biol.* 166:179-91.
- Gassmann, R., P. Vagnarelli, D. Hudson, and W.C. Earnshaw. 2004b. Mitotic chromosome formation and the condensin paradox. *Exp Cell Res.* 296:35-42.
- Gentry, M.S., and R.L. Hallberg. 2002. Localization of *Saccharomyces cerevisiae* protein phosphatase 2A subunits throughout mitotic cell cycle. *Mol Biol Cell.* 13:3477-92.
- Geymonat, M., A. Spanos, P.A. Walker, L.H. Johnston, and S.G. Sedgwick. 2003. In vitro regulation of budding yeast Bfa1/Bub2 GAP activity by Cdc5. *J Biol Chem.* 278:14591-4.
- Giet, R., and D.M. Glover. 2001. *Drosophila* aurora B kinase is required for histone H3 phosphorylation and condensin recruitment during chromosome condensation and to organize the central spindle during cytokinesis. *J Cell Biol.* 152:669-82.
- Gillett, E.S., C.W. Espelin, and P.K. Sorger. 2004. Spindle checkpoint proteins and chromosome-microtubule attachment in budding yeast. *J Cell Biol.* 164:535-46.
- Glotzer, M., A.W. Murray, and M.W. Kirschner. 1991. Cyclin is degraded by the ubiquitin pathway. *Nature.* 349:132-8.
- Goh, P.Y., and J.V. Kilmartin. 1993. NDC10: a gene involved in chromosome segregation in *Saccharomyces cerevisiae*. *J Cell Biol.* 121:503-12.
- Gorbsky, G.J. 2004. Mitosis: MCAK under the aura of Aurora B. *Curr Biol.* 14:R346-8.
- Goshima, G., and M. Yanagida. 2000. Establishing biorientation occurs with precocious separation of the sister kinetochores, but not the arms, in the early spindle of budding yeast. *Cell.* 100:619-33.

- Goto, H., Y. Yasui, E.A. Nigg, and M. Inagaki. 2002. Aurora-B phosphorylates Histone H3 at serine28 with regard to the mitotic chromosome condensation. *Genes Cells*. 7:11-7.
- Gruber, S., C.H. Haering, and K. Nasmyth. 2003. Chromosomal cohesin forms a ring. *Cell*. 112:765-77.
- Guacci, V., D. Koshland, and A. Strunnikov. 1997. A direct link between sister chromatid cohesion and chromosome condensation revealed through the analysis of MCD1 in *S. cerevisiae*. *Cell*. 91:47-57.
- Haering, C.H., J. Lowe, A. Hochwagen, and K. Nasmyth. 2002. Molecular architecture of SMC proteins and the yeast cohesin complex. *Mol Cell*. 9:773-88.
- Hagstrom, K.A., and B.J. Meyer. 2003. Condensin and cohesin: more than chromosome compactor and glue. *Nat Rev Genet*. 4:520-34.
- Hanks, S., K. Coleman, S. Reid, A. Plaja, H. Firth, D. Fitzpatrick, A. Kidd, K. Mehes, R. Nash, N. Robin, N. Shannon, J. Tolmie, J. Swansbury, A. Irrthum, J. Douglas, and N. Rahman. 2004. Constitutional aneuploidy and cancer predisposition caused by biallelic mutations in BUB1B. *Nat Genet*. 36:1159-61.
- Hansen, D.V., A.V. Loktev, K.H. Ban, and P.K. Jackson. 2004. Plk1 Regulates Activation of the Anaphase Promoting Complex by Phosphorylating and Triggering SCF β TrCP-dependent Destruction of the APC Inhibitor Emi1. *Mol Biol Cell*.
- Hardwick, K.G., R.C. Johnston, D.L. Smith, and A.W. Murray. 2000. MAD3 encodes a novel component of the spindle checkpoint which interacts with Bub3p, Cdc20p, and Mad2p. *J Cell Biol*. 148:871-82.
- Hardwick, K.G., R. Li, C. Mistrot, R.H. Chen, P. Dann, A. Rudner, and A.W. Murray. 1999. Lesions in many different spindle components activate the spindle checkpoint in the budding yeast *Saccharomyces cerevisiae*. *Genetics*. 152:509-18.
- Hardwick, K.G., and A.W. Murray. 1995. Mad1p, a phosphoprotein component of the spindle assembly checkpoint in budding yeast. *J Cell Biol*. 131:709-20.
- Hardwick, K.G., E. Weiss, F.C. Luca, M. Winey, and A.W. Murray. 1996. Activation of the budding yeast spindle assembly checkpoint without mitotic spindle disruption. *Science*. 273:953-6.
- Hartwell, L.H., and T.A. Weinert. 1989. Checkpoints: controls that ensure the order of cell cycle events. *Science*. 246:629-34.
- Hauf, S., R.W. Cole, S. LaTerra, C. Zimmer, G. Schnapp, R. Walter, A. Heckel, J. van Meel, C.L. Rieder, and J.M. Peters. 2003. The small molecule Hesperadin reveals a role for Aurora B in correcting kinetochore-microtubule attachment and in maintaining the spindle assembly checkpoint. *J Cell Biol*. 161:281-94.
- He, X., D.R. Rines, C.W. Espelin, and P.K. Sorger. 2001. Molecular analysis of kinetochore-microtubule attachment in budding yeast. *Cell*. 106:195-206.
- Hilioti, Z., Y. Chung, Y. Mochizuki, C.F. Hardy, and O. Cohen-Fix. 2001. The anaphase inhibitor Pds1 binds to the APC/C-associated protein Cdc20 in a destruction box-dependent manner. *Curr Biol*. 11:1347-52.

- Hisamoto, N., K. Sugimoto, and K. Matsumoto. 1994. The Glc7 type 1 protein phosphatase of *Saccharomyces cerevisiae* is required for cell cycle progression in G2/M. *Mol Cell Biol.* 14:3158-65.
- Hofmann, C., I.M. Cheeseman, B.L. Goode, K.L. McDonald, G. Barnes, and D.G. Drubin. 1998. *Saccharomyces cerevisiae* Duo1p and Dam1p, novel proteins involved in mitotic spindle function. *J Cell Biol.* 143:1029-40.
- Howell, B.J., D.B. Hoffman, G. Fang, A.W. Murray, and E.D. Salmon. 2000. Visualization of Mad2 dynamics at kinetochores, along spindle fibers, and at spindle poles in living cells. *J Cell Biol.* 150:1233-50.
- Howell, B.J., B. Moree, E.M. Farrar, S. Stewart, G. Fang, and E.D. Salmon. 2004. Spindle checkpoint protein dynamics at kinetochores in living cells. *Curr Biol.* 14:953-64.
- Hoyt, M.A. 2000. Exit from mitosis: spindle pole power. *Cell.* 102:267-70.
- Hoyt, M.A., L. Totis, and B.T. Roberts. 1991. *S. cerevisiae* genes required for cell cycle arrest in response to loss of microtubule function. *Cell.* 66:507-17.
- Hsu, J.Y., Z.W. Sun, X. Li, M. Reuben, K. Tatchell, D.K. Bishop, J.M. Grushcow, C.J. Brame, J.A. Caldwell, D.F. Hunt, R. Lin, M.M. Smith, and C.D. Allis. 2000. Mitotic phosphorylation of histone H3 is governed by Ipl1/aurora kinase and Glc7/PP1 phosphatase in budding yeast and nematodes. *Cell.* 102:279-91.
- Hu, F., Y. Wang, D. Liu, Y. Li, J. Qin, and S.J. Elledge. 2001. Regulation of the Bub2/Bfa1 GAP complex by Cdc5 and cell cycle checkpoints. *Cell.* 107:655-65.
- Hwang, L.H., L.F. Lau, D.L. Smith, C.A. Mistrot, K.G. Hardwick, E.S. Hwang, A. Amon, and A.W. Murray. 1998. Budding yeast Cdc20: a target of the spindle checkpoint. *Science.* 279:1041-4.
- Hwang, L.H., and A.W. Murray. 1997. A novel yeast screen for mitotic arrest mutants identifies DOC1, a new gene involved in cyclin proteolysis. *Mol Biol Cell.* 8:1877-87.
- Indjeian, V.B., B.M. Stern, and A.W. Murray. 2005. The centromeric protein Sgo1 is required to sense lack of tension on mitotic chromosomes. *Science.* 307:130-3.
- Iouk, T., O. Kerscher, R.J. Scott, M.A. Basrai, and R.W. Wozniak. 2002. The yeast nuclear pore complex functionally interacts with components of the spindle assembly checkpoint. *J Cell Biol.* 159:807-19.
- Ito, H., Y. Fukuda, K. Murata, and A. Kimura. 1983. Transformation of intact yeast cells treated with alkali cations. *J Bacteriol.* 153:163-8.
- Jablonski, S.A., G.K. Chan, C.A. Cooke, W.C. Earnshaw, and T.J. Yen. 1998. The hBUB1 and hBUBR1 kinases sequentially assemble onto kinetochores during prophase with hBUBR1 concentrating at the kinetochore plates in mitosis. *Chromosoma.* 107:386-96.
- Jackson, P.K., and A.G. Eldridge. 2002. The SCF ubiquitin ligase: an extended look. *Mol Cell.* 9:923-5.
- Jackson, P.K., A.G. Eldridge, E. Freed, L. Furstenthal, J.Y. Hsu, B.K. Kaiser, and J.D. Reimann. 2000. The lore of the RINGS: substrate recognition and catalysis by ubiquitin ligases. *Trends Cell Biol.* 10:429-39.

- Janke, C., J. Ortiz, J. Lechner, A. Shevchenko, M.M. Magiera, C. Schramm, and E. Schiebel. 2001. The budding yeast proteins Spc24p and Spc25p interact with Ndc80p and Nuf2p at the kinetochore and are important for kinetochore clustering and checkpoint control. *Embo J.* 20:777-91.
- Janke, C., J. Ortiz, T.U. Tanaka, J. Lechner, and E. Schiebel. 2002. Four new subunits of the Dam1-Duo1 complex reveal novel functions in sister kinetochore biorientation. *Embo J.* 21:181-93.
- Jaspersen, S.L., J.F. Charles, R.L. Tinker-Kulberg, and D.O. Morgan. 1998. A late mitotic regulatory network controlling cyclin destruction in *Saccharomyces cerevisiae*. *Mol Biol Cell.* 9:2803-17.
- Jaspersen, S.L., and M. Winey. 2004. The budding yeast spindle pole body: structure, duplication, and function. *Annu Rev Cell Dev Biol.* 20:1-28.
- Jones, M.H., J.B. Bachant, A.R. Castillo, T.H. Giddings, Jr., and M. Winey. 1999. Yeast Dam1p is required to maintain spindle integrity during mitosis and interacts with the Mps1p kinase. *Mol Biol Cell.* 10:2377-91.
- Jones, M.H., X. He, T.H. Giddings, and M. Winey. 2001. Yeast Dam1p has a role at the kinetochore in assembly of the mitotic spindle. *Proc Natl Acad Sci U S A.* 98:13675-80.
- Kang, J., I.M. Cheeseman, G. Kallstrom, S. Velmurugan, G. Barnes, and C.S. Chan. 2001. Functional cooperation of Dam1, Ipl1, and the inner centromere protein (INCENP)-related protein Sli15 during chromosome segregation. *J Cell Biol.* 155:763-74.
- Kim, J.H., J.S. Kang, and C.S. Chan. 1999. Sli15 associates with the ipl1 protein kinase to promote proper chromosome segregation in *Saccharomyces cerevisiae*. *J Cell Biol.* 145:1381-94.
- Kim, S.H., D.P. Lin, S. Matsumoto, A. Kitazono, and T. Matsumoto. 1998. Fission yeast Slp1: an effector of the Mad2-dependent spindle checkpoint. *Science.* 279:1045-7.
- Kosco, K.A., C.G. Pearson, P.S. Maddox, P.J. Wang, I.R. Adams, E.D. Salmon, K. Bloom, and T.C. Huffaker. 2001. Control of microtubule dynamics by stu2p is essential for spindle orientation and metaphase chromosome alignment in yeast. *Mol Biol Cell.* 12:2870-80.
- Kramer, E.R., N. Scheuringer, A.V. Podtelejnikov, M. Mann, and J.M. Peters. 2000. Mitotic regulation of the APC activator proteins CDC20 and CDH1. *Mol Biol Cell.* 11:1555-69.
- Lampson, M.A., K. Renduchitala, A. Khodjakov, and T.M. Kapoor. 2004. Correcting improper chromosome-spindle attachments during cell division. *Nat Cell Biol.* 6:232-7.
- Lan, W., X. Zhang, S.L. Kline-Smith, S.E. Rosasco, G.A. Barrett-Wilt, J. Shabanowitz, D.F. Hunt, C.E. Walczak, and P.T. Stukenberg. 2004. Aurora B phosphorylates centromeric MCAK and regulates its localization and microtubule depolymerization activity. *Curr Biol.* 14:273-86.

- Lavoie, B.D., K.M. Tuffo, S. Oh, D. Koshland, and C. Holm. 2000. Mitotic chromosome condensation requires Brn1p, the yeast homologue of Barren. *Mol Biol Cell*. 11:1293-304.
- Li, R., and A.W. Murray. 1991. Feedback control of mitosis in budding yeast. *Cell*. 66:519-31.
- Li, W., Z. Lan, H. Wu, S. Wu, J. Meadows, J. Chen, V. Zhu, and W. Dai. 1999. BUBR1 phosphorylation is regulated during mitotic checkpoint activation. *Cell Growth Differ*. 10:769-75.
- Li, X., and R.B. Nicklas. 1997. Tension-sensitive kinetochore phosphorylation and the chromosome distribution checkpoint in praying mantid spermatocytes. *J Cell Sci*. 110 (Pt 5):537-45.
- Li, Y., J. Bachant, A.A. Alcasabas, Y. Wang, J. Qin, and S.J. Elledge. 2002. The mitotic spindle is required for loading of the DASH complex onto the kinetochore. *Genes Dev*. 16:183-97.
- Losada, A., M. Hirano, and T. Hirano. 1998. Identification of *Xenopus* SMC protein complexes required for sister chromatid cohesion. *Genes Dev*. 12:1986-97.
- Losada, A., M. Hirano, and T. Hirano. 2002. Cohesin release is required for sister chromatid resolution, but not for condensin-mediated compaction, at the onset of mitosis. *Genes Dev*. 16:3004-16.
- Luo, X., G. Fang, M. Coldiron, Y. Lin, H. Yu, M.W. Kirschner, and G. Wagner. 2000. Structure of the Mad2 spindle assembly checkpoint protein and its interaction with Cdc20. *Nat Struct Biol*. 7:224-9.
- Luo, X., Z. Tang, J. Rizo, and H. Yu. 2002. The Mad2 spindle checkpoint protein undergoes similar major conformational changes upon binding to either Mad1 or Cdc20. *Mol Cell*. 9:59-71.
- Maeshima, K., and U.K. Laemmli. 2003. A two-step scaffolding model for mitotic chromosome assembly. *Dev Cell*. 4:467-80.
- Mao, Y., A. Abrieu, and D.W. Cleveland. 2003. Activating and Silencing the Mitotic Checkpoint through CENP-E-Dependent Activation/Inactivation of BubR1. *Cell*. 114:87-98.
- Margottin-Goguet, F., J.Y. Hsu, A. Loktev, H.M. Hsieh, J.D. Reimann, and P.K. Jackson. 2003. Prophase destruction of Emi1 by the SCF(betaTrCP/Slimb) ubiquitin ligase activates the anaphase promoting complex to allow progression beyond prometaphase. *Dev Cell*. 4:813-26.
- Martin-Lluesma, S., V.M. Stucke, and E.A. Nigg. 2002. Role of Hec1 in spindle checkpoint signaling and kinetochore recruitment of Mad1/Mad2. *Science*. 297:2267-70.
- Mayer, M.L., I. Pot, M. Chang, H. Xu, V. Aneliunas, T. Kwok, R. Newitt, R. Aebersold, C. Boone, G.W. Brown, and P. Hieter. 2004. Identification of protein complexes required for efficient sister chromatid cohesion. *Mol Biol Cell*. 15:1736-45.
- McClelland, M.L., R.D. Gardner, M.J. Kallio, J.R. Daum, G.J. Gorbsky, D.J. Burke, and P.T. Stukenberg. 2003. The highly conserved Ndc80 complex is required for

- kinetochore assembly, chromosome congression, and spindle checkpoint activity. *Genes Dev.* 17:101-14.
- Measday, V., D.W. Hailey, I. Pot, S.A. Givan, K.M. Hyland, G. Cagney, S. Fields, T.N. Davis, and P. Hieter. 2002. Ctf3p, the Mis6 budding yeast homolog, interacts with Mcm22p and Mcm16p at the yeast outer kinetochore. *Genes Dev.* 16:101-13.
- Measday, V., and P. Hieter. 2004. Kinetochore sub-structure comes to MIND. *Nat Cell Biol.* 6:94-5.
- Meraldi, P., V.M. Draviam, and P.K. Sorger. 2004. Timing and checkpoints in the regulation of mitotic progression. *Dev Cell.* 7:45-60.
- Michaelis, C., R. Ciosk, and K. Nasmyth. 1997. Cohesins: chromosomal proteins that prevent premature separation of sister chromatids. *Cell.* 91:35-45.
- Mihich, E., and L. Hartwell. 1997. Eighth Annual Pezcoller Symposium: genomic instability and immortality in cancer. *Cancer Res.* 57:4437-41.
- Millband, D.N., and K.G. Hardwick. 2002. Fission yeast Mad3p is required for Mad2p to inhibit the anaphase-promoting complex and localizes to kinetochores in a Bub1p-, Bub3p-, and Mph1p-dependent manner. *Mol Cell Biol.* 22:2728-42.
- Minshull, J., A. Straight, A.D. Rudner, A.F. Dernburg, A. Belmont, and A.W. Murray. 1996. Protein phosphatase 2A regulates MPF activity and sister chromatid cohesion in budding yeast. *Curr Biol.* 6:1609-20.
- Moore, A., and L. Wordeman. 2004. The mechanism, function and regulation of depolymerizing kinesins during mitosis. *Trends Cell Biol.* 14:537-46.
- Murata-Hori, M., and Y.L. Wang. 2002. The kinase activity of aurora B is required for kinetochore-microtubule interactions during mitosis. *Curr Biol.* 12:894-9.
- Murnion, M.E., R.R. Adams, D.M. Callister, C.D. Allis, W.C. Earnshaw, and J.R. Swedlow. 2001. Chromatin-associated protein phosphatase 1 regulates aurora-B and histone H3 phosphorylation. *J Biol Chem.* 276:26656-65.
- Murray, A.W. 2004. Recycling the cell cycle: cyclins revisited. *Cell.* 116:221-34.
- Musacchio, A., and K.G. Hardwick. 2002. The spindle checkpoint: structural insights into dynamic signalling. *Nat Rev Mol Cell Biol.* 3:731-41.
- Nasmyth, K. 2002. Segregating sister genomes: the molecular biology of chromosome separation. *Science.* 297:559-65.
- Ng, R., J. Ness, and J. Carbon. 1986. Structural studies on centromeres in the yeast *Saccharomyces cerevisiae*. *Basic Life Sci.* 40:479-92.
- Nonaka, N., T. Kitajima, S. Yokobayashi, G. Xiao, M. Yamamoto, S.I. Grewal, and Y. Watanabe. 2002. Recruitment of cohesin to heterochromatic regions by Swi6/HP1 in fission yeast. *Nat Cell Biol.* 4:89-93.
- Ohkura, H., I.M. Hagan, and D.M. Glover. 1995. The conserved *Schizosaccharomyces pombe* kinase plo1, required to form a bipolar spindle, the actin ring, and septum, can drive septum formation in G1 and G2 cells. *Genes Dev.* 9:1059-73.
- Ono, T., Y. Fang, D.L. Spector, and T. Hirano. 2004. Spatial and temporal regulation of Condensins I and II in mitotic chromosome assembly in human cells. *Mol Biol Cell.* 15:3296-308.

- Ono, T., A. Losada, M. Hirano, M.P. Myers, A.F. Neuwald, and T. Hirano. 2003. Differential contributions of condensin I and condensin II to mitotic chromosome architecture in vertebrate cells. *Cell*. 115:109-21.
- Orr-Weaver, T.L., and R.A. Weinberg. 1998. A checkpoint on the road to cancer. *Nature*. 392:223-4.
- Ortiz, J., O. Stemmann, S. Rank, and J. Lechner. 1999. A putative protein complex consisting of Ctf19, Mcm21, and Okp1 represents a missing link in the budding yeast kinetochore. *Genes Dev*. 13:1140-55.
- Ouspenski, II, O.A. Cabello, and B.R. Brinkley. 2000. Chromosome condensation factor Brn1p is required for chromatid separation in mitosis. *Mol Biol Cell*. 11:1305-13.
- Pan, J., and R.H. Chen. 2004. Spindle checkpoint regulates Cdc20p stability in *Saccharomyces cerevisiae*. *Genes Dev*. 18:1439-51.
- Peters, J.M. 2002. The anaphase-promoting complex: proteolysis in mitosis and beyond. *Mol Cell*. 9:931-43.
- Peters, J.M. 2003. Emi1 proteolysis: how SCF(beta-Trcp1) helps to activate the anaphase-promoting complex. *Mol Cell*. 11:1420-1.
- Petersen, J., and I.M. Hagan. 2003. *S. pombe* Aurora Kinase/Survivin Is Required for Chromosome Condensation and the Spindle Checkpoint Attachment Response. *Curr Biol*. 13:590-7.
- Pfleger, C.M., and M.W. Kirschner. 2000. The KEN box: an APC recognition signal distinct from the D box targeted by Cdh1. *Genes Dev*. 14:655-65.
- Pidoux, A.L., and R.C. Allshire. 2004. Kinetochore and heterochromatin domains of the fission yeast centromere. *Chromosome Res*. 12:521-34.
- Pines, J. 1999. Four-dimensional control of the cell cycle. *Nat Cell Biol*. 1:E73-9.
- Pinsky, B.A., S.Y. Tatsutani, K.A. Collins, and S. Biggins. 2003. An Mtw1 complex promotes kinetochore biorientation that is monitored by the Ipl1/Aurora protein kinase. *Dev Cell*. 5:735-45.
- Pot, I., V. Measday, B. Snydsman, G. Cagney, S. Fields, T.N. Davis, E.G. Muller, and P. Hieter. 2003. Chl4p and iml3p are two new members of the budding yeast outer kinetochore. *Mol Biol Cell*. 14:460-76.
- Rajagopalan, S., A. Bimbo, M.K. Balasubramanian, and S. Oliferenko. 2004. A potential tension-sensing mechanism that ensures timely anaphase onset upon metaphase spindle orientation. *Curr Biol*. 14:69-74.
- Reimann, J.D., E. Freed, J.Y. Hsu, E.R. Kramer, J.M. Peters, and P.K. Jackson. 2001a. Emi1 is a mitotic regulator that interacts with Cdc20 and inhibits the anaphase promoting complex. *Cell*. 105:645-55.
- Reimann, J.D., B.E. Gardner, F. Margottin-Goguet, and P.K. Jackson. 2001b. Emi1 regulates the anaphase-promoting complex by a different mechanism than Mad2 proteins. *Genes Dev*. 15:3278-85.
- Rhind, N., and P. Russell. 2000. Checkpoints: it takes more than time to heal some wounds. *Curr Biol*. 10:R908-11.

- Rieder, C.L., R.W. Cole, A. Khodjakov, and G. Sluder. 1995. The checkpoint delaying anaphase in response to chromosome monoorientation is mediated by an inhibitory signal produced by unattached kinetochores. *J Cell Biol.* 130:941-8.
- Rigaut, G., A. Shevchenko, B. Rutz, M. Wilm, M. Mann, and B. Seraphin. 1999. A generic protein purification method for protein complex characterization and proteome exploration. *Nat Biotechnol.* 17:1030-2.
- Rudner, A.D., and A.W. Murray. 2000. Phosphorylation by Cdc28 activates the Cdc20-dependent activity of the anaphase-promoting complex. *J Cell Biol.* 149:1377-90.
- Sampath, S.C., R. Ohi, O. Leismann, A. Salic, A. Pozniakovski, and H. Funabiki. 2004. The chromosomal passenger complex is required for chromatin-induced microtubule stabilization and spindle assembly. *Cell.* 118:187-202.
- Schwab, M., A.S. Lutum, and W. Seufert. 1997. Yeast Hct1 is a regulator of Clb2 cyclin proteolysis. *Cell.* 90:683-93.
- Schwab, M., M. Neutzner, D. Mocker, and W. Seufert. 2001. Yeast Hct1 recognizes the mitotic cyclin Clb2 and other substrates of the ubiquitin ligase APC. *Embo J.* 20:5165-75.
- Schwartz, K., K. Richards, and D. Botstein. 1997. BIM1 encodes a microtubule-binding protein in yeast. *Mol Biol Cell.* 8:2677-91.
- Seeley, T.W., L. Wang, and J.Y. Zhen. 1999. Phosphorylation of human MAD1 by the BUB1 kinase in vitro. *Biochem Biophys Res Commun.* 257:589-95.
- Shah, J.V., E. Botvinick, Z. Bonday, F. Furnari, M. Berns, and D.W. Cleveland. 2004. Dynamics of centromere and kinetochore proteins; implications for checkpoint signaling and silencing. *Curr Biol.* 14:942-52.
- Sharp-Baker, H., and R.H. Chen. 2001. Spindle checkpoint protein Bub1 is required for kinetochore localization of Mad1, Mad2, Bub3, and CENP-E, independently of its kinase activity. *J Cell Biol.* 153:1239-50.
- Shirayama, M., W. Zachariae, R. Ciosk, and K. Nasmyth. 1998. The Polo-like kinase Cdc5p and the WD-repeat protein Cdc20p/fizzy are regulators and substrates of the anaphase promoting complex in *Saccharomyces cerevisiae*. *Embo J.* 17:1336-49.
- Shou, W., R. Azzam, S.L. Chen, M.J. Huddleston, C. Baskerville, H. Charbonneau, R.S. Annan, S.A. Carr, and R.J. Deshaies. 2002. Cdc5 influences phosphorylation of Net1 and disassembly of the RENT complex. *BMC Mol Biol.* 3:3.
- Sironi, L., M. Mapelli, S. Knapp, A. De Antoni, K.T. Jeang, and A. Musacchio. 2002. Crystal structure of the tetrameric Mad1-Mad2 core complex: implications of a 'safety belt' binding mechanism for the spindle checkpoint. *Embo J.* 21:2496-506.
- Sironi, L., M. Melixetian, M. Faretta, E. Prosperini, K. Helin, and A. Musacchio. 2001. Mad2 binding to Mad1 and Cdc20, rather than oligomerization, is required for the spindle checkpoint. *Embo J.* 20:6371-82.
- Sonoda, E., T. Matsusaka, C. Morrison, P. Vagnarelli, O. Hoshi, T. Ushiki, K. Nojima, T. Fukagawa, I.C. Waizenegger, J.M. Peters, W.C. Earnshaw, and S. Takeda.

2001. Scc1/Rad21/Mcd1 is required for sister chromatid cohesion and kinetochore function in vertebrate cells. *Dev Cell*. 1:759-70.
- Sorger, P.K., K.F. Doheny, P. Hieter, K.M. Kopski, T.C. Huffaker, and A.A. Hyman. 1995. Two genes required for the binding of an essential *Saccharomyces cerevisiae* kinetochore complex to DNA. *Proc Natl Acad Sci U S A*. 92:12026-30.
- Sorger, P.K., F.F. Severin, and A.A. Hyman. 1994. Factors required for the binding of reassembled yeast kinetochores to microtubules in vitro. *J Cell Biol*. 127:995-1008.
- Stern, B.M., and A.W. Murray. 2001. Lack of tension at kinetochores activates the spindle checkpoint in budding yeast. *Curr Biol*. 11:1462-7.
- Strunnikov, A.V., J. Kingsbury, and D. Koshland. 1995. CEP3 encodes a centromere protein of *Saccharomyces cerevisiae*. *J Cell Biol*. 128:749-60.
- Sudakin, V., G.K. Chan, and T.J. Yen. 2001. Checkpoint inhibition of the APC/C in HeLa cells is mediated by a complex of BUBR1, BUB3, CDC20, and MAD2. *J Cell Biol*. 154:925-36.
- Sudakin, V., and T.J. Yen. 2004. Purification of the mitotic checkpoint complex, an inhibitor of the APC/C from HeLa cells. *Methods Mol Biol*. 281:199-212.
- Tanaka, T., M.P. Cosma, K. Wirth, and K. Nasmyth. 1999. Identification of cohesin association sites at centromeres and along chromosome arms. *Cell*. 98:847-58.
- Tanaka, T., J. Fuchs, J. Loidl, and K. Nasmyth. 2000. Cohesin ensures bipolar attachment of microtubules to sister centromeres and resists their precocious separation. *Nat Cell Biol*. 2:492-9.
- Tanaka, T.U., N. Rachidi, C. Janke, G. Pereira, M. Galova, E. Schiebel, M.J. Stark, and K. Nasmyth. 2002. Evidence that the Ipl1-Sli15 (Aurora kinase-INCENP) complex promotes chromosome bi-orientation by altering kinetochore-spindle pole connections. *Cell*. 108:317-29.
- Tang, Z., R. Bharadwaj, B. Li, and H. Yu. 2001a. Mad2-Independent inhibition of APCCdc20 by the mitotic checkpoint protein BubR1. *Dev Cell*. 1:227-37.
- Tang, Z., B. Li, R. Bharadwaj, H. Zhu, E. Ozkan, K. Hakala, J. Deisenhofer, and H. Yu. 2001b. APC2 Cullin protein and APC11 RING protein comprise the minimal ubiquitin ligase module of the anaphase-promoting complex. *Mol Biol Cell*. 12:3839-51.
- Tang, Z., H. Shu, D. Oncel, S. Chen, and H. Yu. 2004. Phosphorylation of Cdc20 by Bub1 Provides a Catalytic Mechanism for APC/C Inhibition by the Spindle Checkpoint. *Mol Cell*. 16:387-97.
- Taylor, S.S., E. Ha, and F. McKeon. 1998. The human homologue of Bub3 is required for kinetochore localization of Bub1 and a Mad3/Bub1-related protein kinase. *J Cell Biol*. 142:1-11.
- Taylor, S.S., D. Hussein, Y. Wang, S. Elderkin, and C.J. Morrow. 2001. Kinetochore localisation and phosphorylation of the mitotic checkpoint components Bub1 and BubR1 are differentially regulated by spindle events in human cells. *J Cell Sci*. 114:4385-95.

- Tournier, S., Y. Gachet, V. Buck, J.S. Hyams, and J.B. Millar. 2004. Disruption of astral microtubule contact with the cell cortex activates a Bub1, Bub3, and Mad3-dependent checkpoint in fission yeast. *Mol Biol Cell*. 15:3345-56.
- Uhlmann, F., F. Lottspeich, and K. Nasmyth. 1999. Sister-chromatid separation at anaphase onset is promoted by cleavage of the cohesin subunit Scc1. *Nature*. 400:37-42.
- van Breugel, M., D. Drechsel, and A. Hyman. 2003. Stu2p, the budding yeast member of the conserved Dis1/XMAP215 family of microtubule-associated proteins is a plus end-binding microtubule destabilizer. *J Cell Biol*. 161:359-69.
- Vanoosthuyse, V., R. Valsdottir, J.P. Javerzat, and K.G. Hardwick. 2004. Kinetochores targeting of fission yeast mad and Bub proteins is essential for spindle checkpoint function but not for all chromosome segregation roles of Bub1p. *Mol Cell Biol*. 24:9786-801.
- Vass, S., S. Cotterill, A.M. Valdeolmillos, J.L. Barbero, E. Lin, W.D. Warren, and M.M. Heck. 2003. Depletion of Drad21/Scc1 in Drosophila cells leads to instability of the cohesin complex and disruption of mitotic progression. *Curr Biol*. 13:208-18.
- Vodermaier, H.C., C. Gieffers, S. Maurer-Stroh, F. Eisenhaber, and J.M. Peters. 2003. TPR subunits of the anaphase-promoting complex mediate binding to the activator protein CDH1. *Curr Biol*. 13:1459-68.
- Waizenegger, I.C., S. Hauf, A. Meinke, and J.M. Peters. 2000. Two distinct pathways remove mammalian cohesin from chromosome arms in prophase and from centromeres in anaphase. *Cell*. 103:399-410.
- Wang, H., D. Liu, Y. Wang, J. Qin, and S.J. Elledge. 2001a. Pds1 phosphorylation in response to DNA damage is essential for its DNA damage checkpoint function. *Genes Dev*. 15:1361-72.
- Wang, X., J.R. Babu, J.M. Harden, S.A. Jablonski, M.H. Gazi, W.L. Lingle, P.C. de Groen, T.J. Yen, and J.M. van Deursen. 2001b. The mitotic checkpoint protein hBUB3 and the mRNA export factor hRAE1 interact with GLE2p-binding sequence (GLEBS)-containing proteins. *J Biol Chem*. 276:26559-67.
- Wang, Y., and D.J. Burke. 1997. Cdc55p, the B-type regulatory subunit of protein phosphatase 2A, has multiple functions in mitosis and is required for the kinetochores/spindle checkpoint in *Saccharomyces cerevisiae*. *Mol Cell Biol*. 17:620-6.
- Warren, C.D., D.M. Brady, R.C. Johnston, J.S. Hanna, K.G. Hardwick, and F.A. Spencer. 2002. Distinct chromosome segregation roles for spindle checkpoint proteins. *Mol Biol Cell*. 13:3029-41.
- Weiss, E., and M. Winey. 1996. The *Saccharomyces cerevisiae* spindle pole body duplication gene MPS1 is part of a mitotic checkpoint. *J Cell Biol*. 132:111-23.
- Wheatley, S.P., A.J. Henzing, H. Dodson, W. Khaled, and W.C. Earnshaw. 2004. Aurora-B phosphorylation in vitro identifies a residue of survivin that is essential for its localization and binding to inner centromere protein (INCENP) in vivo. *J Biol Chem*. 279:5655-60.

- Wigge, P.A., and J.V. Kilmartin. 2001. The Ndc80p complex from *Saccharomyces cerevisiae* contains conserved centromere components and has a function in chromosome segregation. *J Cell Biol.* 152:349-60.
- Williams, B.C., Z. Li, S. Liu, E.V. Williams, G. Leung, T.J. Yen, and M.L. Goldberg. 2003. Zwilch, a new component of the ZW10/ROD complex required for kinetochore functions. *Mol Biol Cell.* 14:1379-91.
- Winey, M., P. Baum, L. Goetsch, and B. Byers. 1991. Genetic determinants of spindle pole body duplication in budding yeast. *Cold Spring Harb Symp Quant Biol.* 56:705-8.
- Winey, M., and E.T. O'Toole. 2001. The spindle cycle in budding yeast. *Nat Cell Biol.* 3:E23-7.
- Wittmann, T., A. Hyman, and A. Desai. 2001. The spindle: a dynamic assembly of microtubules and motors. *Nat Cell Biol.* 3:E28-34.
- Wojcik, E., R. Basto, M. Serr, F. Scaerou, R. Karess, and T. Hays. 2001. Kinetochore dynein: its dynamics and role in the transport of the Rough deal checkpoint protein. *Nat Cell Biol.* 3:1001-7.
- Wu, H., Z. Lan, W. Li, S. Wu, J. Weinstein, K.M. Sakamoto, and W. Dai. 2000. p55CDC/hCDC20 is associated with BUBR1 and may be a downstream target of the spindle checkpoint kinase. *Oncogene.* 19:4557-62.
- Yamaguchi, S., A. Decottignies, and P. Nurse. 2003. Function of Cdc2p-dependent Bub1p phosphorylation and Bub1p kinase activity in the mitotic and meiotic spindle checkpoint. *Embo J.* 22:1075-87.
- Yamano, H., J. Gannon, H. Mahbubani, and T. Hunt. 2004. Cell cycle-regulated recognition of the destruction box of cyclin B by the APC/C in *Xenopus* egg extracts. *Mol Cell.* 13:137-47.
- Yao, X., A. Abrieu, Y. Zheng, K.F. Sullivan, and D.W. Cleveland. 2000. CENP-E forms a link between attachment of spindle microtubules to kinetochores and the mitotic checkpoint. *Nat Cell Biol.* 2:484-91.
- Yoon, H.J., A. Feoktistova, B.A. Wolfe, J.L. Jennings, A.J. Link, and K.L. Gould. 2002. Proteomics analysis identifies new components of the fission and budding yeast anaphase-promoting complexes. *Curr Biol.* 12:2048-54.
- Yoshida, S., K. Asakawa, and A. Toh-e. 2002. Mitotic exit network controls the localization of Cdc14 to the spindle pole body in *Saccharomyces cerevisiae*. *Curr Biol.* 12:944-50.
- Zachariae, W. 1999. Progression into and out of mitosis. *Curr Opin Cell Biol.* 11:708-16.
- Zachariae, W., and K. Nasmyth. 1999. Whose end is destruction: cell division and the anaphase-promoting complex. *Genes Dev.* 13:2039-58.
- Zeitlin, S.G., R.D. Shelby, and K.F. Sullivan. 2001. CENP-A is phosphorylated by Aurora B kinase and plays an unexpected role in completion of cytokinesis. *J Cell Biol.* 155:1147-57.
- Zheng, L., Y. Chen, and W.H. Lee. 1999. Hec1p, an evolutionarily conserved coiled-coil protein, modulates chromosome segregation through interaction with SMC proteins. *Mol Cell Biol.* 19:5417-28.